INCLUSIVE PRODUCTION OF REAL PHOTONS AT LARGE TRANSVERSE MOMENTUM IN QUANTUM CHROMODYNAMICS

by

© Christos Papavassiliou

A thesis submitted to the Faculty of Graduate Studies and Research in partial fulfillment of the requirements for the degree of Master of Science.

Department of Physics
McGill University
Montreal, Quebec, Canada.

August, 1980

ABSTRACT

Inclusive production of real photons in p-p, π^--p and $\bar{p}$-p collisions at large transverse momenta (p_T) is studied in QCD and compared with existing data. Apart from the quark gluon and quark-antiquark contribution, corrections due to Bremsstrahlung of photons ($q+q \rightarrow q+q+\gamma$) and to parton intrinsic transverse momenta are taken into account. It is shown that $p+p \rightarrow \gamma+X$ provides one of the best determinations of the gluon distribution in the proton. Hadron production opposite-side a large-p_T photon trigger is also studied. It is shown that the difference between the momentum sharing (x_e) distributions of $\pi^-+p \rightarrow \gamma+\pi^{\pm}+X$ and $\pi^+ + p \rightarrow \gamma+\pi^{\pm}+X$ provides a good determination of the gluon fragmentation function to a pion.

SOMMAIRE

Nous étudions la production inclusive de photons réels dans les collisions p-p, π^--p et $\bar{p}$-p à grands moments transverses (p_T), dans la contexte de la Chromodynamique Quantique et nous la comparons avec les resultats d'experiences. Nous ajoutons aux contributions quark-gluon et quark-antiquark les corrections dues au rayonnement de freinage des quarks ($q+q \rightarrow q+q+\gamma$) et au moment transversal intrinsèque des partons (k_T). Nous démontrons que la réaction $p+p \rightarrow \gamma + X$ donne la meilleure détermination de la distribution gluonique du proton. Nous étudions aussi la production à grand p_T d'un hadron et un photon aux directions opposés. Nous demontrons que la difference entre les distributions de partage de moment (x_e) des rèactions $\pi^- + p \rightarrow \gamma + \pi^\pm + X$ et $\pi^+ + p \rightarrow \gamma + \pi^\pm + X$ fournit une bonne determination de la fonction de fragmentation d'un gluon à un pion.

ACKNOWLEDGMENTS

This thesis contains some research work I did at McGill University, during the academic year 1979-1980. I wish to thank the staff, research associates and fellow graduate students of the Physics Department, for their assistance and for many helpful and stimulating discussions.

Special thanks are due to my thesis advisor and collaborator, Professor A.P. Contogouris for suggesting this subject of research, for his constant encouragement and help during the course of the research and for his many valuable suggestions regarding the presentation of this thesis. The work on which this thesis is based would never have achieved its present form without the input of my friend and collaborator Stavros Papadopoulos, whose criticism, explanations and valuable suggestions I much appreciate. I have also had the pleasure to receive help in my work from the explanations, advise and criticism of Drs. Ernest Argyres, Bruce Campbell, Jochen Kripfganz, Claude Leroy, Argyris Nicolaidis and Pierre Valin.

Finally, many thanks are due to my fellow graduate student, Nader Mobed for correcting some of my spelling mistakes and Mrs. June Yamazaki for her careful typing of the manuscript.

TABLE OF CONTENTS

TABLE OF CONTENTS - Cont'd.

TABLE OF CONTENTS - Cont'd.

Στούς γονεῖς μου,

Κατερίνα καί Δημήτρη.

INTRODUCTION

The continuous search for a better understanding of the nature of the strong force and the underlying hadronic structure has led physicists to postulate quarks as the fundamental constituents of the hadronic matter[1] and Quantum Chromodynamics (QCD) as the suitable Field Theory that describes their interactions (Chapt. I, Sect. 3). In the physical picture that emerges the strong forces between the quarks are mediated by massless vector bosons - the so-called gluons[2] - which posses the remarkable property of interacting also directly among themselves. This property stems from the fact that QCD is a Yang-Mills theory; theories of this type are the only ones that are renormalizable and at the same time can describe self-interacting vector particles. It is true that much of the development of QCD is due to the perfection, in the 40's, of the most (up to now) accurate theory of Nature, Quantum Electrodynamics (QED) (see Chapt. I, Sec. 1). However, the self interaction property of the gluons (Figs. 1,2) is in striking contrast with that of the mediators of the electromagnetic force in QED, the photons; these can only self-interact indirectly (via electron loops, see Fig. 3).

This self-interaction of the gluons results into a decrease of the effective quark-gluon coupling (g_s), at large energy and momentum transfers. This important property is called Asymptotic Freedom. Apparently, asymptotic freedom

makes possible a perturbation expansion at sufficiently high energies and momentum transfers.

These are the basic ideas behind the approach of perturbative QCD, which had a number of important successes in the past few years. These ideas and certain of these successes will be discussed in some detail in the subsequent sections.

The above outline indicates the significance of gluon in the whole QCD approach. It is then of outmost importance to consider and study physical processes in which the presence of gluons is directly manifest. Such a process is precisely the production of direct photons at large transverse momentum (p_T) in hadron-hadron collisions. Perturbative QCD predicts that, because of the subprocesses[3)-(7)]

$$q + g \rightarrow q + \gamma \; ; \; q + \bar{q} \rightarrow g + \gamma$$

there should be significant yields of direct γ's at large p_T. Clearly these subprocesses are made possible only because of the presence of gluons (g). Experimental verification of the theoretical predictions concerning these yields constitutes an essential test of perturbative QCD.

Even without gluons and QCD some direct photons (in hadronic collisions) will be present at large p_T. This follows by straightforward application of the Vector Dominance Model (VDM) (see Chapt. II, Sect. 4). However, the point is (see also Chapt. III, Sect. 3), that perturbative QCD

predicts direct γ yields exceeding at least one order of magnitude those of VDM.

In Chapt. I we explain to some extent the basic properties of QCD, by comparing this theory with its predecessors (QED and Weak Interactions theories). We mainly discuss the predictions related to the Asymptotic Freedom property of QCD and the "survival" of Feynman's parton model when QCD corrections are switched on.

In Chapt. II we calculate in detail the one-particle inclusive cross-section for the production of real photons in p-p collisions and compare with available data. We carry calculations for centre of mass energies $\sqrt{s}$=31, 45, 53, 63 GeV for a large p_T range: $2 \lesssim p_T \lesssim 12$ GeV. In p-p collisions we take into account the correction due to the quark Bremsstrahlung of photons. Then some predictions for photon production in $\pi^- - p$ and $\bar{p}$-p collisions are given. Confirmation of these predictions in future experiments will provide more evidence in favour of the Quantum Chromodynamic picture of the strong interactions.

Finally and in order to extract the maximum information possible from experiments involving real photons, we take advantage of the simplicity of the formalism and try to isolate the so far unknown gluon fragmentation function (to a pion). This is done in Chapter IV. A summary of our work and conclusions as well as a discussion of possible corrections are presented in Chapter V.

CHAPTER I

THEORETICAL BACKGROUND

1.1 Field theories

Quantum Electrodynamics[1] (QED) is an example of a successful field theory. The Lagrangian of QED read

$$\mathcal{L}_{QED} = -\frac{1}{4} F_{\mu\nu}(x) F^{\mu\nu}(x) + i\psi(x)\gamma^{\mu}\partial_{\mu}\psi(x) - m\bar{\psi}(x)\psi(x) - e\bar{\psi}(x)\gamma^{\mu}\psi(x)A_{\mu}(x) \qquad (1.1a)$$

where

$$F_{\mu\nu}(x) = \partial_{\mu}A_{\nu}(x) - \partial_{\nu}A_{\mu}(x) \qquad (1.1b)$$

is the electromagnetic field tensor and $A_{\mu}(x)$ the vector potential describing the photon field. The first term in (1.1a) describes free radiation. The second and third terms are associated to free matter, spin 1/2 objects of mass m. The last term is the interaction between matter and radiation, where e denotes the electric charge of the matter field ($e^2/4\pi = \alpha_{e.m}$, is the fine structure constant $\hbar = c = 1$).

Quantization can be carried out according to general techniques[1]. The theory that emerges is a relativistic quantum field theory with a well defined perturbation expansion parameter ($\alpha_{e.m}$) and with a remarkable quantitative success. This success lies on the empirical fact that there exist objects in Nature carrying charge, the leptons

(electrons, muons) whose dominant interaction is electromagnetic.

Observables have been confronted with perturbative approximations to the equations of motion of QED, to the remarkable accuracy of a few parts per million.

Another example of a successful field theory is the unified theory of electromagnetic and Weak Interactions (the W-S-GIM model)[2],[3] which describes the interaction of quarks and leptons. The Lagrangian of the theory is rather long[4]. Two basic interactions in Nature are unified in a Yang-Mills[5] gauge theory, with the intermediate vector bosons $W^{\pm}$, Z_o and photons as the gauge bosons. The dissimilarity between weak and electromagnetic interactions is attributed to a spontaneous breakdown of the gauge symmetry[6]. Quantization[7] as well as renormalization problems[8] have been successfully solved and calculations of higher order loop corrections can be safely carried out. In this particular theory, technically speaking, the generators of the weak group[4] are flavour charges with the "exotic" names: up, down, strange, charm, bottom etc., characterizing thus the dynamics as Flavourdynamics. The observed hadrons are members of irreducible represenations of flavour-SU(N) obtained from tensor products of the constituent quarks: $q\bar{q}$ for Mesons; qqq for Baryons. One of the great successes of the theory was the detection at CERN of the weak neutral currents.

After the successful advent of QED and of the W-S-GIM

theories, physicists learned that various interactions among elementary particles are mediated by the exchange of vector mesons, the already mentioned gauge bosons. This is a technical lesson of great heuristic value and has been applied with much success in the construction of a theory of strong interactions (SI).

The property of "Asymptotic Freedom" mentioned in the Introduction makes Yang-Mills theories the best candidates for a theory of SI. However, in such an approach one faces the difficulty of what to choose as the Strong gauge group. The answer came from experiment and phenomenology: one must introduce one more degree of freedom for the quarks the colour degree of freedom.

1.2 Colour

The phenomenological reasons for introducing colour are the following:

(i) Quark Statistics[9],[10]

The scheme that emerges is as follows: Baryons are quark triplets and each quark appears with three different colours: yellow, blue and red. The baryon wave function is then symmetric in space and spin, but antisymmetric in colour. Furthermore, all observables in Nature are assumed to be colour singlets. This is the so called confinement hypothesis. Mathematically we have:

$$|qq'q''\rangle \longrightarrow \frac{1}{\sqrt{6}} \epsilon^{\alpha\beta\gamma} |q_\alpha q'_\beta q''_\gamma\rangle \qquad (1.2)$$

where q,q',q'' are the various quark flavours, α, β, γ, are the colour indices, and $\epsilon^{\alpha\beta\gamma}$ is the fully antisymmetric three index tensor. Similarly for mesons:

$$|qq'\rangle \longrightarrow \frac{1}{\sqrt{3}} |q^\alpha q'_\alpha\rangle \qquad (1.3)$$

The three colours are associated with the fundamental representation $\underline{3}$ of the gauge group $SU(3)_c$ colour. Colour symmetry is assumed to be an exact one in contrast with the flavour symmetry which does not correspond to exact conservation laws. Also $SU(3)_c$ symmetry is a local symmetry, and this fact is reflected in the use of Yang-Mills fields by the Lagrangian of the theory (see Sec. 3).

(ii) <u>The $\pi^0 \to 2\gamma$ decay</u>.

Using PCAC[11] one can relate this decay to the coupling of the axial vector current to two photons. <u>In the soft pion limit</u>[11),(12)] this coupling is given by a short distance term[(f_1)] coming from the V.V.A triangle diagram (Fig. 4). Then the π^0 width is given by:

$$\Gamma(\pi^0 \to 2\gamma) = 7.87 \left(\frac{N}{3}\right)^2 eV \qquad (1.4)$$

A theory with 3 colours predicts $\Gamma(\pi^0 \to 2\gamma) = 7.87$ eV which is in excellent agreement with the experimental value of 7.95 eV.

(iii) The ratio of the cross-sections:

$$R = \frac{\sigma(e^+e^- \rightarrow \text{hadrons})}{\sigma(e^+e^- \rightarrow \mu^+\mu^-)} \qquad (1.5)$$

is well predicted by a 3-colour theory, at least at large c.m. energy. The fact that $SU(3)_c$ symmetry is an exact one leads us to the following possible picture for the Strong Interactions: The colour forces (strong forces) between quarks are mediated by massless vector bosons - the so-called gluons - much the same as photons mediate the electromagnetic forces between charged leptons. The gluons are the gauge fields belonging to the adjoint representation of $SU(3)_c$ and there are eight of them, one associated with each generator of the group $SU(3)_c$. In the case of QED, the photon field is the gauge field associated with the generator of the abelian group U(1): the group of gauge transformations. The crucial difference between QED and QCD is that, because of the non-abelian structure of $SU(3)_c$, the gluons have self-interactions described by a Yang-Mills Lagrangian.

In the next paragraph we will define the Quantum Chromodynamic theory of Strong Interactions and we will trace out some useful QCD properties.

1.3 QCD

The QCD Lagrangian is:[14]

$$\mathcal{L}_{QCD}(x) = -\frac{1}{4} F^{(a)}_{\mu\nu}(x) F_{(a)}^{\mu\nu}(x) + i \sum_{j=1}^{n} \bar{q}^{\alpha}_{j}(x) \gamma^{\mu} (D_{\mu})_{\alpha\beta} q^{\beta}_{j}(x) -$$

$$- \sum_{j=1}^{n} m_j \bar{q}^{\alpha}_{j}(x) q_{\alpha j}(x) + \text{"gauge fixing" term} +$$

$$+ \text{"Fadeev - Popov" term} \qquad (1.9)$$

The theory described by the above Lagrangian is a renormalizable field theory of the SI. The fundamental constituents are spin 1/2 Fermi fields, the quarks [$q^{\alpha}_{j}(x)$] which carry fractional electric charge (see Appendix C) and nonabelian spin 1 gauge fields, the gluons [$A^{(a)}_{\mu}(x)$] which interact with the quarks as well as among themselves.

Explicitly, the various terms in the Lagrangian are:

$$\text{(i)} \quad F^{(a)}_{\mu\nu}(x) = \partial_{\mu} A^{(a)}_{\nu}(x) - \partial_{\nu} A^{(a)}_{\mu} + g f_{abc} A^{(b)}_{\mu}(x) A^{(c)}_{\nu}(x) \qquad (1.10)$$

where:

$F^{(a)}_{\mu\nu}(x)$, a=1,...,8 are the Yang-Mills field strengths.

$A^{(a)}_{\mu}(x)$, are the gluon fields

μ , ν , are space time indices

g , is the QCD coupling constant

f_{abc} , are the structure constants of the SU(3) algebra, given by:

$$[\, T^{(a)}, T^{(b)} \,] = i f_{abc} T^{(c)} \qquad (1.11)$$

where $T^{(a)}$ are the eight generators of the SU(3) algebra.

It is instructive to compare (1.10) with (1.1b). The non-abelian interaction is contained in the second term of (1.10).

(ii) q_j^α, q_j^β are four component Dirac spinors associated with each quark field of colour α and flavour j

(iii) $$(D_\mu)_{\alpha\beta} = \delta_{\alpha\beta}\partial_\mu - ig\sum_{a=1}^{8}\frac{1}{2}\lambda^{(a)}_{\alpha\beta}A^{(a)}_\mu(x) \qquad (1.12)$$

is the covariant derivative acting on the quark colour components with:

$\lambda^{(a)}_{\alpha\beta}$ the eight 3×3 Gell-Mán matrices. We have then:

$$(T^{(a)})_{\alpha\beta} = \frac{1}{2}\lambda^{(a)}_{\alpha\beta} \qquad (1.13a)$$

and for the structure constants,

$$(T^{(a)})_{bc} = -if_{abc} \qquad (1.13b)$$

(iv) The only arbitrary parameters in the theory are the coupling constant g and the quark masses m_j.

(v) The terms "Gauge Fixing" and "Fadeev-Popov" in Eq. (1.9) are results of the covariant quantization of the theory[7],[8] and they are given by:

$$\text{"Gauge fixing"} = -\frac{1}{2\alpha}\partial_\mu A^\mu_{(a)}(x)\,\partial^\nu A^{(a)}_\nu(x) \qquad (1.14)$$

where α is a gauge parameter (not to be confused with the colour indices) and

$$\text{"Fadeev-Popov"} = \partial_\mu \bar{\varphi}_{(a)}(x) \partial^\mu \varphi_{(a)}(x) - g f_{abc} A^{(a)}_\mu(x) \partial^\mu \bar{\varphi}^{(b)}(x) \varphi^{(c)}(x) \tag{1.15}$$

where $\varphi_{(a)}(x)$ is a set of eight massless complex scalar fields which propagate in closed loops only and obey Fermi statistics[4],[15], the so-called "Fadeev-Popov" ghosts.

In QCD, quarks of a fixed flavour and gluons interact via the term:

$$g \sum_a \frac{1}{2} \lambda^{(a)}_{\alpha\beta} \bar{q}^{(a)}_\alpha(x) \gamma^\mu q^{(a)}_\beta(x) A^{(a)}_\mu(x) \tag{1.16}$$

This vertex and the QED analogon are presented graphically in Fig. 5.

The new feature in the QCD Lagrangian as compared to the QED (1.1a), is the presence of fundamental interactions among the gluon fields themselves. As contrasted with QED, where photon-photon (gauge boson) interactions are induced via electron loops only (see Fig. 3), in QCD these self-interactions are due to the presence of the coupling constant g already at the level of the field strengths [see Eq. (1.10)]. Self gluon interactions are of two types:

(a) Those involving 3-gluon fields:

$$-\frac{1}{2} g f_{abc} \left(\partial_\mu A^{(a)}_\nu(x) - \partial_\nu A^{(a)}_\mu(x) \right) A^\mu_{(b)}(x) A^\nu_{(c)}(x) \tag{1.17}$$

represented graphically in Fig. (1).

(b) Those involving 4-gluon fields:

$$-\frac{1}{4}g^2 f_{abc} f_{ade} A^{(b)}_{\mu}(x) A^{(c)}_{\nu}(x) A^{\mu}_{(d)}(x) A^{\nu}_{(e)}(x) \qquad (1.18)$$

represented graphically in Fig. 2.

1.4 "Asymptotic Freedom" and "Infrared Slavery".

In an attempt to understand the short-distance behaviour of QED Gell-Man and Low[16] and independently Stueckelberg and Peterman[17] developed the concept of Renormalization Group Invariance (RG equation). The RG equation together with the operator product expansion (OPE, developed by K.G. Wilson)[18] have been proved to be potential tools for understanding the hadronic interactions at Short Distances.

In QED, the effective charge at short distances becomes larger as a consequence of vacuum polarization (see Fig. 6). Applying RG techniques we find that the coupling constant is given by:

$$\frac{1}{\alpha(Q^2)} \cong \frac{1}{\alpha(m_e^2)} - \frac{1}{3\pi} \log \frac{Q^2}{m_e^2} \qquad (1.19)$$

where Q^2 is the 4-momentum transfer of the virtual cloud and m_e is the renormalized electron mass. The situation in QCD is totally different (Fig. 7). The existence of 3-gluon and 4-gluon couplings that contribute to the QCD vacuum polarization (see Figs. 7(b),7(c)) produce a relative

plus sign in the analogous to (1.19) QCD term, namely[f2]

$$\frac{1}{\alpha_s(Q^2)} \cong \frac{1}{\alpha_s(M^2)} + \frac{33-2f}{12\pi} \log \frac{Q^2}{M^2} \qquad (1.20)$$

where α_s the strong coupling constant[f3], Q^2 as before, M of a few hundres of MeV (usually $\approx$ 500 MeV) and f the number of flavours. This relative sign results in a continuous decrease of the α_s when Q^2 increases; as we mentioned in the Introduction this renders possible a perturbative approach (around α_s) at short distances. Quarks then are almost free from mutual strong interactions, in other words, the short-distance behaviour of the Green's functions of QCD is governed by free field theory (the old quark model of Feynman[19] without gluons). This is the remarkable property of Asymptotic Freedom. It means that corrections to the free field behaviour can be computed perturbatively and the specific theoretical predictions of QCD can thus be tested. However at large distances (much larger than 10^{-14} cm, (the infrared limit) QCD becomes a strong coupling theory.

However one basic question seems to have no answer up to the moment: What is the mechanism (certainly of a non-perturbative nature) that confines colour? Or, otherwise, why quarks and gluons, which appear in the field equations, do not appear in the hadronic spectrum? This is the problem of "Infrared Slavery" or "colour confinement". Together with this difficulty QCD faces some other difficulties as

well as, for example, questions relative to the origin of the quark masses, the flavour and the leptonic quantum numbers. In this thesis we do not attempt to answer any of these questions.

1.5 Deep inelastic scattering in the parton model and in QCD.

One of the most important areas for testing QCD is deep inelastic lepton scattering on nucleon target[20],[21] (Fig.8a). The total cross section is characterized by two variables: The square of the 4-momentum transferred from the lepton to the hadron, $Q^2<0$, and the transferred energy ν. Let us define also x as: $x \equiv -Q^2/2m_H\nu$ where m_H is the mass of the target hadron.

The main experimental fact is that the cross section or more accurately the structure functions (for a definition see Ref. 19), are practically independent of Q^2 and depend only on x. This has been argued by Bjorken[22] on the basis of the Adler sum rule[23]. He proposed that as $Q^2 \to \infty$ and $\nu \to \infty$ (the Bjorken limit), the deep inelastic structure functions scale in x:

$$\nu W_2(\nu, Q^2) \xrightarrow[\text{Bjorken limit}]{} F_2(x) \qquad (1.21)$$

where

$$\int d\nu W_2(\nu, Q^2) = \int \frac{dx}{x} F_2(x) = Q^2\text{-independent} \qquad (1.22)$$

with similar expressions for the other structure functions. At that time scaling seemed to be supported by experiment even at moderate values of Q^2 ($Q^2 \gtrsim 1\,GeV^2$).

Today deviations from the scaling behaviour have been detected[24],[26]. Asymptotic freedom has a bearing on this interesting phenomenon and QCD, as an asymptotically free theory, is expected to predict those scaling deviations. We shall now explain this to some extent.

The scaling behaviour naturally arises in the simple constituent picture of the hadrons formulated by Feynman[19],[27] (Parton model). Partons are assumed to suffer confining interactions which are characterized by a (long) time constant τ_L of order 1/M where M is a typical hadron mass. For large momentum transfers there is another time scale, τ_S, much shorter than τ_L defined as : $\tau_S \sim 1/Q$. These interactions may be treated by an Impulse approximation scheme:[19] The partons are considered as essentially free and "on shell" (i.e. with fixed small mass as $Q^2 \to \infty$) and the full process is assumed to factorize into a convolution of the probability of finding a parton within a hadron with the cross section for the hard process involving the parton.

The general structure of the deep inelastic cross section in the parton model (of one kind of parton for simplicitly) reads schematically:

$$d\sigma_{Hadron}(P,Q) = \int \frac{dx}{x} F(x)\, d\sigma_{parton}(xP,Q) \qquad (1.24)$$

where x is the Bjorken variable. Its physical meaning is clear: x is the fraction of the original hadron momentum P carried by the parton.

To make contact with the coloured quark-gluon theory outlined in the previous section we make the identification of the partons with the quarks and gluons.

Politzer[28] tried to pursue this program by calculating Feynman quark-gluon diagrams to some order in α_s. Let us examine a concrete example. In e-p deep inelastic scattering and to the lowest order in α_s we have the Born term [Fig. 8(a)]; now in QCD there are also gluon corrections (Fig. 8). However, in calculating the corresponding contributions, one encounters infinities that tend to spoil the perturbation expansion.

These are of various types:[29]-[31]

a) "Infrared" singularities; divergencies associated with soft-gluon emission [Figs. 8(b), 8(c)], which are cancelled by divergencies arising from virtual gluon corrections [Figs. (d),(e),(f)].

b) "Mass" singularities; they occur when a quark emits a collinear gluon because the quark can remain on mass shell. This is, in general, a disease of massless charged particles[f4] (Fig. 9). As a result of Politzer's analysis the structure of $d\sigma_{parton}$ of Eq. (1.24) reads as follows:

$$d\sigma_{parton} = \delta\left(\frac{y}{x} - 1\right) + \alpha_s P\left(\frac{y}{x}\right) \log\frac{Q^2}{p^2} + \dots \quad (1.25)$$

where p is the 4-momentum of the constituent and P(y/x) are functions calculable from perturbation theory. Politzer argued[28] that the divergent piece in (1.25) does not really belong to the $d\sigma_{parton}$ but to the structure function F(x).

For the moments of $d\sigma_{parton}$, the following "factorization" of infrared divergencies has been proven to all orders in perturbation theory (for all logs)[30]:

$$d\sigma^{n}_{parton}\left[\alpha_s(M^2), \log\frac{Q^2}{M^2}, \log\frac{p^2}{M^2}\right] = \tag{1.26}$$

$$= d\tilde{\sigma}^{n}_{parton}\left[\alpha_s(M^2), \log\frac{Q^2}{M^2}, 0\right] P^n\left[\alpha_s(M^2), \log\frac{p^2}{M^2}\right]$$

M is an arbitrary mass scale that has been introduced to formally separate long from short distance effects. There are, of course, corrections to Eq. (1.26) of order p^2/Q^2, but we neglect them as $p^2 \to 0, Q^2 \to \infty$. By choosing $M^2 \sim Q^2$ (taking advantage of the renormalization group equation), $d\tilde{\sigma}_{parton}$ essentially becomes the usual parton model cross section, expanded in powers of $\alpha_s(Q^2)$, but where only the infrared finite pieces are retained. Such cross sections are, of course, calculable. The factors P^n combine with the moments of the original parton distribution functions F(x) to give effective Q^2-dependent parton distribution functions $F'(x,Q^2)$. These functions are process independent and thus universal. This fact is summarized in the formula:

$$d\sigma_{Hadron}(Q^2) = \int \frac{dx}{x} F(x,Q^2)\, d\tilde{\sigma}_{parton}\left[\alpha_s(Q^2)\right] \tag{1.27}$$

The Q^2-dependence of $F(x,Q^2)$ certainly leads to violation of Bjorken scaling, [see Eq. (1.22)].

In this way the parton model scheme miraculously survives. However now the structure functions, or equivalently the parton distributions, are Q^2-dependent. This Q^2-dependence is calculable more easily by solving the Altarelli-Parisi equations which will be the subject of our next section.

1.6. The Altarelli-Parisi equations. Intuitive approach to the violations of scaling.

Altarelli and Parisi studied[32] for the first time the Q^2 evolution of the parton distribution functions to lowest order in α_s. The fact that both quark and gluon carry colour charge, results in two coupled first order integrodifferential equations which govern the Q^2 evolution of the distribution functions. Let us introduce $g(x,t)$ as the density of gluons (summed over colours) inside the proton, in the infinite momentum frame. Then the Altarelli-Parisi equations read:

$$\frac{dq^i(x,t)}{dt} = \frac{\alpha_s(t)}{2\pi}\int_x^1 \frac{dy}{y}\left[\sum_{j=1}^{2f} q^j(y,t) P_{qq}^{ij}\left(\frac{x}{y}\right) + g(y,t) P_{qg}^{i}\left(\frac{x}{y}\right)\right] \tag{1.28}$$

$$\frac{dg(x,t)}{dt} = \frac{\alpha_s(t)}{2\pi}\int_x^1 \frac{dy}{y}\left[\sum_{i=1}^{2f} q^i(y,t) P_{gq}^{i}\left(\frac{x}{y}\right) + g(y,t) P_{gg}\left(\frac{x}{y}\right)\right] \tag{1.29}$$

t is defined by: $t=\log Q^2/Q_o^2$ where Q_o^2 is a suitable normalization point. The indices i and j run over quarks and antiquarks of all flavours. The number of quarks as seen by the current probe changes by two mechanisms: a quark originally at higher energy, may loose momentum by radiating a gluon, or, a gluon inside the proton may produce a quark-antiquark pair. Similarly the number of gluons changes because a quark may radiate a gluon or a gluon may split into two gluons. The functions P_{qq}, P_{qg}, P_{gq}, P_{gg} (the so called Splitting, or Altarelli-Parisi functions) are completely calculable from perturbative QCD and are indicated in Fig. 10 together with the diagrams used for their calculation. The components of the Anomalous dimension matrix γ^n (which govern the Q^2-dependence of the structure functions) are related to the splitting functions by relations of the form:

$$\int_0^1 dz\, z^{n-1} P_{qq}(z) \propto \gamma_{qq}^n \qquad (1.30)$$

To order α_s, equations like Eqns. (1.28), (1.29) exist also for fragmentation functions and for polarized quark and gluon distributions[40],[41].

In phenomenological applications one uses directly the quark and gluon Q^2-dependent distribution functions. [See Chapter II, Eq. (2.2)] To illustrate the usual approach of determining the Q^2-dependence we shall restrict ourselves to the valence part of $F_2(x,Q^2)$. Defining the moments $M_n(Q^2)$ of $F_2(x,Q^2)$ by:[33]

$$M_n(Q^2) = \int_0^1 dx\, x^{n-1} F_2(x,Q^2) \qquad (1.31)$$

one finds[32]:

$$M_n(Q^2) = M_n(Q_0^2)\, e^{-\frac{\gamma^n}{2\beta_0}(t-t_0)} \qquad \alpha)$$

where

$$t = \log\log\frac{Q^2}{\Lambda^2} \quad , \quad \beta_0 = 11 - \frac{2}{3}f \qquad \beta)$$

$\Lambda \approx 0.5$ GeV and f is the number of flavours. These equations are contained, of course, in the Altarelli-Parisi equations [Eqn. (1.28)] as a special case (valence part only). Thus, once the moments of the structure functions are specified at a reference value $Q^2 = Q_0^2$, then their Q^2 evolution is uniquely determined by QCD in the leading logarithm approximation. However, in applications we use the hard scattering formula [Eq. (2.2)] which involves direct use of the structure functions. Thus we need to: (i) Invert the moments in Eq. (1.31) and (ii), parametrize the $F(x,Q^2)$s by relatively simple to handle and, of course, accurate formulas. At present we possess parametrizations for quark-valence, distributions in the leading[34],[35] as well as in the next to leading order[36] and for sea and gluon distributions only in the leading order.

One particularly simple way to parametrize distribution and fragmentation functions is that proposed by Parisi and Sourlas[37] and further developed in Ref. 38. The distribution functions are parametrized as:

$$F(x,Q^2) = x^{\beta}(1-x)^{\alpha(Q^2)} \sum_{k=0}^{N} C_k x^k \qquad (1.32)$$

k is a number of Jacobi polynomials which we use to approximate $F(x,Q^2)$ in the interval $0<x<1$. C_k are "constants" of the parametrization[39]. The idea behind this parametrization is the following: The singular parts of $F(x,Q^2)$, for $x\to 1$ and $x\to 0$, are factored out in Eq. (1.32) in the form $x^{\beta}(1-x)^{\alpha}$; thus the remaining polynomials $\sum_{k=0}^{N} C_k x^k$ converge fast enough to permit a simple and accurate parametrization of the structure functions.

CHAPTER II

REAL PHOTON PRODUCTION IN HADRON-HADRON COLLISIONS IN QCD.

2.1 Hadron-hadron collisions and the production of hadrons at large p_T.

Hadron-hadron scattering differs from lepton-hadron since now both particles are composite. The carrier of the interaction is not a virtual photon or weak boson but a virtual quark or gluon, or a system of quarks and gluons (diquarks etc.). The fact that now the gluon participates directly in the hard scattering subprocesser introduces one major phenomenological difficulty: the gluon distribution function, which is not probed directly in deep-inelastic scattering, and thus it cannot be measured experimentally. Nevertheless, large p_T physics has contributed much in shaping our understanding of the nature of the perturbative QCD regime, so it is worthwhile to examine it closely.

The first application of the parton model to large-p_T hadron production was carried out by Berman, Bjorken and Kogut[1],[2] (BBK model); this is based on a generalization of Feynman's parton model. Here all large-p_T hadron production arises from the quark-quark subprocess $qq \to qq$, which proceeds by exchange of a vector meson (gluon).

If the produced hadron emerges at $\theta_{c.m} = 90°$ relative to the beam-target axis (c.m of the initial hadrons), then

the BBK model predicts that the inclusive cross-section exhibits scaling in x_T:

$$E\frac{d\sigma}{d^3p}(h_1+h_2 \longrightarrow h + X) = s^{-2} f(x_T) = p_T^{-4} g(x_T) \qquad (2.1)$$

where $x_T = 2p_T/\sqrt{s}$, p_T is the transverse momentum of the produced hadron, $\sqrt{s}$ is the total c.m. energy ($\approx 2E_{inc}$), and $(E,\vec{p})$ is the 4-momentum of the produced hadron. Unfortunately, confrontations of (2.1) with data[3] strongly discouraged simple interpretations based on point like parton interactions. The reason was that the experimental value for the p_T exponent in (2.1) turned out to be ≈ -8. This important finding brought into fashion the Constituent Interchange Model (CIM model)[4] which predicts scaling and p_T^{-8} for the one particle inclusive (1PI) cross-section. In this particular model quark-meson (q-M) scattering dominates. CIM makes explicit use of the dimensional counting rules[5],[6] which predict a p_T^{-8} behaviour for the 1PI cross-section and thus fits the data at $p_T \lesssim 7$ GeV. However, insufficient explanation for the absence of q-q subprocesses as well as the dissimilarity observed between the trigger jet and the away-side jet favoured quark-quark scattering over quark-Meson one[7]-[11].

In the summer of 1976, experiments in deep inelastic lepton-nucleon scattering confirmed earlier theoretical

expectations[12],[3] by providing evidence for violations of scaling[14]. Those early theoretical calculations were done in the context of QCD, which predicts logarithmic deviations from scaling (at least at high energies) and are of great importance in large p_T physics; the structure functions that explicitly enter the hard scattering formula (see below) are now slowly varying at large momentum transfers. This important experimental finding together with the fact that scaling violations arise naturally in QCD marked the adoption of QCD as the leading candidate for a theory of Strong Interactions.

In the beginning scale violations in large-p_T hadron production were introduced by taking into account QCD requirements in an approximate way[15]-[18]. Later on parton distributions in a tractable form satisfying more exact QCD requirements became available[19],[20].

Furthermore, QCD requires that, in addition to qq→qq, subprocesses like qg→qg, gg→gg etc, contribute in large-p_T hadron production. These contributions were first calculated by Combridge, Kripfganz and Ranft[21] and by Cutler and Sivers[22] and found to be very significant.[23]

Finally, several reasons pointed out the necessity of introducing some "primordial" transverse momentum k_T to the initial partons. A main reason was the experimental information on the p_T distribution of dileptons produced in hadron-hadron collisions (see also Chapter III, Sec. 3.2).

With all these ingredients taken into account successful phenomenological analyses of data on $p+p \to \pi + X$ at p_T ranging up to ~16 GeV were carried out[24]-[25]. It should also be stressed that more recent data in the large p_T region ($p_T \gtrsim 7$ GeV) support now a behaviour $\sim p_T^{-6} g(x_T)$ which is much in favour of the QCD approach[26]-[28].

In the Introduction we explained to some extent how scale violations are introduced into the structure functions by factorization of mass singularities. By taking advantage of factorization[29] we can immediately write down the expression for the inclusive cross section of large-p_T production of a hadron[30] (see Fig. 11)

$$E\frac{d\sigma}{d^3p}(h_1+h_2\to h+X) =$$

$$= \sum_{\substack{\text{quarks}\\ \text{gluons}}} \int_0^1 dx_1 dx_2 \frac{dx_3}{x_3^2} F_{q_1/h_1}(x_1,Q^2)\, F_{q_2/h_2}(x_2,Q^2)\, D_{h/q_3}(x_3,Q^2) \times$$

$$\times \delta(\hat{s}+\hat{t}+\hat{u}) \frac{\hat{s}}{\pi} \frac{d\sigma^{(Born)}}{d\hat{t}}(q_1+q_2\to q_3+q_4)\Big|_{\substack{\hat{s}=x_1x_2s\\ \hat{t}=x_1/x_3\,t\\ \hat{u}=x_2/x_3\,u}} \qquad (2.2)$$

The various terms are:

$\frac{d\sigma^{(Born)}}{d\hat{t}}$: The Born term contribution to the elastic cross section for qq, qg, gg scattering, calculated using the running coupling constant $\alpha_s(Q^2)$. Q^2 is the "large" variable of the subprocess (proportional to p_T^2).

$F_{q_1;q_2/h_1;h_2}(x_{q_1;q_2}, Q^2)$: determine the probabilities the partons $q_1;q_2$ to emerge from hadrons $h_1;h_2$, with fraction $x_{q_1;q_2}$ of the linear momentum of the hadron at the value Q^2 (distribution functions).

$D_{h/q_3}(x_3, Q^2)$: determines the probability for the parton q_3 to fragment to hadron h, carrying away a fraction x_3 of the momentum along the direction of the parton q_3 at the value Q^2 (fragmentation function.)

$\hat{s}, \hat{t}, \hat{u}$: are the Mandelstam variables for the subprocesses.

The fragmentation function $D_{h/q}(x_3, Q^2)$ can be calculated from $e^+e^- \to h X$ and is related to the distribution function $F_{q/h}$ (at least to the lowest order) by the Gribov-Lipatov reciprocity relations[31]. It is to be noted that the existence of the fragmentation function $D_{h/q}$, which behaves as $(1-x_3)^m$, suppresses significantly the cross section at large x_3 (or large p_T). An illustrative example is the hadronic production of neutral pions ($h_1 + h_2 \to \pi^0 + X$); this involves a fragmentation function $D_{\pi^0/q}$ or $D_{\pi^0/g}$ (for $q \to \pi^0$ or $g \to \pi^0$), which suppresses the cross section as p_T increases.

We turn now our attention to large p_T direct photons.

2.2 Direct photon production to $O(\alpha_s)$

In perturbative QCD, and to the lowest non trivial order in both coupling constants (α_s and $\alpha_{e.m}$), large p_T photons can be produced by the Feynman diagrams (a) and (b) of Fig. 13, together with their crossed ones. These diagrams are the so-called "Compton" ($qg \to q\gamma$) and "Annihilation" diagrams ($\bar{q}q \to \gamma g$).

Compton scattering is expected to dominate in proton-proton collisions since the gluon distribution in the proton is stronger than the antiquark distribution which enters the "Annihilation" contribution (for the relative strengths of these distributions, see Chapt. III, Sec. 3.3 and Ref. 47). To this order, the same diagrams that give real photons generate also some transverse momentum of the virtual photons in the Drell Yan production of lepton pairs of large invariant mass M[32]. The expansion in α_s is still valid because of the large momentum flow in the q-g (or q-$\bar{q}$) diagram which is now sustained by the transverse momentum (p_T) of the produced photon ($\alpha_s(p_T^2)$) instead of the mass M of the lepton pair ($\alpha_s(M^2)$). The Drell-Yan diagram $q\bar{q} \to \gamma^* \to \ell^+\ell^-$, which is the Born term in $\ell^+\ell^-$ production does not produce photons at large p_T.

It has been pointed out by several authors[32]-[34], that QCD might give large direct photon yields through the perturbative diagrams that we mentioned before. A convenient way is to consider the ratio of the cross sections:

$$\frac{\gamma}{\pi^0} = \frac{E d\sigma(h_1+h_2 \to \gamma+X)/d^3p}{E d\sigma(h_1+h_2 \to \pi^0+X)/d^3p} \qquad (2.3)$$

Now photons are electromagnetically coupled to quarks (point-coupling) and their weaker (than the π^0) coupling is compensated by the fact that their production does not involve any fragmentation function. Thus one expects the ratio γ/π^0 to increase with x_T, following the decrease of the fragmentation function of quarks and gluons to a pion (32), (34).

Earlier calculations found rather high direct photon yields without taking into account scale[32),(33] violations. Explicit and consistent use of scale violating quark and gluon distributions somewhat diminishes the rate $h_1 + h_2 \rightarrow \gamma + X$ [35]

In our work we calculate direct photon production in pp, $\bar{p}p$, and $\pi^- p$ collisions with scale violating quark and gluon distributions [including also the photon Bremsstrahlung contribution, see Sect. (2.3)]. In particular for pp collisions we predict a γ/π^0 ratio (for large-p_T and s)

$$\left(\frac{\gamma}{\pi^0}\right)_{QCD} \cong 0.2 \sim 0.3$$

and comparable or even higher ratios (see Chapter III, Sec. 3.3) for $\pi^- p$ and $\bar{p}p$. We believe that verification of these predictions provides a very important test of QCD.

The kinematics for $h_1 + h_2 \rightarrow \gamma + X$ are illustrated in Fig. 12.

Then the Mandelstam variables at the hadronic level are

$$s = (P_1 + P_2)^2 = 2P_1P_2 \qquad (2.4)$$

$$t = (P_1 - p)^2 = -2P_1p \qquad (2.5)$$

$$u = (P_2 - p)^2 = -2P_2p \qquad (2.6)$$

with $p^2=0$, $P_1^2\approx 0$, $P_2^2\approx 0$, where p, P_1, P_2 are the 4-momenta of the real photon, the beam (target) and the target (beam) respectively.

At the constituent level we have:

$$\hat{s} = (x_1P_1 + x_2P_2)^2 = x_1x_2 2P_1P_2 = x_1x_2 s \qquad (2.7)$$

$$\hat{t} = (x_1P_1 - p)^2 = -x_1 2P_1p = x_1 t \qquad (2.8)$$

$$\hat{u} = (x_2P_2 - p)^2 = -x_2 2P_2p = x_2 u \qquad (2.9)$$

The inclusive cross section for the production of real photons can be calculated directly from the QCD Born graphs plus factorization theorem. Here we would like to show how it can be deduced from the expression (2.2). First, the fragmentation function $D_{h/q_3}(x_3, Q^2)$ is replaced by a delta function at $x_3=1$:

$$D_{h/q_3}(x_3, Q^2) \equiv \delta(x_3 - 1) \qquad (2.10)$$

This is the exact mathematical formulation of the fact that the photon has a point-like coupling to the quarks. By introducing (2.10) into (2.2) and performing the x_3-integration we get:

$$\left(E\frac{d\sigma}{d^3p}\right)_{\alpha_s} = \sum_{q_1,q_2}\int_0^1 dx_1\int_0^1 dx_2\, F_{q_1/A}(x_1,Q^2)F_{q_2/B}(x_2,Q^2)\times$$

$$\times\frac{\hat{s}}{\pi}\frac{d\sigma^{(Born)}}{d\hat{t}}(q_1q_2)\,\delta(\hat{s}+\hat{t}+\hat{u}) + A\longleftrightarrow B \qquad (2.11)$$

where $\hat{s},\hat{t}$ and $\hat{u}$ are given by (2.7),(2.8), and (2.9). Using the following property of the delta function:

$$\int dx_2\,\delta[f(x_2)] = \left|\frac{\partial f(x_2)}{\partial x_2}\right|^{-1}_{x_2=a}$$

with $x_2=a$ being the solution of $f(x_2)=0$, we can eliminate one integration in (2.11) thus getting finally:

$$\left(E\frac{d\sigma}{d^3p}\right)_{\alpha_s} = \frac{1}{\pi}\sum_{q_1,q_2}\int_{x_{1,min}}^1 dx_1 F_{q_1/A}(x_1,Q^2)F_{q_2/B}(x_2,Q^2)\times$$

$$\times\frac{x_1x_2s}{(x_1s+u)}\frac{d\sigma}{d\hat{t}}(q_1q_2) + A\longleftrightarrow B \qquad (2.12)$$

Here x_1 and x_2 are given by:

$$x_2 = -\frac{x_1t}{x_1s+u}\quad;\quad x_{1,min} = \frac{-u}{s+t} \qquad (2.13\,a,b)$$

(2.13a) comes from the relation $\hat{s}+\hat{t}+\hat{u}=0$, if translated in terms of the s,t,u invariants. (2.13b) is obtained from

the condition $0 \lesssim x_2 \lesssim 1$. Now if we choose the photon to emerge at $\vartheta_{c.m} = 90^\circ$ (perpendicular to the beam-target axis), then in the c.m. of the colliding hadrons the Madelstam variables become:

$$t = u = -\sqrt{s}\, p \tag{2.14}$$

and

$$\hat{t} = -\frac{1}{2} x_1 x_T s \tag{2.15}$$

$$\hat{u} = -\frac{1}{2} x_2 x_T s \tag{2.16}$$

with $x_T = 2p_T/\sqrt{s}$ and $\sqrt{s}/2$ the c.m energy of the almost massless beam (or target). Inserting (2.14) back into (2.12) we finally get:

$$\left(E\frac{d\sigma}{d^3p}\right)^{\vartheta=90^\circ}_{\alpha_s} = \frac{2}{\pi}\sum_{q_1,q_2}\int_{x_1,min}^{1} dx_1 F_{q_1|A}(x_1,Q^2) F_{q_2|B}(x_2,Q^2) \times$$

$$\times \frac{1}{(2x_1 - x_T)} \frac{d\sigma^{(Born)}_{q_1 q_2}}{d\hat{t}} + A \leftrightarrow B \tag{2.17}$$

where now:

$$x_{1,min} = \frac{x_T}{2 - x_T} \tag{2.18}$$

and

$$x_2 = \frac{x_1 x_T}{2x_1 - x_T} \tag{2.19}$$

In the expression (2.17), we have also redefined the distribution functions according to the scheme:

$$F_{q_1/A}(x_1,Q^2) \rightarrow x_1 F_{q_1/A}(x_1,Q^2) \quad \text{etc} \qquad (2.20)$$

The summation Σ_{q_1,q_2} runs over quark flavours (d,s,u, neglecting charm) and gluon.

The subprocesses differential cross sections have been calculated by a direct application of the Feynman rules for QCD[38]. This calculation can be easily carried out using the Feynman gauge for the gluon: (this is certainly correct when there is only one gluon involved)[36],

$$\sum_{\text{spins}} \epsilon^{\mu} \epsilon^{*\mu'} = -g^{\mu\mu'} \qquad (2.21)$$

where ϵ^{μ} is the gluon polarization vector. For the colour sums the following identity among the colour matrices is needed:

$$\left(T^a\right)_{ij}\left(T^a\right)_{ke} = \frac{1}{2}\left(\delta_{il}\delta_{jk} - \frac{1}{N}\delta_{ij}\delta_{ke}\right) \qquad (2.22)$$

where a is the gluon colour (1,2,...8) and i,j,k,l are the quark colours (1,2,3). N=3 for colour SU(3). The quarks and gluons are considered to be massless. Finally the cross sections are summed over final colours and averaged over the initial ones.

We list here the result of the calculation. For the "Annihilation" ($q\bar{q}\rightarrow\gamma g$) cross section we get:

$$\frac{d\sigma^{q\bar{q}}}{d\hat{t}} = e_q^2 \frac{8\pi\alpha\alpha_s}{9\hat{s}^2}\left(\frac{\hat{t}}{\hat{u}} + \frac{\hat{u}}{\hat{t}}\right) = \frac{d\sigma^{q\bar{q}}}{d\hat{u}} \qquad (2.23)$$

and for the "Compton" ($qg \to q\gamma$):

$$\frac{d\sigma^{qg}}{d\hat{t}} = e_q^2 \frac{\pi\alpha\alpha_s}{3\hat{s}^2}\left(-\frac{\hat{s}}{\hat{u}} - \frac{\hat{u}}{\hat{s}}\right) \neq \frac{d\sigma^{qq}}{d\hat{u}} \qquad (2.24)$$

In these formulas the quark charge e_q is given in units of the electron charge, $\alpha_{e.m}$ is the electromagnetic coupling constant (unless otherwise specified) and $\alpha_s(Q^2)$ is the QCD running coupling constant for four flavours:

$$\alpha_s(Q^2) = \frac{12\pi}{25 \log\left(\frac{Q^2}{\Lambda^2}\right)} \qquad (2.25)$$

$\Lambda^{(f_s)}$ is the strong interaction scale ≈ 0.5 GeV. This value has been found by the authors of Ref. (37) by fitting the asymptotic-freedom formulas (beyond the leading approximation) to the moments of F_3. The data they used were those of the BEBC group[38] (for another set of data see Ref. 39).

We have now listed all the ingredients to proceed in the calculation of real photon production to (α_s). Details from the structure functions that enter (2.17) as well as discussion of the kinematics for the k_T effects will be given in Chapter III.

2.3. The Bremsstrahlung contribution to direct photon production.

The QCD radiative corrections to the Drell-Yan formula ($q\bar{q} \to \gamma^* \to$ lepton pair), to $O(\alpha_s)$, are the "Compton" [Fig. 13(a)] and "Annihilation" [Fig. 13(b)] subprocesses. Then the

"Bremsstrahlung" ($qq \to qq\gamma$) diagrams [Fig. 13(c)] contributes an $\mathcal{O}(\alpha_s^2)$ correction. However, it involves quark valence distributions which are stronger than the antiquark and gluon distributions that enter the Drell-Yan formula as well as the "Annihilation" and the "Compton" cross section. Thus in proton-proton collisions, the apparent supression of this subprocess by powers of α_s can be effectively compensated, in certain kinematical regions, by the relative strength of the quark distribution inside a proton, resulting thus in a sizeable Bremsstrahlung cross section. This is indeed the case when one approaches the kinematic boundary of the reaction $p+p \to \ell^+\ell^- X$ which corresponds to dilepton mass $M \to \sqrt{S}$ [40]-[42].

This particular $\mathcal{O}(\alpha_s^2)$ contribution, can be even more significant in the case where the $\ell^+\ell^-$ -pairs are produced with large transverse momenta, obviously due to the absence of the $q\bar{q} \to \gamma^* \to \ell^+\ell^-$ Born term. Again this is found to be the case at large lepton pair p_T [43],[44].

But now, as we have discussed in Sect. 2.2, the same QCD diagrams that contribute to the transverse momentum of the lepton pairs, give also real photons at large p_T. Thus we may anticipate that the Bremsstrahlung diagrams [Fig. 13(c_1), 13(c_2)], give a nonnegligible contribution to direct γ production in p-p collisions, as well.

This contribution has been recently calculated in detail. [45]-[47]. The dominant parts arise from two characteristic

kinematic configurations[48]

(i) The intermediate gluon almost collinear with one of the scattered quarks [Fig. 13(c_1)].

(ii) The emitted photon almost collinear with one of the final quarks [Fig. 13(c_2)].

We shall discuss each configuration separately.

The calculation of the contribution from the configuration (i) is very similar to that of the $O(\alpha_s^2)$ contribution to lepton-pair production at large p_T[43],[44]. First, this contribution introduces a singular term proportional to $\log(Q^2/\mu^2)$ where μ is some regularization mass. This "mass singularity" (see Introduction) is absorbed, by well-known procedures, into the gluon distribution function, thus implementing (to $O(\alpha_s)$) the Q^2 dependence of $F_{g/h}(x,Q^2)$. However we are also left with a finite correction term. The magnitude of this correction term depends, to some extent, on the definition of the gluon density inside the quark[43]-[48] which is of the general form:

$$G_{g/q}(x,Q^2) = \frac{\alpha_s}{2\pi}\left[P_{gq}(x)\log\frac{Q^2}{-p_1^2} + u_{gq}(x)\right] \qquad (2.26)$$

Here P_{gq} is a probability function[51] (see Fig. 10).

$$P_{gq}(x) = C_F\frac{1+(1-x)^2}{x} \qquad (2.27)$$

$C_F = 4/3$ for colour SU(3). To specify the function $u_{gq}(x)$ some convention is necessary. Following Ref. 48 we consider

the longitudinal structure function $F_L(x,Q^2)$ of deep inelastic scattering, we calculate the $O(\alpha_s^2)$ correction due to the subprocess $q+\gamma^* \to q+q+\bar{q}$ (γ^*, the deep inelastic virtual photon) and specify $u_{gq}(x)$ by comparing to this correction[46]. We find:

$$u_{gq}(x) \simeq -P_{gq}(x)\left(2\log x + 2 - \frac{1}{x}\right) - C_F\frac{2-x}{x} \qquad (2.28)$$

Thus the gluon density inside a quark, Eq. (2.26), is fully specified.

To give the correction term arising from the configuration (i) it is convenient to introduce the covariant variables ξ and η defined as follows:

$$\xi = \frac{2P_1P}{S} \quad , \quad \eta = \frac{2P_2P}{S} \qquad (2.29a)$$

where P_1, P_2 are the 4-momenta of the initial quarks and p is the 4-momentum of the photon (Fig. 14). We also express the 4-momentum k of the gluon in terms of Sudakov variables α, β, ℓ[43]:

$$K_1 \simeq \alpha P_1 - \beta P_2 - \ell \qquad (2.29b)$$

Then, after carrying the integrations with respect to ℓ and β and after absorption of the mass singularity we obtain the correction term:

$$\frac{d\sigma^{(i)}}{d^4Q}_{corr}(S,\xi,\eta;\alpha_s) = \frac{2\pi\alpha_{em}e_q^2}{3S^2}\left(\frac{\alpha_s}{\pi}\right)\int\frac{d\alpha}{\alpha}\,\delta\left(1-\xi-\frac{\eta}{\alpha}\right)\frac{K(\alpha;\xi,\eta)}{\alpha} \qquad (2.30a)$$

where

$$K(\alpha;\xi,\eta) \simeq \frac{1}{2\pi}\left\{ P_{gq}(\alpha)\log\frac{\beta_m Q^2}{\alpha s} - u_{gq}(\alpha) - C_F\frac{2-\alpha}{\alpha}\right\} \times$$

$$\times\left(\frac{\alpha}{\eta}+1-\xi\right) \qquad (2.30b)$$

In (2.30) the quantity $\frac{\alpha}{\eta}+1-\xi$ is proportional to the squared amplitude for $qg\to q\gamma$ expressed as a mixture of covariant and Sudakov variables. The region of integration in (2.30a) is specified from the requirement $k_{10}-k_{20}\geq 0$ (see Fig. 14), where k_{10}, k_{20} are the time components of the 4-momenta k_1, k_2. This requirement implies:

$$1+\alpha-\beta-\xi-\eta \geq 0 \qquad (2.31)$$

In addition to (2.31) we have also to take into account the restriction $0\leq\alpha,\beta\leq 1$[43]. Then $\beta_{max}=1+\alpha-\xi-\eta$. Furthermore for a photon at $\vartheta_{c.m}=90^\circ$ we get[47]:

$$\xi = \eta = \frac{x_T}{2}, \quad \beta_{max}-\alpha = 1-x_T \qquad (2.32)$$

where as in Sect. 2.2, $x_T=2p_T/\sqrt{s}$ and p_T is the transverse momentum of the photon.

We turn now to the contribution of the kinematic configuration (ii) [γ almost parallel to a final quark, Fig. 13(c_2)]. The contribution of this to the cross section for

$q+q\to q+q+\gamma$ is:

$$\frac{d\sigma^{(ii)}}{d^4Q} \simeq \frac{2\pi\alpha_{e.m}}{3\hat{s}^2} e_q^2 \left(\frac{\alpha_s}{\pi}\right)^2 \int \frac{d\alpha}{\alpha} \delta\left(\alpha - \frac{\eta}{x_T}\right) P_{\gamma q}\left(\frac{\eta}{\alpha}\right) \times$$

$$\times \log \frac{s(\beta_{max}-\alpha)}{\mu^2} \left|M(\alpha)\right|^2_{qq\to qq} \qquad (2.33)$$

with

$$\eta = \alpha x_T \,, \quad P_{\gamma q}(x_T) = \frac{1+(1-x_T)^2}{x_T} \qquad (2.34)$$

and

$$\left|M(\alpha)\right|^2_{qq\to qq} = C_F \frac{1+(1-\alpha)^2}{\alpha^2} \qquad (2.35)$$

$M_{qq\to qq}$ being proportional to the q-q elastic scattering amplitude (Fig. 15).

In Eq. (2.33) the term $\sim P_{\gamma q} \log s/\mu^2$ is the leading term of the fragmentation function of a quark to a photon; notice that it introduces an s-dependence (or a $Q^2 \sim p_T^2$ -dependence). This fragmentation function to the leading order in α_s is given by:

$$D_{\gamma/q}(x,s) = \frac{\alpha_{e.m}}{2\pi} e_q^2 P_{\gamma q}(x) \left[\log \frac{s}{\mu^2} + u_{\gamma q}(x)\right] \qquad (2.36)$$

The function $u_{\gamma q}(x)$ can be specified by calculating the cross section of $e^+e^- \to \gamma + X$ [45] (see Fig. 16).

Finally:

$$u_{\gamma q}(x) = \log(1-x) + \frac{3}{2} \qquad (2.37)$$

We can now easily recognise the term log(1-x) in Eq. (2.33), in the form $\log(\beta_{max}-\alpha)$, if we take also into account Eq. (2.34) and Eq. (2.31).

In our calculations we replace $\mu^2 \to \Lambda_e^2$ and use $\Lambda_e = 0.5$ GeV. (see also Ref. 45). In principle, Λ_e should be determined by fitting data on $e^+e^- \to \gamma + X$ with the form (2.36). Unfortunately, such data are not yet available (May 1980).

The complete correction term from $qq \to qq\gamma$ arising from both configurations (i) and (ii) is:

$$\frac{d\sigma}{d^4Q} \simeq \frac{d\sigma^{(i)}}{d^4Q}_{corr} + \frac{d\sigma^{(ii)}}{d^4Q}$$

To obtain the Bremsstrahlung correction to the physical process $A+B \to \gamma + X$ we convolute $d\sigma/d^4Q$ with the Q^2-dependent quark distribution functions:

$$\left(E\frac{d\sigma}{d^3p}\right)^{(Brems)} = \sum_{q_1 q_2} \int \frac{dx_1 dx_2}{x_1 x_2} F_{q_1/A}(x_1, Q^2) F_{q_2/B}(x_2, Q^2) \left(\frac{d\sigma}{d^4Q}\right)^{q_1 q_2 \to q_1 q_2 \gamma} \qquad (2.38)$$

A final remark must be made for the further use of the parton distributions that enter Eq. (2.38): Even with our well defined prescription for obtaining the non-leading finite term, our numerical estimates are at best approximate. For a consistent analysis, the parton distributions should be determined from deep inelastic scattering data using the next to leading order formulae[37),(51),(52)]. However, even for valence quarks, the parton distributions are presently only leading logarithm estimates. Anyway, a bigger uncertainty is introduced by the unknown gluon

distribution function (see Chapter III, Sect. 3.3).

We turn now our attention to some other contributions, which are not of the conventional QCD type.

2.4 Other contributions. Vector mesons and CIM.

(i) Vector mesons.

According to the Vector Dominance model (VDM) there is a direct coupling of the various neutral vector mesons V and the photon (see Fig. 17). In our discussion we shall consider only the "light" vector mesons, ρ, ω and Φ.

For the experimental ratio (γ/π^0), VDM predicts:

$$\left(\frac{\gamma}{\pi^0}\right)_{VDM} \cong \frac{\alpha_{e.m}}{4} \sum_V \left(\frac{V}{\pi^0}\right)\left(\frac{\gamma_V^2}{4\pi}\right)^{-1} \qquad (2.39)$$

$\gamma_V^2/4\pi$ are the various couplings for the vector mesons: $\gamma_\omega^2/4\pi = 5.4$, $\gamma_\Phi^2/4\pi = 4.7$, $\gamma_\rho^2/4\pi = 0.64$ [53]. The ratios (V/π^0) are defined as in Eq. (2.3) and, for $p_T \approx 4$, are taken to be: [54]-[58], [f6]

$$\frac{\omega}{\pi^0} \cong 0.4 \quad , \quad \frac{\Phi}{\pi^0} \cong 0.04 \quad , \quad \frac{\rho}{\pi^0} \cong 0.8$$

A direct application of Eq (2.39), using the above data gives:

$$\left(\frac{\gamma}{\pi^0}\right)_{VDM} \times 100 \cong 0.24\% \qquad (2.40)$$

This is indeed very small, much smaller than that predicted

by QCD (see Refs.[32]-[34] and Chapt. III). In subsequent comparisons of our theoretical predictions with experiment we shall neglect the VDM contribution.

(ii) The Constituent Interchange Model (CIM)

The CIM[60]-[62] predicts direct photon yields at large p_T, through the following basic mechanisms:

a) Prompt processes: $qM \to q'\gamma$, $q\bar{q} \to M\gamma$, where M stands for meson,

b) Final Bremsstrahlung processes: $qM \to q'g\,(q' \to \gamma)$, $qM \to q'M\,(q' \to \gamma)$

Explicit application of the dimensional counting rules[59]-[62], together with a proper normalization (see below), shows that in the CIM dominant source of high p_T photons is the prompt process $qM \to q'\gamma$ shown in Fig. 18. For this particular subprocess, CIM predicts an inclusive cross section of the form:

$$E\frac{d\sigma}{d^3p}(pp \to \gamma X) \propto p_T^{-6} f(x_T) \qquad (2.41)$$

and a $(\gamma/\pi^0_{exp}) \sim 10\%$ at $p_T = 3.7$ GeV.

In this estimate, the CIM normalization constant, usually denoted by a_M[62], is taken to be $a_M \approx 2$ GeV^2. In this way CIM predicts significant photon yields also at larger p_T. Recently, however, it has been argued[63] that a_M is of the order of 10^{-2} GeV; then the CIM contribution is unimportant. We consider that the question of normalization of the CIM contribution is unsettled, at present.

Nevertheless, on general grounds[61],[64],[65], we may anticipate an expansion of the 1 particle inclusive cross section of the form:

$$E_c \frac{d\sigma}{d^3p_c}(AB \to CX) = \frac{f(x_T,\theta_{cm})}{p_T^4} + \frac{g(x_T,\theta_{cm})}{p_T^6} + \frac{h(x_T,\theta_{cm})}{p_T^8} + \dots \qquad (2.42)$$

$$\downarrow \qquad \downarrow \qquad \downarrow$$

$$\text{QCD 2-2} \qquad qM \to qg \qquad qM \to qM$$

(neglecting logarithmic corrections). It is certainly of great importance to obtain theoretical and/or phenomenological information on the magnitude and shape of the functions $f(x_T,\theta_{cm})$, $g(x_T,\theta_{cm})$, etc., entering the nonleading terms (higher twists) of Eq. (2.42).

We have chosen in this work not to include CIM contributions; instead we present careful and detailed calculations using only the aforementioned QCD contributions (Sects. 2.3, 2.2). The final comparison with experiment will show us if in order to understand the "perturbative regime" ($p_T \geq 4$) of photon production we have to resort to other models as the CIM.

Having thus formulated our problem, we proceed now to compare the results of our calculation with experiment and give some predictions for the cases where experimental data are not yet available.

CHAPTER III

CALCULATIONS AND COMPARISON WITH EXPERIMENT

3.1 Distribution functions in QCD

It is customary in the phenomenology of large p_T physics, to split the quark structure functions $F_{q/A}$, into a "valence" (q_v) and a "sea" (t_q) part. There is however, no rigorous theoretical justification for this splitting[1].

Quark structure functions are available for valence and sea quarks of different flavours as a result of recent accumulation of accurate lepto-production data[2],[7]. Their Q^2-dependence has also been found to be consistent with QCD predictions.

The gluon distribution function is not directly probed in leptoproduction, and reliable determinations are difficult to obtain[8]-[12]. Thus, in the present work, we are obliged to make certain choices. For the gluon distribution inside the proton we choose two characteristic forms:

(I) A "strong" gluon distribution: $\sim (1+9x)(1-x)^4$; we notice that as $x\to 1$, the gluon distribution behaves like $(1-x)^4$, in accord with more recent considerations based on the Altarelli-Parisi evolution equations[13]. Also we notice that the factor $1+9x$ enchances the gluon distribution at intermediate x. Such a form was first proposed in Ref. 14, on the basis of their QCD analysis of $p+p\to\pi^0+X$ at large p_T; for a recent justification see Ref. 15.

(II). A "weak" gluon distribution: $\sim (1-x)^5$, n=5 on account of old counting rules (Chapt. II, Ref. 5-6).

In our work we are interested in inclusive photon production in pp, $\bar{p}p$ and $\pi^- p$ collisions. For the various distribution functions inside the proton we adopt the following notation:

$$F_{q/p}(x,Q^2) = q \quad , \quad q = u, d, s, \bar{u}, \bar{d}, \bar{s}, \tag{3.1}$$

with:

$$u(x,Q^2) = u_v(x,Q^2) + t(x,Q^2) \tag{3.2}$$

$$d(x,Q^2) = d_v(x,Q^2) + t(x,Q^2) \tag{3.3}$$

$$s = \bar{s} = \bar{u} = \bar{d} = t(x,Q^2) \tag{3.4}$$

where $u_v(x,Q^2)$, $d_v(x,Q^2)$ and $t(x,Q^2)$ are the momentum distributions of u-valence, d-valence and sea quarks and an SU(3)-symmetric sea has been assumed. Similarly when q is a gluon we set:

$$F_{g/p}(x,Q^2) \equiv g(x,Q^2) \tag{3.5}$$

Also notice the relations $F_{\bar{q}/\bar{p}}(x,Q^2) \equiv F_{q/p}(x,Q^2)$ which will be useful for the applications in $\bar{p}p \to \gamma + X$.

We present calculations with two different sets of parton distributions (I) and (II). (Corresponding to the forms (I) and (II) of the gluon distribution mentioned above.)

Set (I)[16] uses input distributions $F(x,Q_0^2)$ determined essentially by counting rules. The Q^2-dependence is obtained by Mellin - inverting the QCD predicted moments [see also Chapter I, Eq. (1.31)][17], and fitting the predictions with relatively simple forms based on improved parametrizations of the Buras-Gaemers type (see Appendix A for details). Here for later purposes we present only the u-valence and gluon distribution of this set (Fig. 19)[18]. In set (I):

$$\Lambda = 0.5 \text{ GeV} \tag{3.6}$$

and as we mentioned before, the gluon distribution is of the "weak" form:

$$g(x,Q^2) \equiv 2.4\,(1-x)^5 \tag{3.7}$$

with $Q_0^2 = 1.8$ GeV^2.

Set (II) uses the following input distributions[18],[19]:

$$u_v(x,Q_0^2) = x(1-x)^3(c_0 + c_1T_1 + c_2T_2 + c_3T_3) + x^{1/2}(1-x)^3(c_0' + c_1'T_1) \tag{3.8}$$

$$d_v(x,Q_0^2) = x(1-x)^4(d_0 + d_1T_1 + d_2T_2 + d_3T_3) +$$

$$+ x^{1/2}(1-x)^4(d_0' + d_1' T_1) \qquad (3.9)$$

with

$$t(x,Q_0^2) = \bar{u}(x,Q_0^2) = \bar{d}(x,Q_0^2) = 2\bar{s}(x,Q_0^2) =$$

$$= 0.275(1-x)^{10} \qquad (3.10)$$

In the formulas above $T_n = T_n(2x-1)$ are Tchebycheff polynomials and c_n, c_n', d_n, d_n' are given in Table 1.

In set (II) the Q^2 dependence is obtained by exact QCD moment requirements and numerical inversion of Mellin transforms[19]. This exact result has been parametrized in Ref. 20 and is based on an improved Parisi-Sourlas method. In Fig. 19 well illustrated the u-valence and gluon distributions of Set (II), including their Q^2-dependence. In this set:

$$\Lambda = 0.4 \text{ GeV} \qquad (3.11)$$

and, as we mentioned before, the gluon distribution is of the "strong" form:

$$g(x,Q_0^2) = 0.866(1+9x)(1-x)^4 \qquad (3.12)$$

with Q_o^2 =4 Gev .

All these parametrizations have been chosen so that they satisfy the momentum sum rule:

$$\sum_i \int \frac{dx}{x} F_i(x,Q_o^2) = 1 \qquad (3.13)$$

where i runs over all quark and antiquark flavours and over the gluon.

For the parton distributions inside the pion we present calculations for two different sets of input distributions hereafter called Set (i), Set (ii). Both of them are parametrized as follows:

$$F_{u/\pi^+}(x,Q_o^2) = V(x,Q_o^2) + \xi(x,Q_o^2) \qquad (3.14)$$

$$F_{u/\pi^-}(x,Q_o^2) = \xi(x,Q_o^2) \qquad (3.15)$$

and $F_{\bar{d}/\pi^+} \equiv F_{u/\pi^+}$ etc. (see Appendix B). In Eqns. (3.14), (3.15), V is the valence part of the distribution and ξ is the sea part. Then, at $Q^2 = Q_o^2 = 3$ GeV^2 and $\Lambda = 0.5$ GeV, the two sets consist of:

(i) Forms determined from old counting rules (Chapt. II, Refs. 5-6)

$$V(x,Q_o^2) = \frac{3}{4} x^{1/2}(1-x) \;, \quad \xi(x,Q_o^2) = 0.1(1-x)^5 \qquad (3.16)$$

$$F_{g/\pi^\pm}(x,Q_o^2) = 2(1-x)^3 \equiv g_\pi \qquad (3.17)$$

(ii) The following forms:

$$V(x,Q_0^2)=\frac{2}{\pi}\,x^{1/2}(1-x)^{1/2}\ ,\ \xi(x,Q_0^2)=0.042(1-x)^4$$
$$Fg/\pi^{\pm}(x,Q_0^2)=1.35(1-x)^2\equiv g_\pi \qquad (3.18)$$

In set (ii), the form of V (valence distribution) has been determined by fits on certain $\pi^-+N\to\mu^+\mu^-+X$ data[21],[f7], and the forms of ξ and $Fg/\pi^{\pm}$ are taken more in accord with recent theoretical considerations[23]. In Appendix B we give the details (constants and parametrized forms) of these two sets of distributions.

It is known[18],[22] that there is an ambiguity in the choice of the large variable Q^2, that enters the running coupling constant $\alpha_s(Q^2)$ and the parton distributions $F(x,Q^2)$. For indication we mention here some possible choices:

$$Q^2=-\hat{t}\ ,\quad Q^2=(\hat{s}\hat{t}\hat{u})^{1/3}$$
$$Q^2=\hat{s}\ ,\quad Q^2=\frac{2\hat{s}\hat{t}\hat{u}}{(\hat{s}^2+\hat{t}^2+\hat{u}^2)} \qquad (A1)$$

Throughout our work we make the following simple choice:

$$Q^2=2p_T^2 \qquad (3.19)$$

This can be argued as follows[18]: Due to the fact that the distributions $F(x,Q^2)$ decrease fast as $x\to 1$ (see Fig. 19), much of the contribution to the integral in Eq. (2.17), comes from the region:

$$x_1 \approx x_2 \approx x_T$$

Then in view of the relations (2.15),(2.16) and $\hat{s}+\hat{t}+\hat{u}\approx 0$, (A1) becomes:

$$Q^2 = 2\,p_T^2 \quad , \quad Q^2 = 2.5\,p_T^2$$
$$Q^2 = 4\,p_T^2 \quad , \quad Q^2 = \frac{4}{3}\,p_T^2 \qquad (A2)$$

Clearly, the choice $Q^2=2p_T^2$ is somewhere between the extremes. There are rather small quantitative differences with these choices of Q^2. For example in going from $Q^2=2p_T^2$ to $Q^2=2\hat{s}\hat{t}\hat{u}/(\hat{s}^2+\hat{t}^2+\hat{u}^2)$ typically changes the total single photon yield by no more than 20%[18].

3.2 The parton k_T effects.

Another ingredient in the QCD description of large p_T direct photon (and hadron) production is the transverse momentum distribution (k_T) of the incident partons inside their parent hadrons[24]-[28]. Experimentally the transverse momentum distribution of muon pairs produced at Fermilab and at the ISR was observed to be rather wide[29]-[31]. Simple

QCD fits require an average value $\langle k_T \rangle \approx$ 0.7 GeV[32]. However more recent determinations suggest a not too large $\langle k_T \rangle \approx$ 0.3-0.5 GeV. This is the amount of "primordial" or "intrinsic" k_T required to fit the Fermilab data, if the contribution of the diagrams of Fig. 13(a),(b) and that of higher order QCD graphs corresponding to soft (multiple) gluon Bremsstrahlung are taken into account[33],[34]. Anyway, in all our calculations we use

$$\langle k_T \rangle = 0.5 \ GeV \tag{3.20}$$

To include the k_T effects we shall modify Eq. (2.11) and Eq. (2.38). Suppose that each constituent has a transverse momentum k_T. Following Ref. 35, we introduce the light cone variables:

$$(k_i^+, k_i^-, \vec{k}_{Ti}) \tag{3.21}$$

where

$$k_i^{\pm} = k_{i0} \pm k_{i3} \ , \ k_i = x_i P_i \ , \ i = 1,2 \tag{3.22}$$

(P_i as in Chapter II, Sect. 2). The subprocess invariants become:

$$\hat{s} = s\left(x_1 + \frac{k_1^+}{\sqrt{s}}\right)\left(x_2 + \frac{k_2^-}{\sqrt{s}}\right) - \left(\vec{k}_{T1} + \vec{k}_{T2}\right)^2 \tag{3.23}$$

$$\hat{t} = -s\left(x_1 - \frac{x_T}{2}\right)\left(\frac{k_1^-}{\sqrt{s}} - \frac{x_T}{2}\right) - \left(\vec{k}_{T1} - \vec{P}_T\right)^2 \tag{3.24}$$

$$\hat{u} = -s\left(x_2 - \frac{x_T}{2}\right)\left(\frac{k_2^+}{\sqrt{s}} - \frac{x_T}{2}\right) - \left(\vec{k}_{T2} - \vec{P}_T\right)^2 \tag{3.25}$$

where:

$$k_1^- = \frac{1}{x_1\sqrt{s}}\left(k_{T1}^2 + k_1^2\right) \quad , \quad k_2^+ = \frac{1}{x_2\sqrt{s}}\left(k_{T2}^2 + k_2^2\right) \qquad (3.26)$$

and the structure functions are now $\vec{k}_T$-dependend i.e. $F_{q_1/A}(x_1, \vec{k}_{T1}, Q^2)$ etc. In the above equations we have exhibited explicitly the dependence of the subprocess invariant on the parton invariant masses in order to show some controversy that exists due to the way these quantities are handled. In the "on-shell" kinematics approach[27),(36)-(38)] the partons remain close to the mass shell in the presence of $\vec{k}_T$, while with "off-shell", kinematics[28), (39),(40)] k_i^2 becomes large and negative for large k_T^2 and/or x near 1. With "on-shell", kinematics and all masses set to zero Eq. (2.11) becomes:

$$\left(E\frac{d\sigma}{d^3p}\right)_{\alpha_s} = \sum_{q_1,q_2}\int dx_1 d^2k_{T1} dx_2 d^2k_{T2} F_{q_1/A}(x_1, \vec{k}_{T1}, Q^2) \times$$

$$\times F_{q_2/B}(x_2, \vec{k}_{T2}, Q^2)\frac{\hat{s}}{\pi}\frac{d\sigma^{(q_1q_2)}}{d\hat{t}}\delta(\hat{s}+\hat{t}+\hat{u}) + A\leftrightarrow B \qquad (3.27).$$

with $\hat{s},\hat{t},\hat{u}$ given by Eqns. (3.23)-(3.26) with $k_1^2 = k_2^2 = 0$.

To complete the calculation, the form of $F(x, \vec{k}_T, Q^2)$ must be specified. We proceed, similarly to Ref. 36, with the usual and convenient factorized Ansatz [27),(38)]

$$F(x, \vec{k}_T, Q^2) = F(x, Q^2)\, g(\vec{k}_T) \qquad (3.28)$$

with $$\int d^2_{K_T} g(\vec{K_T}) = 1 \quad ; \qquad (3.29)$$

there is, however, no rigorous theoretical justification for this form. The k_T distribution is expected to be strongly damped at large k_T. We have chosen, as in Ref. 36, a Gaussian form for $g(k_T)$:

$$g(K_T) = \frac{b^2}{\pi} \exp(-b^2 K_T^2) \qquad (3.30)$$

with:

$$\langle K_T \rangle = \frac{\pi}{2b} = 0.5 \text{ GeV} \qquad (3.31)$$

From Eqns. (3.23)-(3.26) we can easily see that for a given value of $\vec{K_{T1}}$, and for fixed X_1 and X_T, $\hat{t}$ is smallest when $\vec{K_{T1}}$ is in the direction of $\vec{p_T}$. Physically this means that for a $\hat{t}$ channel exchange, the parton q_1 prefers to line up in the direction of the trigger. However for $\vec{K_{T1}} = \vec{p_T}$ and $X_1 = \frac{X_T}{2}$, $\hat{t}$ vanishes and e.g. the cross-section (2.32), blows up.

Of course, for $\langle K_T \rangle$ = 0.5 GeV such poles become significant when p_T becomes smaller than ~1 GeV; and then use of simple perturbative QCD will be very unwise. Anyway, in order to avoid these poles the more common method is to introduce a regularizing mass:[18],[27]

$$\hat{s} \to \hat{s} + M^2 \;, \quad \hat{t} \to \hat{t} - M^2 \;, \quad \hat{u} \to \hat{u} - M^2 \qquad (3.32)$$

so that $\hat{t}_{min} = -M^2$ etc.; M is chosen to be of the order of 1 GeV.

Recently calculations based on "off-shell" constituent kinematics[39]-[44] have been carried out. In this way the poles $\hat{s}, \hat{t}, \hat{u} \approx 0$ lie outside the allowed phase space boundary and there is no need of cut-off. For the k_T effects in e.g. $pp \to \pi^0 X$, the result of these calculations is that, at ISR energies and $p_T \simeq 2$ GeV and with $\langle k_T \rangle \simeq 0.8$ GeV, they increase the inclusive cross-section by a factor of ~ 2. In $pp \to \gamma X$ we expect the k_T effects to be less important because, as a function of p_T at fixed s, $pp \to \gamma X$ is less steep than $pp \to \pi^0 X$.

Details for the calculation of multifold integrals of the type of Eq. (3.27), can be found in Appendix A of Ref. 36.

In Fig. 22 (b), we show the magnitude of the k_T effects for $pp \to \gamma + X$ at various c.m energies. $\sigma(k_T)$ denotes $(E d\sigma/d^3p)$ with $\langle k_T \rangle = 0.5$ GeV and $\sigma(0)$ the same with $\langle k_T \rangle = 0$ (no k_T-effect). We notice that, as in $pp \to \pi^0 X$, with increasing p_T, the k_T-effects become unimportant.

As it is expected, "off-shell" and "on-shell" calculated k_T effects affect very little the single photon inclusive cross-section when a moderate average k_T, like $\langle k_T \rangle = 0.5$ GeV, is assumed[45]. This is true for either an "off-shell" or an "on-shell" calculation. However for larger $\langle k_T \rangle$ and at sufficiently low p_T there is a significant difference.[39]

3.3 The $p+p \rightarrow \gamma + X$ cross-section and the γ/π^0 ratio.

The experimental situation in photon production is encouraging. There are at least four collaborations (March 1980) that have already reported results (final or preliminary). These are the CERN-Rome-Brookhaven-Adelphi (CRBA), the Athens-Athens-Brookhaven-CERN (A^2BC) the Fermilab-Johns Hopkins (FJH) and the CCOR (CERN-Columbia-Oxford-Rockefeller) collaborations (see References 46-50). When this work was almost finished we had results from A^2BC and CRBA, and some preliminary results from CCOR. Thus only these data will appear in our work. In particular the A^2BC collaboration has measured direct photon production in pp collisions, at the CERN Intersection Storage Rings (ISR), for c.m energies $31 \leq \sqrt{s} \leq 63$ GeV. and photon transverse momenta up to 9 GeV, using segmented lead/liquid-argon colorimeters which are described in detail in their publications. They detect a γ/π^0 ratio of order 40% at $p_T = 9$ GeV and no significant energy dependence. It should be noted that over the full p_T range they measure, the two photons from π^0 decay are individually resolved in almost every case, providing a very clear π^0 signature. Also $\eta \rightarrow 2\gamma$, $\omega \rightarrow \pi^0\gamma$ and $\eta' \rightarrow 2\gamma$ decays have been subtracted. It is to be noted that most of the background comes from π^0 and η decays where one of the decay photons misses the calorimeter; contributions of other mesons to the γ/π^0 ratio are negligible[f8].

Before comparing our predictions with the data we would like to illustrate the effects of scale violations in the total photon cross section, as well as the relative strength of the "Compton" (qg) and "Annihilation" ($q\bar{q}$) subprocesses. Consider e.g. Set (II) (see Sect. 3.1) for the parton distributions. In Fig. 20 we present the results of our calculation using Eqn. (2.17) only. In presenting our results for γ/π^0 we have divided our predictions for $E d\sigma(pp\to\gamma+X)/d^3p$ by the experimental cross-sections for $E d\sigma(pp\to\pi^0+X)/d^3p$ [denoted by π^0 (expt)]. Because of experimental errors as well as some differences between data of different collaborations, we represent π^0(expt) by a band.

(i) As it is expected, the "Compton" contribution (qg) in all three energies (see Fig. 20a,b,c), is at least one order of magnitude greater than ($q\bar{q}$) in medium p_T($\simeq$6-7 GeV) and almost four orders at large p_T(9-14 GeV).

(ii) It is a common feature of all three figures (three different energies) that nonscaling distribution functions (i.e. with Q^2-dependence) reduce the total photon yield by one order of magnitude at high p_T with a corresponding decrease of the γ/π^0 ratio. For example, in Fig. 20(b) ($\sqrt{S}$=53), the γ/π^0 predicted for one collaboration (CCOR, first solid line from below), at $p_T\sim$10 GeV is $\sim$20% while the scaling prediction (first dashed line from below), gives almost 100%! Taking into account that $qg\to q\gamma$ dominates $pp\to\gamma X$ (see (i)), we can understand this difference

as mainly due to the scale violations in the gluon distribution (for an illustration of their effect see Fig. 19).

Next we would like to illustrate the magnitude of the Bremsstrahlung contribution. For this we reproduce Fig. 21 from Ref. 52. There, R_γ is defined as:

$$R_\gamma = \frac{E d\sigma^{(Brems)}/d^3p}{E d\sigma^{(qg)}/d^3p} \qquad (3.33)$$

and has been calculated using Eqns. (2.38), (2.28), (2.17) and the Set (I) of parton distribution functions. Clearly in general, Bremsstrahlung makes a sizeable correction ($R_\gamma \sim 1$), in particular as we approach the kinematic boundary $x_T \to 1$. Most of the correction is due to collinear γ emission (see Chapter II, Sect. 3). In Fig. 22(a) we present $(E d\sigma/d^3p)^{(Born)}_{\alpha_s}$ and $(E d\sigma/d^3p)^{(Brems)}$ for two different energies. For the lowest energy ($\sqrt{S}$=31 GeV) we clearly see that as $x_T \to 1$ the Bremsstrahlung contribution makes an important correction, as has been expected[f9].

Now we would like to compare our predictions with data on the ratio of γ/π^0, [Figs. 23(a), 23(b)]. When the contribution of $qg \to q\gamma$ (dominant sub-process) is calculated with a gluon distribution $g(x,Q^2) \sim (1-x)^5$ (Set I), the predictions fall somewhere below the data of the A^{2}BC[46],[47]; however, they are consistent with the data of CCOR[48],[51].

When we use $g(x,Q^2) \sim (1+9x)(1-x)^4$ we are in better agreement with the $\bar{A}^2$BC collaboration [Fig. 23(b)]. In this calculation k_T effect has been taken into account according to Sect. 3.2.

In Fig. 24 we compare our results with recent data on the ratio γ/π^0 [46]. Our theoretical predictions on γ have been divided by π^0 data of the same collaboration [47]. It is to be noted that, in general, our predictions even with a strong $g(x,Q^2)$ lie below these data [f10].

At present there is some difference between large p_T π^0 data from different experiments [53], [54], [47]. To avoid such uncertainties, in Fig. 25 we present directly our theoretical predictions (including k_T effects and the Bremsstrahlung correction) on $E\,d\sigma/d^3p(pp\to\gamma X)$. We also present data of various collaborations. Whenever a collaboration gives only γ/π^0 we have multiplied by their own π^0. Again, of course $\bar{A}^2$BC data favour a strong gluon distribution. However data of the CCOR collaboration [48] at not too large p_T appear to favour a weak $g(x,Q^2)$.

3.4. Predictions for $\pi^- p \to \gamma X$ and $\bar{p}p \to \gamma X$.

We consider photon production by pion and anti-proton beams. Since π^- $(\bar{u}d)$ and $\bar{p}(\bar{u}\bar{u}\bar{d})$ contain valence $\bar{q}$, the large p_T inclusive cross-sections are controlled by the "Annihilation" $(q\bar{q})$ subprocess (see Fig. 13). The Bremsstrahlung corrections are expected to be small and will be neglected.

Concerning $\pi^- p \to \gamma X$ predictions are somewhat uncertain

due to ambiguities in the quark valence distribution and, to a less extent, in the gluon distribution inside the pion. As we mentioned in Sect.3.1, we present results for two different sets of input distributions for the pion (set (i) and set (ii)). The parton distributions inside the proton are from Ref. 16 (Set (I)). Figs. 26(a) and 26(b) illustrate only the effect of scale violations in the parton distributions; again it is a sizeable effect. Fig. 26(a) has been calculated with set (i) for the pion distributions and Fig. 26(b) with set (ii). In these figures k_T-effects are not included in the calculations of $\pi^- p \to \gamma X$.

Fig. 27 presents our results for $\pi^- p \to \gamma X$ at $\vartheta_{c.m}=90°$ and $\sqrt{s}=19.4$ GeV (as before). Now k_T effects have been taken into account with $\langle k_T \rangle = 0.5$ GeV. Naturally the set (ii) [Fig. 27(b)] leads to somewhat large photon yields, since the valence $\bar{q}$ distribution is rather stronger than that of set (i). With the $\pi^- p \to \pi^0 X$ experimental cross-section, in all four digures, taken as indicated[55], at $p_T \sim 6$ GeV we predict $\gamma/\pi^0 \simeq 20-30\%$.

Now we turn to $\bar{p}p \to \gamma X$. The theoretical predictions are less ambiguous because the dominant contribution contains valence q and $\bar{q}$. We use Set (I) of parton distributions inside the proton (including scale violations). Our predictions for $E d\sigma(\bar{p}p \to \gamma X)/d^3p$, $\vartheta_{c.m}=90°$ are shown in Figs. 28 and 29. In Fig. 28 we show again the effect of scale violations (without k_T effects in $\bar{p}p \to \gamma X$). In Fig. 29 we include k_T effects, Eqn. 3.27, taking as before,

$\langle K_T \rangle = 0.5$ GeV. For the π^0 experimental cross-section (not measured yet) we have chosen the $\bar{p}+p \to \pi^0 + X$ cross-section as indicated (expt) assuming:

$$E\frac{d\sigma}{d^3p}(\bar{p}p \to \pi^0 X) \sim E\frac{d\sigma}{d^3p}(pp \to \pi^0 X) \quad (3.34)$$

at each energy. Now the predicted photon yields are significantly larger; the reason is that both subprocesses "Compton" and "Annihilation" give sizeable contribution.

We note that recently the ratio:

$$R = \frac{E\, d\sigma(\bar{p}p \to \pi^0 X)/d^3p}{E\, d\sigma(pp \to \pi^0 X)/d^3p} \quad (3.35)$$

has been calculated by the authors of Ref. 56. This ratio is very close to unity for large energy variations confirming the correctness of our guess, Eq. (3.37).

CHAPTER IV

PHOTON HADRON CORRELATIONS AT OPPOSITE SIDES

4.1 Two-hadron inclusive cross-sections (hadron trigger).

The experimental study of two (and more) particle distributions has revealed that the large p_T events have three components[1]-[3],

i) Towards jet. The density of large p_T particles produced on the same side as the trigger particle peaks in the trigger direction.

ii) Away jet. A clustering of large p_T particles is observed also in the away side of the trigger.

iii) Low p_T cloud. This background of small p_T particles is a nuissance, since both in practice and in principle, it is hard to distinguish particles in the jets from particles in the background.

Another feature is that the momenta (p_{out}) of particles normal to the plane defined by the beam and trigger direction are limited[4],[5] (see Fig. 30). The p_{out} distribution falls rapidly with a mean value $\langle p_{out} \rangle = 500$ MeV.

The above jet structure is a natural consequence of hard scattering pictures of large p_T reactions.

Consider the reaction $A+B \rightarrow h_1 + h_2 + X$ with the two hadrons observed with large transverse momenta p_{T1}, p_{T2} in opposite directions in the c.m of the initial hadrons. Again, we assume that the reaction takes place via the $qq \rightarrow qq$, $qg \rightarrow qg$, $gg \rightarrow gg$ etc. subprocesses. By taking advantage of factorization[6]

we can immediately write down the expression for the inclusive cross-section[7] of large-p_T production of two hadrons (see Fig. 30).

$$\sigma_{12}(p_{T1},p_{T2},s) \equiv E_1 E_2 \frac{d\sigma}{(d^3p_1)(d^3p_2)} = \frac{16}{\pi s x_{T1}^2 x_{T2}^2} \sum_{\substack{q_1,q_2,\\ q_3,q_4}} \int \frac{dx_1}{(1+\eta)^2} x_1 F_{q_1/A}(x_1,Q^2) \times$$

$$\times F_{q_2/B}(x_2,Q^2) \tan^2\left(\frac{\theta_1}{2}\right) \frac{d\sigma}{d\hat{t}}^{(q_1q_2\to q_3q_4)} D_{h_1/q_3}\left(\frac{x_{T1}}{z},Q^2\right) D_{h_2/q_4}\left(\frac{x_{T2}}{z},Q^2\right) \times$$

$$\times \delta(\varphi_1-\varphi_2+\pi) \quad + \quad A \longleftrightarrow B \qquad (4.1)$$

where

$$x_2 = x_1 \tan\frac{\theta_1}{2} \tan\frac{\theta_2}{2} \quad , \quad \eta = \tan\frac{\theta_1}{2} \cot\frac{\theta_2}{2}$$

$$z = \frac{2x_1 \tan\theta_1/2 \tan\theta_2/2}{\tan\theta_1/2 + \tan\theta_2/2} \qquad (4.2)$$

$$Q^2 = \frac{x_1^2 s \tan^2\theta_1/2}{1+\eta} \quad , \quad x_{Ti} = \frac{2p_{Ti}}{\sqrt{s}} \qquad i = 1,2$$

The limits of integration are given by

$$\left[x_{T1}\left(\frac{1+\eta}{2\tan\theta_1/2}\right), x_{T2}\left(\frac{1+\eta}{2\tan\theta_1/2}\right)\right]_{max} \lesssim x_1 \lesssim 1 \qquad (4.3)$$

Details of the derivation of Eq. (4.1) can be found in Ref. 7. The functions that enter Eq. (4.1) have been explained in Chapter II, Sect. 2.1. However the gluon fragmentation function that explicitly enters this equation deserves further attention. This is because not too much is known for this important fragmentation function.

Large p_T production of hadrons is the only hard process to which the fragmenting gluons can considerably contribute to the leading order. Particularly in Eq. (4.1), gluons and quarks fragment incoherently to produce the observed hadrons (h_1,h_2). Available data, however, do not provide any evidence for gluon jets different from quark ones; this, at first sight, seems to render impossible the isolation of the gluon fragmentation function using Eq. (4.1). In Sect. 5.2 we will demonstrate how this problem can be overcome.

In reaction (4.1), parton k_T effects are known to be unimportant[8],[9]; an opposite-side hadron with a large p_T almost eliminates the trigger bias (see also Chapter III, Sect. 3.2).

For later use we shall define here the transverse momentum sharing (x_e) distributions. Consider a particle in the hemisphere opposite the trigger, with transverse momentum p_{T2} and call p_{x2} the projection of p_{T2} on the beam-trigger plane (see Fig.30). We define:

$$x_e = \frac{p_{x2}}{p_{T1}} \qquad (4.4)$$

where p_{T1} is the transverse momentum of the trigger. The x_e variable denotes the percentage of the transverse momentum p_T balanced by the individual hadrons in the opposite hemisphere. The x_e distributions are defined by:

$$\frac{d\sigma}{dx_e} = \int_{\Delta p_{out}} dp_{out} \int_{\Delta \eta_2} d\eta_2 \frac{d\sigma}{dx_e d\eta_2 dp_{out} d^3p_1} \qquad (4.5)$$

where η_2 is the pseudo-rapidity ($\eta_2 = -\log(\tan\theta_2/2)$) of the secondary and p_{out} is the component of the secondary's momentum normal to the beam-trigger plane. Since[10]

$$d\eta\, dp_x dp_{out} = \frac{d^3p}{E} \qquad (4.6)$$

we rewrite (4.5) as:

$$\frac{d\sigma}{\Delta\eta_2 dx_e} = p_{T1} \int_{\Delta p_{out}} dp_{out} E_1 E_2 \frac{d\sigma}{(d^3p_1)(d^3p_2)} \qquad (4.7)$$

The ranges $\Delta\eta_2$ and Δp_{out} are specified by experiment.

4.2 Photon-hadron inclusive cross-section (photon trigger).

In this chapter we are interested in reactions of the kind:

$$A + B \longrightarrow \gamma(p_{T1}) + h_{opp}(p_{T2}) + X \qquad (4.8)$$

where the hadron h is produced at opposite sides to a large p_T photon trigger.

To the leading order in the QCD running coupling constant, two subprocesses contribute in this reaction

(i) $q(\bar{q})g \to q(\bar{q})\gamma$ "Compton" scattering. The hadron h results as the fragmentation of a quark (antiquark).

(ii) $q\bar{q} \to g\gamma$ "Annihilation" subprocess. The hadron h results as the fragmentation of a gluon.

Bremsstrahlung corrections should, in general, be important for A=B=p. However, subsequently we consider the reactions $\pi^{\pm} + p \to \gamma + h_{opp} + X$ and, in fact, isolate the contribution of $q\bar{q} \to \gamma g$; in this case, Bremsstrahlung is not important and we shall neglect it.

We shall demonstrate here how we can derive the γ-h inclusive cross section from the h-h one. As in Chapter II, Sect. 2.1, due to the direct quark-photon coupling the "fragmentation" function is simply:

$$D_{\gamma/q_3}\left(\frac{x_{T1}}{z}\right) \equiv \delta\left(\frac{x_{T1}}{z} - 1\right) \qquad (4.9)$$

Also, if we choose $\theta_1 = \theta_2 = 90°$ (γ-h at 90° relative to A-B) and use Eq. (4.2) and (4.9), Eq. (4.1) becomes: (F12), (11)

$$\sigma_{12} \equiv E_1 E_2 \frac{d\sigma}{(d^3p_1)(d^3p_2)} = \frac{4}{\pi s x_{T1}^2 x_{T2}^2} \sum_{q_1 q_2; q_3} \int \frac{dx_1}{x_1} z^2 F_{q_1/A}(x_1, Q^2) \times$$

$$F_{q_2/B}(x_2, Q^2) \frac{d\sigma^{(q_1 q_2)}}{d\hat{t}} \delta\left(\frac{x_{T1}}{z} - 1\right) D_{h/q_4}\left(\frac{x_{T2}}{z}\right) \delta(\varphi_1 - \varphi_2 + \pi) + A \leftrightarrow B \qquad (4.10)$$

Using the first delta function to eliminate the integration, we get:

$$\sigma_{12} = \frac{4}{\pi S x_{T2}^2} F_A(x_{T1}) F_B(x_{T1}) \frac{d\sigma}{d\hat{t}} D\left(\frac{x_{T2}}{x_{T1}}\right) \delta(\varphi_1 - \varphi_2 + \pi) + A \leftrightarrow B \qquad (4.11)$$

In the above equation we have suppressed quark, gluon indices and Q^2-dependence for convenience. $\frac{d\sigma}{d\hat{t}}$ are given in Eqs. (2.23) and (2.24) and they have to be calculated now using:

$$z = x_1 = x_2 = x_{T1} = x_{T2} = x \qquad (4.12)$$

Let us consider now distributions in transverse momentum sharing (x_e), which have given important information in similar experiments with large-p_T hadron triggers.[5),(9),(10] If we choose γ-h to emerge "back to back" (see Fig. 30), then $\varphi_2 \approx 180°$ and in view of the relation (4.12), Eq. (4.4) becomes:

$$x_e = \frac{p_{x2}}{p_{T1}} = \frac{p_{T2}}{p_{T1}} = \frac{x_{T2}}{x_{T1}} \qquad (4.13)$$

Now the transverse momentum sharing (x_e) distribution, [Eq. (4.7)] becomes:

$$S \overset{\text{def}}{\equiv} \frac{1}{\Delta\eta_2} \frac{d\sigma}{dx_e} = p_{T1} \int_{\Delta p_{out}} dp_{out}\, \sigma_{12} \simeq$$

$$\simeq p_{T1} p_{T2} \sigma'_{12} \qquad (4.14)$$

In the derivation of Eq. (4.14) we have used:

$$p_{out} = p_{T2}\sin\psi_2 \quad , \quad \psi_2 = \varphi_1 - \varphi_2 + \pi$$

and

$$\sigma_{12} = \sigma'_{12}\,\delta(\psi_2) \qquad (4.15)$$

By using $x_{Ti}=2p_{Ti}/\sqrt{s}$, i=1,2 and Eqs. (4.14), (4.13) and (4.12), Eq. (4.11) finally becomes:

$$S \simeq \frac{1}{\pi x_e}\sum_{q_1,q_2,q_4} F_{q_1/A}(x,Q^2)\,F_{q_2/B}(x,Q^2)\,\frac{d\sigma}{d\hat{t}}\,D_{h/q_4}(x_e,Q^2) + A\leftrightarrow B \qquad (4.16)$$

(see also Appendix D). For the Q^2 variable we make again the simple choice: $Q^2=2p_T^2$.

4.3 The gluon fragmentation function. Experimental prospects.

In general the sum in Eq. (4.16) involves quark and gluon fragmentation functions. We can isolate, however, the latter by considering differences of appropriate x_e distributions.

Let us take B≡p(proton) and let S_A^h denote the x_e distribution for A+p→γ+h+x (opposite side). We define also:

$$\sigma^{q_1q_2} = \frac{e_q^{-2}}{\pi x_e}\left.\frac{d\sigma^{q_1q_2}}{d\hat{t}}\right|_{x_1=x_2=x} \quad , q_1,q_2 = q,\bar{q},g \qquad (4.17)$$

where $d\sigma/d\hat{t}$ are given by Eq. (2.23) and Eq. (2.24). We indicate the "Compton" and "Annihilation" part of S by splitting it into two parts:

$$S_A^h = S_A^h(qg) + S_A^h(q\bar{q}) \quad . \qquad (4.18)$$

Furthermore, we define

$$S_{A-\bar{A}}^h = S_A^h - S_{\bar{A}}^h \qquad (4.19)$$

We also assume that h is identical to its own antiparticle (eg. $h=\pi^o$ or $h=\pi^+ + \pi^-$). After some manipulation it can be shown (see Appendix D) that:

$$S_{A-\bar{A}}^h = S_{A-\bar{A}}^h(q\bar{q}) = -\sigma^{q\bar{q}} D_{h/g} \sum_q e_q^2 (F_{q/A} - F_{\bar{q}/A}) \times$$

$$\times (F_{q/p} - F_{\bar{q}/p}) \qquad (4.20)$$

where the summation is over quarks only. Notice also that $(F_{q/A}-F_{\bar{q}/A})$, $(F_{q/p}-F_{\bar{q}/p})$ are valence quark distributions only. Thus knowledge of them allows the extraction of the gluon fragmentation function $D_{h/g}$ from data on:

$$S_A^h : \quad A + p \rightarrow \gamma + h + X$$

$$S_{\bar{A}}^h : \quad \bar{A} + p \rightarrow \gamma + h + X \qquad (4.21)$$

where A can be a proton or a π^+ etc.

Now if we want to sum Eq. (4.20) for a particular choice of A and h we must use the decomposition of the distributions that is given in Eqs. (3.2),(3.3),(3.4),(3.14),(3.15) together with the quark charge assignments (see also Appendix D).

Also we decompose the fragmentation functions as follows:

$$D^{V+\xi} \overset{def}{\equiv} D_{\pi^+/u} = D_{\pi^-/\bar{u}} = D_{\pi^+/\bar{d}} = D_{\pi^-/d} \qquad (4.22)$$

$$D^{\xi} \overset{def}{\equiv} D_{\pi^+/d} = D_{\pi^-/\bar{d}} = D_{\pi^-/u} = D_{\pi^+/\bar{u}} \qquad (4.23)$$

with the obvious composition law:

$$D^{V} \pm D^{\xi} \overset{def}{\equiv} D^{V\pm\xi} \qquad (4.24)$$

In Appendix D we give [together with the proof of Eq. (4.20)] an application when A=π^- and h=π^0 [=$(\pi^+ + \pi^-)/2$, in the quark model]. The final formula in terms of the valence distributions of the pion (V) and the proton (u_v, d_v) is:

$$S^{\pi^0}_{\pi^+-\pi^-} = -\frac{\sigma^{q\bar{q}}}{g} D_{\pi/g} V(4u_v - d_v) \qquad (4.25)$$

where $D\pi/g \equiv D\pi/g\ (x_e, Q^2)$, $d_v \equiv d_v(x,Q^2)$ and $u_v \equiv u_v(x,Q^2)$. Thus experimental information on the LHS of Eq. (4.25) together with V, u_v and d_v, can determine the gluon fragmentation function to a pion.

Eq. (4.25) involves measurement of the x_e-distributions of the following reactions:

$$S^{\pi^+}_{\pi^+} : \pi^+ + p \longrightarrow \gamma + \pi^+ + X$$

$$S^{\pi^-}_{\pi^+} : \pi^+ + p \longrightarrow \gamma + \pi^- + X$$

$$S_{\pi^-}^{\pi^+}: \quad \pi^- + p \longrightarrow \gamma + \pi^+ + X \qquad (4.29a)$$

$$S_{\pi^-}^{\pi^-}: \quad \pi^- + p \longrightarrow \gamma + \pi^- + X \qquad (4.29b)$$

Reactions (4.28), or (4.29) can be measured in the same run of the machine; sometimes, however, it is preferable to make two independent runs in order to remove the background easier. Experiments of the type of $S_p^{\pi^+}$ and $S_p^{\pi^-}$ are already under way[12].

4.4 Calculations, discussion and conclusions.

We have calculated the quantity given in formula (4.25) by using two different input fragmentation functions both of the form:

$$\frac{1}{2}\left(D_{\pi^+/g} + D_{\pi^-/g}\right) \equiv D_{\pi^0/g}(x_e, Q^2) = \frac{m+1}{5}(1-x_e)^m \qquad (4.30)$$

In the first, in accord with old counting rules[13], we choose:

$$m = 3 \qquad (4.31)$$

In the second

$$m = 1.5 \qquad (4.32)$$

More recent theoretical considerations combined with the Gribov-Lipatov reciprocity relations[14] would suggest m=2. The choice m=1.5 does not differ much and on the other hand

makes more clear the difference with Eq. (4.31). In both calculations we have introduced scale violations in the distribution and fragmentation functions as predicted by QCD. For the valence nucleon and pion distributions we use the parametrization of Owens and Reya (see Appendices A and B). The Q^2 difference of the fragmentation function $D\pi/g\ (x,Q^2)$ has been calculated by S.L. Papadopoulos[15] using an improved Parisi and Sourlas method; some details are given in Appendix B.

Using Eq. (4.25) and working at fixed x_e, we can also get an idea about the scaling violations in $D\pi/g\ (x_e,Q^2)$.

Our results are shown in Fig. 31 for several trigger transverse momenta p_{T1}. Clearly at large x_e the choice (4.32) leads to differences $S^{\pi^o}_{\pi^- - \pi^+}$ significantly larger. (Factors of 3~4). It is evident that measurement of such physical quantities should give the best, perhaps, determination of gluon fragmentation functions[f11]. As we stressed repeatedly, so far there is no direct information on them.

CHAPTER V

SUMMARY AND CONCLUSIONS

5.1 Summary of our work and conclusions.

In this work we have studied:

(1) The inclusive real photon production, at large p_T in hadronic collisions, making detailed calculations for the typical processer $pp \to \gamma + x$, $\bar{p}p \to \gamma + x$, $\pi^- p \to \gamma + x$.

(2) The inclusive production of photon and hadron at opposite sides. We have shown that by forming certain differences of appropriate 2 P-Inclusive cross-sections we succeed in isolating the gluon fragmentation function.

Our general framework was that of perturbative QCD. The approach can be applied to all such processes involving hadrons in the initial and/or final states. This framework also, interrelates the various processes by permitting the information gained from some of them (eg. deep inelastic leptoproduction) to be used in more complex ones (eg. hadron production in h-h collisions, Drell-Yan production of $\ell^+\ell^-$ - pairs etc.). Therefore, it is possible to make predictions for the latter processes and thus test the theory (QCD) by comparing with available data.

In part (1) of our study we have calculated perturbatively photon production to $\mathcal{O}(\alpha_s)$ in the strong coupling constant for $pp, \bar{p}p, \pi^- p$ and to $\mathcal{O}(\alpha_s^2)$ [Bremsstrahlung correction] for pp collisions only.

In part (2) of our study we have calculated the difference of x_e distributions $S^{\pi^0}_{\pi^+ - \pi^-}$ (following the notation of Chapter IV). As we have seen this particular difference isolates the $q\bar{q} \to g\gamma$ subprocess and subsequently the gluon fragmentation

function.

In our calculations we have used:

(A) the quark distribution functions inside the proton obtained from lepton initiated processes $ep \to e+x$, $\mu p \to \mu+x$ and neutrino and antineutrino interactions.

(B) the quark (valence) distribution function inside the pion, which has been determined by fits on certain $\pi^- + N \to \mu^+\mu^- + X$ data (see Chapter III, Sect. 3.1).

The unknowns in our calculations were the power m determining the shape of the gluon distributions inside the proton and the pion. We did not try to obtain an optimal fit to the data by adjusting these unknowns; instead, but we made two characteristic choices for the input gluon distributions.

As for the partons' average intrinsic (or "primordial") transverse momentum k_T, we have chosen a moderate value $\langle k_T \rangle \approx 0.5$ GeV.

Our detailed conclusions are as follows:

(1) 1-P inclusive cross-sections.

(1A) On the comparison with experiment of the calculated $pp \to \gamma+x$ cross section.

Perturbative QCD predicts a large γ/π^0 ratio, far above the predictions of the Vector Dominance model. In particular at low $x_T (\leq 0.35)$ most of the contribution comes from "Compton Scattering" with the Bremsstrahlung correction being down almost one order of magnitude. However at $x_T \geq 0.4$ Bremsstrahlung becomes comparable to the "Born" term.

The Q^2-dependence of the structure functions, as dictated from QCD, leads to appreciable differences between scaling and non-scaling predictions.

In general, perturbative QCD (based on $\mathcal{O}(\alpha_s)$ and Bremsstrahlung $[\mathcal{O}(\alpha_s^2)]$ diagrams does not seem to match very well the data, particularly at medium and low p_T. At higher p_T it reproduces the main features of the data rather well. Also when k_T effects are included with $\langle k_T \rangle \simeq 0.5$ GeV a better agreement with data is achieved. In particular:

(a) With our moderate $\langle k_T \rangle$ and a "strong" gluon distribution $[\sim(1+9x)(1-x)^4]$ QCD lies somewhat below the A^2BC data (Fig.23(a))

(b) With the same $\langle k_T \rangle$ but with a "weak" gluon distribution $[\sim(1-x)^5]$ the theoretical predictions are even more below the experimental yields (A^2BC) (Fig.23(b))

There are several ways to improve our predictions:

(a) We can use a larger value of $\langle k_T \rangle$ (~1 GeV) (see Ref. 1). However as we have discussed in Sect. 3.2, the amount of "primordial" k_T required to fit the Fermilab data on dilepton production is small: $\langle k_T \rangle \simeq 0.3$ 0.5 GeV (see also Sect. 3.2).

(b) We can take an even stronger gluon distribution inside the proton[2],[3]. However, such a distribution does not appear to be supported by the very recent analysis of Ref. 15 of Chapt. III.

(c) We can introduce Constituent Interchange Model contributions (Fig. 18) which, if taken into account might improve

our theoretical predictions particularly at low p_T [4]. However, recent work [5] indicates that the old problem of CIM normalization is still unsettled.

In view of these reservations and of the fact that the CCOR Collaboration data (on $pp \to \gamma + x$) are somewhat below those of A^2BC (Fig. 25), we would like to await for more accurate experimental information. Anyway, it is evident that A^2BC data favor a "strong" [$\sim(1+9)x(1-x)^4$] gluon distribution; so do the data of FJH and CRBA Collaborations. Certainly precise data on large p_T $pp \to \gamma + x$ can offer one of the best, perhaps, determinations of the gluon distribution inside the proton.

(1B) On the $\bar{p}p \to \gamma + x$ and $\pi^- p \to \gamma + x$ predictions.

Most of the contribution comes from the QCD "Born" terms. For $\pi^- p \to \gamma + x$, $\sqrt{s} \sim 19.4$ GeV and $p_T \sim 6$ GeV) we predict $\gamma/\pi^0 \sim 20-30\%$ and for $\bar{p}p \to \gamma + x$ at $\sqrt{s} \sim 23-53$ GeV and $p_T \sim 6$, $\gamma/\pi^0 \sim 80-100\%$.

The effect of scale violations is important; it reduces the yields by one order of magnitude at large p_T. k_T effects play a minor role particularly at high p_T [Fig. 22(b)]; at low p_T ($\simeq$ 2-4 GeV) they enchance the cross-section by a factor of $\approx$ 1.5.

(2) 2-particle inclusive cross sections.

Opposite sides photon-hadron correlation in perturbative QCD, can help to isolate the gluon fragmentation function if appropriate differences of some x_e distributions are formed.

On the basis of two different choices of the gluon fragmentation function [see Chapter IV, Eq. (4.32)] and taking

into account the size of the involved cross sections in $\pi^{\pm}+p\to\gamma+\pi^{o}{}_{pp}+X$ [f11], we conclude that measurement of the relevant physical quantities (Sect. 5.2) should be able to give important information on the gluon fragmentation function to a pion.

5.2 Overall conclusions. The Moral.

We may briefly summarize our conclusions as follows:

(a) Perturbative QCD essentially accounts for the main features of the large $-p_T$ experimental $pp\to\gamma+x$ and gives definite and clear predictions for $\bar{p}p\to\gamma+x$ and $\pi^- p\to\gamma+x$ reactions.

(b) Precise data on large $-p_T$ $pp\to\gamma+x$ should offer the best, perhaps, determination of the gluon distribution inside the proton.

(c) Data on large p_T photon-hadron correlations in particular in $\pi^{\pm}+p\to\gamma+\pi^{o}{}_{pp}+x$ will give valuable information about the gluon fragmentation function; so far there is no direct information on this.

In carrying out these calculations we have seen that there is a minimum number of free parameters in the theory ("primordial" k_T and gluon distribution and fragmentation functions) which introduces some uncertainties when one tries to give precise quantitative tests of QCD. We share [6] the belief that one should not be discouraged by these uncertainties. The point is that the theory makes predictions for a large number [7],[8] of hard scattering, inclusive, processes:

e^+e^- annihilation, photon-photon collisions, leptoproduction, Drell-Yan, production of hadrons and jets at large transverse momentum in hadronic collisions, etc. A clear disagreement between experiment and theory for any one of these would be enough to invalidate this approach to hadron dynamics. In all cases there is no qualitative disagreement between experiment and theory[7],[8] provided theory is extended to subleading orders when they are non negligible. At the present stage the strongest argument in favour of Quantum Chromodynamics is not so much the success of any individual test, but rather its failure to disagree with experiment in any of a wide variety of potentially fatal tests.

APPENDIX A

Parametrization of the parton distributions for the proton.

Set (I): [Reproduced from J.F. Owens and E. Reya (Ref. 16)].

$$u_v(x,Q^2) + d_v(x,Q^2) = \frac{3}{B(\eta_1, 1+\eta_2)} x^{\eta_1}(1-x)^{\eta_2}$$

$$d_v(x,Q^2) = \frac{1}{B(\eta_3, 1+\eta_4)} x^{\eta_3}(1-x)^{\eta_4}$$

with

$$\eta_1 = 0.7 - 0.176\,\bar{s} \quad , \quad \eta_2 = 2.6 + 0.8\bar{s}$$

$$\eta_3 = 0.85 - 0.24\,\bar{s} \quad , \quad \eta_4 = 3.35 + 0.816\,\bar{s}$$

where $\bar{s} = \log\left[\log(Q^2/\Lambda^2)/\log(Q_o^2/\Lambda^2)\right]$, $Q_o^2 = 1.8$ GeV and $\Lambda \approx 0.5$. The sea (t) and gluon (g) distributions are given by:

$$t(x,Q^2) = A_t(1-x)^{\eta_t} + A'_t(1-x)^{\eta'_t} + B_t e^{-C_t x}$$

$$g(x,Q^2) = A_g(1-x)^{\eta_g} + A'_g(1-x)^{\eta'_g} + B_g e^{-C_g x}$$

with

$$A_t \simeq 0.15 - 0.12\bar{s} + 0.03\bar{s}^2 \quad , \quad A_g \simeq 2.41 - 1.98\bar{s} + 0.44\bar{s}^2$$

$$A'_t \simeq 0.185\,\bar{s} - 0.061\bar{s}^2 \quad , \quad A'_g \simeq 3.6\bar{s} - 1.41\bar{s}^2$$

$$\eta_t \simeq 7.0 + 0.022\bar{s} + 0.004\bar{s}^2 \quad , \quad \eta_g \simeq 5.0 + 1.55\bar{s} - 0.529\bar{s}^2$$

$$\eta'_t \simeq 9.5 + 1.017\bar{s} - 0.105\bar{s}^2 \quad , \quad \eta'_g \simeq 13.8 + 0.79\bar{s} - 0.28\bar{s}^2$$

$$B_t \simeq 0.169\bar{s} + 0.447\bar{s}^2 \quad , \quad B_g \simeq 7.66\bar{s} - 1.46\bar{s}^2$$

$$C_t \simeq 25.89 + 3.96\bar{s} + 1.63\bar{s}^2 \quad , \quad C_g \simeq 36.79 + 12.59\bar{s} - 1.16\bar{s}^2$$

Notice that throughout our work we use momentum distributions. In the valence distributions $B(\eta_i, \eta_j)$ $(i=1,2,3)$ is the Euler Beta function which ensures baryon number conservation for all values of Q^2. These parametrizations are valid for $x \gtrsim 0.02$ and $0 \leq \bar{s} \leq 1.6$.

APPENDIX B

Parametrization of the parton distributions inside the pion.

Set (i): [Reproduced from J.F. Owens and E. Reya (Ref. 16)].

$$V(x,Q^2) = \frac{1}{B(\eta_1, 1+\eta_2)} \; x^{\eta_1}(1-x)^{\eta_2} \qquad (B1)$$

with

$$\eta_1 = 0.5 - 0.1037\,\bar{s} \quad , \quad \eta_2 = 1 + 0.6912\,\bar{s}$$

with $\bar{s} = \log\left[\log(Q^2/\Lambda^2)/\log(Q_0^2/\Lambda^2)\right]$, $Q_0^2 = 3\ \text{GeV}^2$, and $\Lambda \simeq 0.5$ GeV. The sea(ξ) and gluon(g_π) distributions are parametrized as in the proton (see Appendix A) but with:

$$A_\xi \simeq 0.1 - 0.068\,\bar{s} + 0.017\,\bar{s}^2 \quad , \quad A_g \simeq 2.0 - 1.955\,\bar{s} + 0.51\,\bar{s}^2$$

$$A'_\xi \simeq 0.161\,\bar{s} - 0.051\,\bar{s}^2 \quad , \quad A'_g \simeq 3.789\,\bar{s} - 1.784\,\bar{s}^2$$

$$\eta_\xi \simeq 5.0 - 0.265\,\bar{s} + 0.338\,\bar{s}^2 \quad , \quad \eta_g \simeq 3.0 + 1.444\,\bar{s} - 0.585\,\bar{s}^2$$

$$\eta'_\xi \simeq 6.533 + 1.701\,\bar{s} + 0.06\,\bar{s}^2 \quad , \quad \eta'_g \simeq 6.577 + 4.715\,\bar{s} - 1.963\,\bar{s}^2$$

$$B_\xi \simeq 0.144\,\bar{s}^2 + 0.051\,\bar{s}^2 \quad , \quad B_g \simeq 8.125\,\bar{s} - 9.024\,\bar{s}^2$$

$$C_\xi \simeq 29.49 + 3.884\,\bar{s} + 0.586\,\bar{s}^2 \quad , \quad C_g \simeq 57.86 - 24.447\,\bar{s} + 8.688\,\bar{s}^2$$

Set (ii): (Reproduced from S.L. Papadopoulos, Ref. 20)

This parametrization uses an improved Parisi and Sourlas method (Ref. 20). The various distribution functions of the pion are parametrized as:

$$q_j(x,Q^2) = x^{\beta_j}(1-x)^{\alpha_j(5)} \sum_{K=0}^{6} C_{jK}(5)\, x^K \qquad (B.2)$$

The expressions for β_j are given in Table 2. The contants $C_{jk}(Q^2)$ for p_T=2,4,6,8,10 are given in Tables 4,5,6,7 and 8 respectively. The number of Jacobi polynomials that have been used to approximate sufficiently well[20] the q_js', is 7. For both parametrizations [Set (i) and Set (ii)] the following conventional decomposition has been assumed: (see also TABLE 2).

$$u_{\pi^+} = \bar{d}_{\pi^+} = \bar{u}_{\pi^-} = d_{\pi^-} \equiv V + \xi \qquad (B.3)$$

$$\bar{u}_{\pi^+} = d_{\pi^+} = u_{\pi^-} = \bar{d}_{\pi^-} \simeq s_{\pi^\pm} \equiv \xi \qquad (B.4)$$

GLUON FRAGMENTATION FUNCTION $D\pi/g(x_e,Q^2)$.

The parametrization uses the improved Parisi and Souslas method[20],[57] as before. The gluon fragmentation is parametrized as:

$$g_\pi(x_e,Q^2) = x_e^{\beta_g}(1-x_e)^{\alpha_g(5)} \sum_{K=0}^{8} C_{gK}\, x_e^K \qquad (B.5)$$

For the coefficients β_g and $\alpha_g(\bar{s})$ see Table 3. For C_{gk} see Tables 9, 10. ($Q^2 = 3$ GeV).

APPENDIX C

We present here the analytic expressions that enter the 1P inclusive cross-section (Eq. 2.17 and 2.38).

$$\sum_{i,j} e_i^2 F_{q_i/A}(x_1) F_{q_j/B}(x_2) \frac{d\hat{\sigma}}{d\hat{t}} q_i q_j \quad + \quad A \leftrightarrow B$$

where i,j run over all 3 quark and antiquark flavours f and q_i or q_j can be a gluon (for "Compton" scattering). By a (') we distinguish the arguments (x_1, x_2) of the structure functions.

The quark charge assignments are:

$$e_u^2 = e_c^2 = e_{\bar{u}}^2 = e_{\bar{c}}^2 = \frac{4}{9}$$

$$e_s^2 = e_d^2 = e_{\bar{s}}^2 = e_{\bar{d}}^2 = \frac{1}{9}$$

We shall make explicit use of the decompositions given by: Eqs. (3.4), (3.5), (3.6), (3.7), (3.8), (3.18), (3.19) and Eqs. (B3) and (B4) from Appendix B. The $\frac{d\hat{\sigma}}{d\hat{t}} q_i q_j$ and $\frac{d\hat{\sigma}}{d\hat{u}} q_i q_j$ for "Compton" and "Annihilation" are given in Eq. (2.23) and Eq. (2.24) and for Bremsstrahlung in Eqs. (2.30a) and (2.33).

p+p +x, A=B=p, (f runs over $q,\bar{q}$ flavours and gluon).

$p + p \to \gamma + X$, $A = B = p$, (f runs over $q,\bar{q}$ flavours and gluon)

For $q(\bar{q})g \to q(\bar{q})\gamma$:

$$\sum_i^{2f} e_i^2 F_{q_i/p}(x_1) F_{g/p}(x_2) \frac{d\hat{\sigma}}{d\hat{t}} qg \quad + \sum_i^{2f} e_i^2 F_{q_i/p}(x_1) F_{g/p}(x_2) \frac{d\hat{\sigma}}{d\hat{u}} qg =$$

$$\left[e_u^2(F_{u/p}+F_{\bar{u}/p})+e_d^2(F_{d/p}+F_{\bar{d}/p})+e_s^2(F_{s/p}+F_{\bar{s}/p})\right]F'_{g/\pi}\frac{d\sigma}{d\hat{t}}\,qg+$$

$$\left[e_u^2(F'_{u/p}+F'_{\bar{u}/p})+e_d^2(F'_{d/p}+F'_{\bar{d}/p})+e_s^2(F'_{s/p}+F'_{\bar{s}/p})\right]F_{g/p}\frac{d\sigma}{d\hat{u}}\,qg=$$

$$=\frac{1}{9}\left[4u_v+d_v+12t\right]g'\frac{d\sigma}{d\hat{t}}\,qg+\frac{1}{9}\left[4u'_v+d'_v+12t'\right]g\frac{d\sigma}{d\hat{u}}\,qg$$

For $q\bar{q}\to g\gamma$ (f runs over quarks only).

$$\sum_i^f e_i^2 F_{q_i/p}F'_{\bar{q}_i/p}\frac{d\sigma}{d\hat{t}}\,q\bar{q}+\sum_i^f e_i^2 F'_{q_i/p}F_{\bar{q}_i/p}\frac{d\sigma}{d\hat{u}}\,q\bar{q}=$$

$$=\left[e_u^2(F_{u/p}F'_{\bar{u}/p})+e_d^2(F_{d/p}F'_{\bar{d}/p})+e_s^2(F_{s/p}F'_{\bar{s}/p})+\right.$$

$$\left.+e_u^2(F'_{u/p}F_{\bar{u}/p})+e_d^2(F'_{d/p}F_{\bar{d}/p})+e_s^2(F'_{s/p}F_{s/p})\right]\frac{d\sigma}{d\hat{t}}\,q\bar{q}=$$

$$=\frac{1}{9}\left[4(u_vt'+u'_vt)+(d_vt'+d'_vt)+12tt'\right]\frac{d\sigma}{d\hat{t}}\,q\bar{q}$$

<u>For the Bremsstrahlung ($qq\to qq\gamma$) cross section we select:</u>

$$\sum_{i=j}^f e_i^2 F_{q_i/p}F'_{q_j/p}\frac{d\sigma^{(Brems)}}{d\hat{t}}+\sum_{i=j}^f e_i^2 F'_{q_i/p}F_{q_j/p}\frac{d\sigma^{(Brems)}}{d\hat{u}}$$ and

neglecting sea quarks contributions we get:

$$\left[e_u^2F_{u/p}F'_{u/p}+e_d^2F_{d/p}F'_{d/p}\right]\frac{d\sigma^{(Brems)}}{d\hat{t}}+$$

$$+\left[e_u^2F'_{u/p}F_{u/p}+e_d^2F'_{d/p}F_{d/p}\right]\frac{d\sigma^{(Brems)}}{dt}=$$

$$=\frac{1}{9}\left[4uu'+dd'\right]\left(\frac{d\sigma^{(Brems)}}{d\hat{t}}+\frac{d\sigma^{(Brems)}}{d\hat{u}}\right)$$

where u,d now are <u>probability distributions</u>

$\pi^- + p \to \gamma + X$, $A = \pi^-$, $B = p$

For $q(\bar{q})g \to q(\bar{q})\gamma$:

$$\sum_i^{2f} e_i^2 F_{q_i/\pi^-} F'_{g/p} \frac{d\sigma}{d\hat{t}} qg + (\pi^- \leftrightarrow p) =$$

$$= \frac{1}{9}\left[5V + 12\xi\right] g' \frac{d\sigma}{d\hat{t}} qg + \frac{1}{9}\left[4u_v' + d_v' + 12t\right] g_\pi \frac{d\sigma}{d\hat{u}} qg$$

. For $q\bar{q} \to g\gamma$: (f runs over 3 flavours only)

$$\sum_i^{f} e_i^2 F_{q_i/\pi^-} F'_{\bar{q}_i/p} \frac{d\sigma}{d\hat{t}} q\bar{q} + (\pi^- \leftrightarrow p) =$$

$$= \frac{1}{9}\left[12\xi t' + 5Vt' + 4Vu_v' + \xi d_v'\right] \frac{d\sigma}{d\hat{t}} q\bar{q}$$

$\bar{p} + p \to \gamma + x$, $A = p$, $B = \bar{p}$.

For $q(\bar{q})g \to q(\bar{q})\gamma$:

$$\sum_i^{2f} e_i^2 F_{q_i/p} F'_{\bar{q}_i/p} \frac{d\sigma}{d\hat{t}} q\bar{q} + (p \leftrightarrow \bar{p}) =$$

$$= \frac{1}{9}\left[4u_v + d_v + 12t\right] g' \frac{d\sigma}{d\hat{t}} qg + \frac{1}{9}\left[4u_v' + d_v' + 12t'\right] g \frac{d\sigma}{d\hat{u}} qg$$

For $q\bar{q} \to g\gamma$:

$$\sum_i^{f} e_i^2 F_{q_i/p} F'_{\bar{q}_i/\bar{p}} \frac{d\sigma}{d\hat{t}} q\bar{q} + (p \leftrightarrow p) =$$

$$= \frac{1}{9}\left[4uu' + dd' + 7tt'\right] \frac{d\sigma}{d\hat{t}} q\bar{q}$$

APPENDIX D

In the following we shall derive certain relations between the various S symbols defined in (4.13) and prove Eq. (4.15). For $q(\bar{q})g \to q(\bar{q})\gamma$ with the subsequent fragmentation of the quark (antiquark) to a hadron we have:

$$S_A^h(qg) = \sigma^{qg}\left[F_{g/P}\sum_{q,\bar{q}} e_q^2 F_{q/A} D_{h/q} + F_{g/A}\sum_{q,\bar{q}} e_q^2 F_{g/P} D_{h/q}\right] \tag{D1}$$

For $q\bar{q} \to g\gamma$ "Annihilation" with the subsequent fragmentation of the gluon to a hadron, we have:

$$S_A^h(q\bar{q}) = \sigma^{q\bar{q}} D_{h/g}\left[\sum_q e_q^2 (F_{q/A}F_{\bar{q}/A} + F_{\bar{q}/A}F_{q/A})\right] \tag{D2}$$

$D_{h/q}$ is a function of x_e and Q^2. $\sum_q$ runs over quark flavours only, $\sum_{q,\bar{q}}$ over quark-antiquark. From (D1), (D2) and definitions (4.14) we get:

$$S_{A-\bar{A}}^h(qg) = \sigma^{qg} F_{g/P}\sum_q e_q^2 (F_{q/A} - F_{q/\bar{A}})(D_{h/q} - D_{h/\bar{q}}) \tag{D3}$$

where we have used the obvious relation,

$$F_{q/\bar{A}} = F_{\bar{q}/A} \quad \text{and} \quad F_{q/A} = F_{\bar{q}/\bar{A}}$$

and the identity:

$$\sum_{q,\bar{q}} e_q^2 (F_{q/A} - F_{q/\bar{A}}) D_{h/q} = \sum_q e_q^2 (F_{q/A} - F_{q/\bar{A}})(D_{h/q} - D_{h/\bar{q}}) \tag{I}$$

In a similar way and using (I) we get:

$$S^{h}_{A-\bar{A}}(q\bar{q}) = -\sigma^{q\bar{q}} D_{h/g} \sum_q e_q^2 (F_{q/A} - F_{\bar{q}/A})(F_{q/P} - F_{\bar{q}/P}) \qquad (D4)$$

We collect here some necessary formulas for the distribution functions for convenience.

(i) $F_{q/p} = q \qquad e_u^2 = e_c^2 = \frac{4}{9}, \quad e_d^2 = e_s^2 = \frac{1}{9}, \quad q = u,d,s$

$u = u_v + t_u \qquad s = \bar{s} = t_s \qquad \bar{u} = t_u$

$d = d_v + t_d \qquad c = \bar{c} = t_c \qquad \bar{d} = t_d$

(ii) $u - \bar{u} = u_v, \qquad d - \bar{d} = d_v, \qquad s - \bar{s} = 0, \quad c - \bar{c} = 0$

(iii) $u_{\pi^+} - \bar{u}_{\pi^+} = d_{\pi^-} - \bar{d}_{\pi^-} = -(d_{\pi^+} - \bar{d}_{\pi^+}) = -(u_{\pi^-} - \bar{u}_{\pi^-}) = V$

(see also Eqs. (4.22), (4.23), (4.24) for fragmentation functions). Then, using (D.4) and (i),(ii),(iii) we have:

$$S^{\pi^+}_{\pi^+-\pi^-} = -\sigma^{q\bar{q}} D_{\pi^+/g} \sum_q e_q^2 (q_{\pi^+} - \bar{q}_{\pi^+})(q - \bar{q}) =$$

$$= -\frac{\sigma^{q\bar{q}}}{9}\left[4u_v - d_v\right] V D_{\pi^+/g} \qquad (D.5)$$

Using (D3) and (i),(ii),(iii) we get:

$$S^{\pi^+}_{\pi^+-\pi^-}(qg) = \sigma^{qg} F_{g/p} \sum_q e_q^2 (q_{\pi^+} - \bar{q}_{\pi^+})(D_{\pi^+/q} - D_{\pi^+/\bar{q}}) =$$

$$= \frac{5}{9} \sigma^{qg} V D^V F_{g/p} \qquad (D.6)$$

Repeating the calculation (D.5), but with $h = \pi^-$, and assuming $D_{\pi^+/g} = D_{\pi^-/g} = D_{\pi^0/g} = D_{\pi/g}$ we get:

$$S^{\pi^-}_{\pi^+\pi^-}(q\bar{q}) = -\frac{\sigma^{q\bar{q}}}{g}\left[4u_v - d_v\right] V \; D_{\pi^-/g} = (D5) \qquad (D.7)$$

Similarly, using (D3) and $h = \pi^-$ we get:

$$S^{\pi^+}_{\pi^+\pi^-}(qg) = -\frac{5}{g}\sigma^{qg} \; V \; D^V \; F_{g/p} \qquad (D8)$$

If we define: $S^{\pi^0}_{\pi^+\pi^-} = \frac{1}{2}\left(S^{\pi^+}_{\pi^+\pi^-} + S^{\pi^-}_{\pi^+\pi^-}\right)$

and sum (D5),(D6),(D7),(D8) then:

$$S^{\pi^0}_{\pi^+\pi^-} = -\frac{\sigma^{q\bar{q}}}{g}\left[4u_v - d_v\right] V \; D_{\pi/g}$$

Q.E.D.

For more formulas see Ref. 20 of Chapter III.

REFERENCES

INTRODUCTION

1. F. Close, An Introduction to Quarks and Partons, Academic Press, (1979).
2. J. Ellis, "Gluons", TH-2817-CERN preprint (Submitted to Comments on Nuclear and Particle Physics).
3. H. Fritzsch and P. Minkowski, Phys. Lett. 69B (1977) 316.
4. F. Halzen and D.M. Scott, Phys. Rev. Lett. 40 (1978) 1117.
5. R. Ruckl, S. Brodsky and J. Gunion, Phys. Rev. D18 (1978) 2469.
6. A.P. Contogouris, S. Papadopoulos and M. Hongoh, Phys. Rev. D19 (1979), 2607.
7. S. Petrarca and F. Rapuano, Phys. Lett. 88B (1979) 167.

CHAPTER I

1. J.D. Bjorken and S.D. Drell, Relativistic Quantum Mechanics, McGraw Hill (1964).
2. S. Weinberg, Phys. Rev. Lett. 19 (1967) 1264.
3. A. Salam, Elementary Particle Physics: Relativistic Groups and Analyticity, Edited by N. Svartholm, Almquist and Wiskell, (1968), Stockholm.
4. E.S. Abers and B.W. Lee, Phys. Reports 9C (1973) 1.
5. C.N. Yang and R.L. Mills, Phys. Rev. 96 (1954) 191.
6. H. Fritzsch and M. Gell-Mann, Proc. XVI International Conference on High-Energy Physics 2 (1972) 135.

REFERENCES Cont'd.

7. R.P. Feynman, Acta Phys. Polon. 26 (1963) 697.
L.D. Fadeev and Y.N. Popov, Phys. Lett. 25B (1967) 29.
8. G. t'Hooft, Nucl. Phys. 33B (1971) 173; ibid 35B (1971) 167. For a review see: M. Veltman, Proc. of 6th Inter. Conf. on Electron and Photon Interactions at High Energies.
9. O.W. Greenberg, Phys. Rev. Lett. 13 (1964) 598.
10. M. Han and Y. Nambu, Phys. Rev. 139 (1965) 1006.
11. V. de Alfaro, S. Fubini, G. Furlan and G. Rossetti, Currents in Hadron Physics, North-Holland, (1973), Amsterdam.
12. S.L. Adler, Phys. Rev. 137 (1965) 1022B.
13. C. Bouchiat, J. Iliopoulos and Ph. Meyer, Phys. Lett. 38B (1972) 519.
14. E. de Rafael, Quantum Chromodynamics as a Theoretical framework of the Hadronic Interactions, Extract from a course given at the School of Particle Phys. Gif-sur Yvette-4-9 Septembre 1978.
15. J.C. Taylor, Gauge Theories of Weak Interactions, Cambridge Univ. Press (1974) Cambridge.
16. M. Gell-Mann and F.E. Low, Phys. Rev. 95 (1954) 1300.
17. E.C. Stueckelberg and A. Peterman, Helv. Phys. Acta 26 (1953) 499.
18. K.G. Wilson, Phys. Rev. D3 (1971) 1818.
19. R.P. Feynman, Photon-Hadron Interactions, Benjamin, N.Y. (1972).

20. F. Martin and B. Gaillard, TH-2803-CERN preprint (in French) 1979.

21. W.B. Atwood, Lectures at the SLAC Summer Institute on Particle Physics: Quantum Chromodynamics, at Stanford, California. SLAC-PUB-2428 (1979).

22. J.D. Bjorken, Phys. Rev. Lett. 16 (1966) 408.

23. S.L. Adler, Phys. Rev. 143 (1966) 1144.

24. J.S. Poucher et al., Phys. Rev. Lett. 32 (1974) 118.

25. A. Bodek et al., SLAC-PUB-1327.

26. E.M. Riordan, Ph.D. Thesis, MIT LNS R.

27. R.P. Feynman, Phys. Rev. Lett. 23 (1969) 1415.
J.D. Bjorken and E.A. Paschos, Phys. Rev. 185 (1969) 1975.

28. H.D. Politzer, Nucl. Phys. B129 (1977) 301.

29. M.K. Gaillard, TH-03-LAPP preprint (1979).

30. R.K. Ellis, H. Georgi, M. Machacek, H.D. Politzer and G.G. Ross, Nucl. Phys. B152 (1979) 285.

31. J. Ellis and C.T. Sachrajda, Proceedings of the 1979 Cargèse Summer Institute on QUARKS AND LEPTONS July 1979 (TH-2782-CERN preprint).

32. G. Altarelli and G. Parisi, Nucl. Phys. 126B (1977) 298. For a review see: A. Buras, Rev. of Mod. Phys., Vol. 52, No. 1 (1980).

33. For a pedagogical introduction to scale violations see: J.F. Gunion, Lecture notes delivered at U.C. San Diego (1979).

34. A. Buras and K. Gaemers, Phys. Lett. 71B (1977) 186.
Nucl. Phys. 132B (1978) 249.

35. J. Owens and E. Reya, Phys. Rev. D17 (1978) 3003.

36. A. Bialas and A. Büras, Fermilab-Pub-79/73-THY preprint.

37. G. Parisi and N. Sourlas, Nucl. Phys. B151 (1979) 421.

38. S.L. Papadopoulos, Ph.D. Thesis, McGill Univ. (in preparation.

39. C_k are Q^2-dependent (see Ref. 37). However we used the parametrization of Ref. 38 which calculates at each Q^2 a set of values for the C_k.

40. J. Owens, Phys. Lett. 76B (1978) 85.

41. T. Uematsu, Phys. Lett. 79B (1978) 97.

CHAPTER II

1. S. Berman, J. Bjorken and J. Kogut, Phys. Rev. D4 (1971). 3388.

2. S. Ellis and M. Kisslinger, Phys. Rev. D9 (1974) 2027.

3. F. Büsser et al., Phys. Lett. 46B (1973) 471.

4. R. Blakenbecler, S. Bordsky and J. Gunion, Phys. Lett. 39B (1972) 649; Phys. Rev. D6 (1972) 2652; Phys. Lett. 42B (1973) 461; Phys. Rev. D8 (1973) 287.

5. S. Brodsky and G. Farrar, Phys. Rev. Lett. 31 (1973) 1153; Phys. Rev. D11 (1975) 1309.

6. V. Matveev, R.M. Muradyan and A.N. Tavkhelidze, Lett. Nuov. Cim. 7 (1973) 719.

7. J.D. Bjorken, "High-p_T dynamics". Lectures delivered at the SLAC Summer Institute on Particle Physics, July 1975.

8. S. Ellis, M. Jacob and P.V. Landshoff, Nucl. Phys. B108 (1976) 93.

9. G. Ranft and J. Ranft, Nucl. Phys. B110 (1976) 493.

10. R. Baier et al., Nucl. Phys. B118 (1977) 139.

11. J. Kripfganz and J. Ranft, Nucl. Phys. B124 (1977) 353.

12. H.D. Politzer, Phys. Rev. Lett. 30 (1973) 1346.

13. D.J. Gross and F.A. Wilczek, Phys. Rev. Letters 30 (1973) 1343.

14. See Ref. 21 of CHAPT. I for a review.

15. R. Hwa, A. Spiessbach and M. Teper, Phys. Rev. Lett. 36 (1976) 1418; Phys. Rev. D18 (1978) 1475.

16. A.P. Contogouris, R. Gaskell and A. Nicolaidis, Phys. Rev. D17 (1978) 839.

17. E. Fishbach and G. Look, Phys. Rev. D15 (1977) 2576; Phys. Rev. D16 (1977) 1369; Phys. Rev. D16 (1977) 1571.

18. D. Duke, Phys. Rev. D16 (1977) 1375.

19. A. Buras and K. Gaemers, Nucl. Phys. B132 (1978) 249.

20. J. Owens and E. Reya, Phys. Rev. D17 (1978) 3003.

21. B. Combridge, J. Kripfganz and J. Ranft, Phys. Lett. 70B (1977) 234.

22. R. Cutler and D. Sivers, Phys. Rev. D16 (1977) 679.

23. J. Owens, E. Reya and M. Glück, Phys. Rev. D18 (1978) 1501.

24. A.P. Contogouris, R. Gaskell and S. Papadopoulos, Phys. Rev. D17 (1978) 2314.

25. R. Field, Phys. Rev. Lett. 40 (1978) 997.

26. C. Kourkoumeli et al., Phys. Lett. 84B (1979) 271.

27. A. Angelis et al., Phys. Lett. 79B (1978) 505; Physica Scripta 19 (1979) 116.

28. A. Clark et al., Nucl. Phys. B142 (1978) 189.

29. R. Ellis, H. Georgi, M. Machacek, H.D. Politzer and G. Ross, Nucl. Phys. B152 (1979) 285.

30. See Ref. 31, Chapt. I.

31. V. Gribov and I. Lipatov, Sov. J. Nucl. Phys. 15 (1972) 675.

32. See for example: Ref. 4 of Introduction.

33. R. Rückl, S. Brodsky and J. Gunion, Phys. Rev. D18 (1978) 2469.

34. H. Fritzsch and P. Minkowski, Phys. Lett. 69B (1977) 316.

35. See Ref. 6 of Introduction.

36. R. Cutler and D. Sivers, Phys. Rev. D16 (1977) 679.

37. W. Bardeen, A. Buras, D. Duke and T. Muta, Phys. Rev. D18 (1978) 3998.

38. P. Bosetti et al., Nucl. Phys. B142 (1978) 1.

39. J. de Groot et al., Phys. Lett. 82B (1979) 45; Z. Physik. C. Particles and Fields 1 (1979) 143.

40. J. Kripfganz and A.P. Contogouris, Phys. Lett. B84 (1979) 473.

41. A. Contogouris and J. Kripfganz, Phys. Rev. D20 (1979) 2295.

42. A. Schellekens and W. van Neerven, Phys. Rev. D21 (1980) 2619.

43. A. Contogouris, R. Gaskell and L. Marleau, Phys. Rev. D1 (in press).

44. M. Chaichian, M. Hayashi and T. Honkaranta, Univ. of Helsinki preprint HU-TFT-80-9 (1980).

45. P. Aurenche and J. Lindfors, TH-2768-CERN preprint (1980).

46. A. Contogouris, J. Kripfganz, L. Marleau and S. Papadopoulos, Proceedings of the XV Rencontre de Moriond, Les Arcs-Savoie 1980 (to be edited by J. Tran Thanh Van).

47. A.P. Contogouris, S. Papadopoulos and C. Papavassiliou, McGill preprint (1980) (to be published in Nucl. Phys. B).

48. A. Contogouris, L. Marleau and S. Papadopoulos, Phys. Rev. D (in press).

49. G. Altarelli and G. Parisi, Nucl. Phys. B126 (1977). 298.

50. W. Bardeen and A. Buras, Phys. Lett. 86B (1979) 61; A. Buras, Fermilab-Pub-79/17-THY (1979).

51. A. Gonsales-Arroyo, C. Lopez and F.J. Yndurain, Nucl. Phys. B153 (1979) 161.

52. A. Gonsales-Arroyo and C. Lopez, TH-2734-CERN preprint (1979).

53. J. Cumalat, Invited talk in the APS meeting of the division of Particles and Fields, Montreal, October 1979.

54. A.J. Lankford, CERN-EP-Internal report 78-3 (1978).

55. P. Darriulat et al., Nucl. Phys. B107 (1976) 429.

56. M. Della Negra, Proc. 7th International Colloquium on Multiparticle Reactions, Tutzing, West Germany (Max Planck Inst., Munich, 1976) 189.

57. T. Modis et al., Talk 14th Rencontre de Moriond Conference 11-17 March 1979, Les Arcs, Savoire, France.

58. G. Donaldson et al., Phys. Rev. Lett. 36 (1976) 1110.

59. R. Blankenbecler, S. Brodsky and J. Gunion, Phys. Rev. D6 (1972) 2652; Phys. Lett. 42B (1973) 461; R. Blakenbecler and S. Brodsky, Phys. Rev. D10 (1974) 2973; J. Gunion, Phys. Rev. D10, (1974) 242; R. Blankenbecler, S. Brodsky and J. Gunion, Phys. Rev. D12 (1975) 3469.

60. D. Sivers, S. Brodsky and R. Blankenbecler, Phys. Reports 23C, 1 (1976).

61. P. Landshof and T. Polkinghorne, Phys. Rev. D8 (1978) 927.

62. R. Blankenbecler, S. Brodsky and J. Gunion, Phys. Rev. D18 (1978) 900.

63. G. Farrar and G. Fox, Rutgers Univ. preprint RU-79-170.

64. W. Stirling, Invited talk presented at the UK High Energy Physics Forum on Strong Interactions (Abingdon, April, 1979), Cambridge preprint, DAMTP 79/10.

65. D. Jones and J. Gunion, Phys. Rev. D19 (1979) 870.

CHAPTER III.

1. R.P. Feynman, Photon-Hadron Interactions (Benjamin, New York, 1972).

2. B. Gordon et al., Phys. Rev. Lett. 41 (1978) 615.

3. P. Bosetti et al., Nucl. Phys. B142 (1978) 1.

4. de Groot et al., Phys. Lett. 82B (1979) 45.
Zeits. Phys. C (1979) 143.

5. A. Bodek et al., Phys. Review. D20 (1979) 1471.

6. E. Fernandez et al., Phys. Rev. Lett. 43 (1979) 1975.

7. A. Benvenuti et al., Phys. Rev. Lett. 42 (1979) 149.

8. G. Altarelli and Martinelli, Phys. Lett. 76B (1978) 89.

9. H. Anderson, H. Matis and L. Myrianthopoulos, Phys. Rev. Lett. 40 (1978) 1061.

10. M. Glück and E. Reya, Nucl. Phys. B156 (1979) 456.

11. W.K. Tung, Phys. Rev. D17 (1978) 738.

12. A. Mendez and Weiler, Phys. Lett. 83B (1979) 221.

13. G. Altarelli and G. Parisi, Nucl. Phys. B126 (1977) 298.

14. R. Feynman, R. Field and G. Fox, Phys. Rev. D18 (1978) 3320.

15. M. Gluck, E. Hoffmann and E. Reya, Dortmund preprint DO-TH 80/13, May 1980.

16. J. Owens and E. Reya, Phys. Rev. D17 (1978) 3003.

17. M. Gluck and E. Reya, Phys. Rev. D14 (1976) 3034.

18. A.P. Contogouris, S. Papadopoulos and M. Hongoh, Phys. Rev. D19 (1979) 2607.

19. G. Fox, Nucl. Phys. B131 (1977) 107; B134 (1978) 269.

20. S. Papadopoulos, Ph.D. Thesis, McGill Univ. (in preparation).

21. D. McCal et al., Phys. Lett. 85B (1979) 485.

22. B. Combridge, J. Kripfganz and J. Ranft, Phys. Lett. 70B (1977) 234.

23. F. Martin, Phys. Rev. D19 (1979) 1382.
T.A. DeGrand, Nucl. Phys. B151 (1979) 485.

24. J.F. Owens, Phys. Rev. D19 (1979) 3279.
Phys. Rev. D20 (1979) 221.

25. J.F. Owens and J.D. Kimel, Phys. Rev. D18 (1978) 3313.

26. J. Alonso et al., Nucl. Phys. B157 (1979) 498.

27. M. Fontannaz and D. Schiff, Nucl. Phys. B132 (1978) 457.

28. M. Chase, Nucl. Phys. B145 (1978) 189.

29. M. Binkley et al., Phys. Rev. Lett. 37 (1976) 574; H.L. Anderson et al., Phys. Rev. Lett. 37 (1976) 799; Hom et al., Phys. Rev. Lett. 37 (1976) 1374.

30. L. Lederman, in Proceedings of the 1977 European Conference on Particle Physics, Budapest, ed. by L. Jenik and I. Montvay (GRIP, Budapest) I (1978) 303.

31. C.N. Brown, review talk in "Particles and Fields '77", Proceedings of the Annual Meeting of the Division of Particles and Fields of the APS, Argonne (AIP-1978), p. 375; D. Kaplan et al., (Stony Brook-Fermilab-Columbia Collaboration) report, 1977.

32. G. Altarelli, G. Parisi and R. Petronzio, Phys. Lett. 76B (1978) 351 and 356.

33. Yu. L. Dokshitser, D.I. D'Yakonov and S.I. Troyan, Phys. Lett. 79B (1978) 269.

34. G. Parisi and R. Petronzio, TH-2627-CERN preprint.

35. D. Sivers, R. Blankenbecler and S. Brodsky, Phys. Rep. 23C (1976) 1.

36. A.P. Contogouris, R. Gaskell and S. Papadopoulos, Phys. Rev. D17, (1978) 2314.

37. J. Ranft and G. Ranft, Lett. Nuovo Cimento 20 (1977) 669.

38. R. Baier and B. Petersson, Bielefeld preprints BI-TP-77/08 and 77/10 (1977).

39. W. Caswell, R. Horgan and S. Brodsky, Phys. Rev. D18 (1978) 2415.

40. R. Raitio and R. Sosnowski, Helsinki preprint HU-TFT-77-22 (1977).

41. K. Kinoshita et al., Phys. Lett. 68B (1977) 355.

42. P. Landshoff, J. Polkinghorne and R. Short, Nucl. Phys. B28 (1971) 222; S. Brodsky, F. Close and J. Gunion, Phys. Rev. D8 (1973) 3678.

43. K. Kinoshita and Y. Kinoshita, Progr. Theor. Phys. 5 (1978) 60.

44. S. Horgan and P. Scharbach, Phys. Lett. 81B (1979) 215.

45. See Chapt. II, Ref. 64.

46. M. Diakonou et al., Physics Lett. 87B (1979) 292; Phys. Lett. 91B (1980) 296 (Athens-Athens-Brookhaven-CERN Collaboration).

47. M. Diakonou et al., CERN-EP/80-07, to appear in Zeits. fur Physik C.

48. C. Newman, presented at the XV Rencontre de Moriond (CERN-Columbia-Oxford-Rockefeller-Collaboration).

49. E. Amaldi et al., Nucl. Phys. B150 (1979) 326. (Rome-Brookhaven-CERN-Adelphi Collaboration).

50. R. Baltrusaitis et al., Fermilab report 79/38-EXP (1979); Phys. Rev. Lett. 44 (1980) 122.

51. M. Tannenbaum, Rockefeller Univ. COO-2232A-83.

52. See Ref. 46, Chapt. II.

53. P. Darriulat, CERN-EP/80-16.

54. L. Di Lella, CERN-EP/79-145.

55. G. Donaldson et al., Phys. Rev. Lett. 40 (1978) 917.

56. K. Kato and H. Yamamoto, Tokyo Univ. preprint, UT-335 (1980).

57. G. Parisi and N. Sourlas, Nucl. Phys. B151 (1979) 421.

CHAPTER IV.

1. P. Darriulat, in Proceedings of 18th International Conference on High Energy Physics, Tbilisi, U.S.S.R. (1976).

2. P. Darriulat, Rapporteur talk, Proceedings of the International Conference on H.E. Physics, Palermo (1975), p. 840; Lectures at the Summer Institute on Particle Physics, McGill Univ., Montreal (1976).

3. S.D. Ellis and R. Stroynowski, Rev. of Mool. PHys. 49 (1977) 753.

4. Jacob and P. Landshoff, Phys. Reports 48 (1978) 285.

5. P. Darriulat, CERN-EP/80-16, to be published in Ann. Rev. of Nucl. and Particle Science.

6. See Ref. 29, Chapter II.

7. S. Ellis and M. Kisslinger, Phys. Rev. D9 (1974) 2027.

8. M. Fontannaz and D. Sciff, Nucl. Phys. B132 (1978) 457.

9. A.P. Contogouris, R. Gaskell and S. Papadopoulos, Nuovo Cim. 51A (1979) 263.

10. A.P Contogouris and R. Gaskell, Nucl. Phys. B126 (1977) 157; A.P. Contogouris, R. Gaskell and A. Nicolaidis, Phys. Rev. D17 (1978) 2992.

11. R. Baier, J. Engels and B. Petersson, Univ. of Bielefeld preprint, BI-TP 80/07, April 1980.

12. B.S. Nielsen, Talk presented at the XV Rencontre de Moriond, 1980.

13. See Refs. 5 and 6 of Chapter II.

14. See Ref. 31 of Chapt. II.

15. See Ref. 20 of Chapt. III.

CHAPTER V

1. L. Cormell and J. Owens, Florida Univ. preprint, FSU-HEP-030780, March 1980.

2. F. Halzen, M. Dechantsreiter and D.M. Scott, Univ. of Wisconsin preprint, COO-881-140.

3. K. Kato and H. Yamamoto, Tokyo Univ. preprint, UI-335, January 1980.

4. R. Horgan and P. Scharbach, CERN-TH-2836, March 1980.

5. G. Farrar and G. Fox, Rutgers Univ. preprint RU-79-170.

6. B. Campbell, Ph.D. Thesis, McGill Univ. (1980).

7. For a review see: A. Buras, Rev. of Mod. Phys. Vol. 52, No. 1 (1980).

8. R. Field, CALT-68-696 (1978) preprint.

FOOTNOTES

f_1. These "anomalous" terms, which a priori would spoil the renormalizability of the theory, cancel if, as pointed out by Bouchiat, Iliopoulos and Meyer, quarks are taken to be colourful objects carrying three different colours.

f_2. $\alpha_s(Q^2)$ is calculated at the one-loop renormalization level.

f_3. From Eq. (1.20), and the requirement that $\alpha_s \to 0$ as $Q^2 \to \infty$ we get $f \lesssim 16$. This is the maximum number of flavours one can have without loosing the asymptotic freedom property of QCD.

f_4. Kinoshita and Lee and Nauenberg have proved that for inclusive cross sections, the "mass" singularities associated with final state undetected particles, moving parallel to each other, cancel (the KLN theorem) (see Ref. 30 and references therein).

f_5. By fitting the asymptotic freedom formulas to the moments of F_3, Ref. 37 obtains the scale $\overline{\Lambda} \equiv \Lambda \exp[\frac{1}{2}(\ln 4\pi - \gamma_E)]$ where $\gamma_E = 0.5772$ is the Euler-Mascheroni constant, and where Λ is the scale parameter in the leading log order. The term $\ln 4\pi - \gamma_E$ is an artifact of the dimensional regularization scheme used and should be absorbed through a redefinition of Λ.

Footnotes, Cont'd.

f_6. In this particular estimate of the $(\gamma/\pi^0)_{VDM}$ the ratios (V/π^0) have been assumed constant for different energies[54]

f_7. Notice that the data of Ref. 21 correspond to relatively low s and Q^2 $(=M^2_{\mu^+\mu^-})$. It has been pointed out[21] (and verified by our calculations) that for higher Q^2, corresponding to other higher s data, scale violations increase the effective power of 1-x, so that for x large: $V_\pi(x,Q^2) \sim (1-x)^n$, $n \sim 1$.

f_8. For more details, see latest papers of A$^{\text{e}}$BC on direct γ production.

f_9. The results of Ref. 45 of Chapter II, although in agreement with ours, are presented in a way that is somewhat misleading and gives the impression that the whole Bremsstrahlung contribution [Eq. (2.38) of Chapt. II) is always completely negligible. The reason is that Ref. 45 does not count as correction the part of Eq. (2.34) involving the fragmentation of a quark to a photon (collinear photon emission, second term in the integrand of Eq. (2.34); as we discuss in Chapt. II, Sect. 2.3, this part is the most important. We count as correction everything of order $\alpha\alpha_s^2$) or higher, i.e. everything beyond the "Compton" and "Annihilation" subprocesses. [see Figs. 13(a),13(b)].

Footnotes (Cont'd.)

f_{10}. Due to unassigned energy cut and to the demand that no additional reconstructed shower[46] be present in the calorimeter, the experimental γ/π^0 ratios given in our figures do not correspond to fully inclusive conditions. In order to obtain the fully inclusive γ/π^0 ratio, the experimental points of the A^2 BC Collaboration should be multiplied by a common factor of 0.85 ± 0.15.

f_{11}. The magnitude of the cross-sections of Eq. (4.25) is near the limits of present experimental accuracy. In order to improve the yields we can: a) measure both charged (π^+, π^-) particles; then S^{π^0} is multiplied by a factor of 2. b) measure direct γs for 2π geometry; then S^{π^0} is multiplied by 2π. In this way the yields increase by more than one order of magnitude.

f_{12}. This configuration may be suppressed by additional Sudakov form factors just as $pp \to \mu^+\mu^- + X$ at fixed $Q_T \ll Q$ is. This is discussed by Yu.L. Dokshitzer, D.I. Dyakonov and S.I. Troyan, Phys. Reports 58, 5 (1980) 269-395. In this work however we do not investigate this effect.

TABLE CAPTIONS

1. Constants determining the valence distributions of Set II.
2. Constants that enter Set (ii) of the pion distribution functions (Appendix B, Eq. (B2)). G=4/25.
3. Constants that enter the gluon fragmentation functions to a π (Appendix B, Eq. (B5)).
4. Constants C_{jk} for Set (ii) parametrization of the pion distributions (Appendix B, Eq. (B2). Here p_T=2 GeV.
5. Same as in Table 4 but for p_T=4 GeV.
6. Same as in Table 4 but for p_T=6 GeV.
7. Same as in Table 4 but for p_T=8 GeV.
8. Same as in Table 4 but for p_T=10 GeV.
9. Constants C_{gk} for the parametrization of the gluon fragmentation to a π (Appendix B, Eq. (B5)) for the choice m=3 [Eq. (4.31)].
10. Same as in Table 9 but for the choice m=1.5 [Eq. (4.32)].

FIGURE CAPTIONS

Fig. 1. Self gluon fundamental interaction involving 3-gluons corresponding to Eq. (1.17).

Fig. 2. Self gluon fundamental interaction involving 4-gluons corresponding to Eq. (1.18).

Fig. 3. Lowest order photon-photon interaction in QED, induced by an electron loop.

Fig. 4. Diagrams contributing to the vector-vector-axial vector vertex anomaly (triangle anomaly).

Fig. 5. Graphical representation of the interactions corresponding to Eq. (1.16) QCD and its QED analogon.

Fig. 6. Lowest order contribution to charge renormalization in QED.

Fig. 7. Lowest order contributioons to coupling constant renormalization in QCD.

(a) Fermion contribution.

(b),(c) Gauge boson contributions.

(d) Fadeev-Popov "Ghost" contribution.

Fig. 8. Electroproduction off partons to $\mathcal{O}(\alpha_s)$ in QCD: photon + quark (or gluon) $\rightarrow$ anything

Fig. 9. The "square" of diagram (g), Fig. 8. This diagram contains a mass singularity.

Fig. 10. The Altarelli-Parisi splitting functions and their vertices. The distribution $(1-z)_+^{-1}$ is defined by the equation:

FIGURE CAPTIONS (Cont'd.)

Fig. 10. Cont'd. $\int_0^1 dz f(z)/(1-z)_+ \equiv \int_0^1 dz[f(z)-f(1)]/(1-z)$ where $f(z)$ is any function regular at the end points.

Fig. 11. Dominant contribution to $Ed\sigma/d^3p$. The —.—.—.— line represents quarks and gluons, the shaded blobs represent non-scaling distribution and fragmentation functions and the "B" implies that we take the Born term contribution calculated using the effective quark-gluon coupling, Eq. (2.25).

Fig. 12. Kinematics for $h_1+h_2\to\gamma+X$. The —.—.— as in Fig. 11.

Fig. 13. Feynman graphs of QCD subprocesses included in our calculations. (a) and (b): Born terms (contributions of $O(\alpha_s)$), (c) Photon Bremsstrahlung (contributions of $O(\alpha_s^2)$). C_1, C_2 represent the collinear gluon and photon configurations, respectively.

Fig. 14. Kinematics for the Bremsstrahlung contribution.

Fig. 15. The $qq\to qq$ diagram.

Fig. 16. Feynman diagrams for $e^+e^-\to q\bar{q}\gamma$.

Fig. 17. Production of two particles A and B through vector meson decay (VDM). The dark blob indicates the vector meson-photon coupling. γ_V and m_V are the coupling constants and the masses of the various vector mesons, respectively.

FIGURE CAPTIONS (Cont'd.)

Fig. 18. Dominant CIM contributions to direct photon production ($qM \to q'\gamma$). M ≡ meson.

Fig. 19. The u-valence and glue distributions of our calculations as functions of Q^2. (a) Set I (Ref. 16, Chapt. III) (b) Set II (Refs. 18, 19, Chapt. III).

Fig. 20. Contribution of Born terms to the inclusive cross-section for $pp \to \gamma + X$ at $\theta = 90°$ and predictions for the γ_{tot}/π^0 ratio. k_T effects and the Bremsstrahlung correction have not been taken into account.

Fig. 21. The ratio $R = Ed\sigma^{Brems}/d^3p / Ed\sigma^{qg}/d^3p$ in $pp \to \gamma + X$. The parton distributions are from Ref. 16, Chapt. III.

Fig. 22. (a) Contributions of Born terms and of photon Bremsstrahlung to the inclusive cross-section for $pp \to \gamma + X$ at $\theta_{c.m} = 90°$. Solid lines: Total contribution of $\mathcal{O}(\alpha_s)$ (i.e. $qg \to q\gamma$ and $q\bar{q} \to g\gamma$). Dashed lines: Contribution of $\mathcal{O}(\alpha_s^2)$ (i.e. $qq \to qq\gamma$). For comparison at each energy we give the range of the experimental $pp \to \pi^0 + X$. (b) The effect of partons' intrinsic transverse momentum calculated with a gaussian k_T-distribution of $\langle k_T \rangle = 0.5$ GeV. We denote by $\sigma(k_T)$ the $pp \to \gamma + X$ inclusive corss-section with k_T-effects and by $\sigma(0)$ the same cross-section calculated without k_T-effects ($\langle k_T \rangle = 0$).

FIGURE CAPTIONS (Cont'd.)

Fig. 23. Comparison of the theoretical calculations with data on the γ/π^0 ratio, for $pp \to \gamma + X$, using two different input distributions functions for the gluon. Data are from ϕ (Ref. 49), ϕ ϕ (Refs. 46 (a),(b)), ϕ (Ref. 48). (All Refs. are from Chapt. III).

Fig. 24. Predictions for the ratio γ/π^0 ($\theta_{c.m.}=90°$) compared with data of the A^2 BC Collaboration. Dashed lines: Weak gluon distribution [Eq. (3.5)]. Solid lines: Strong gluon distribution [Eq. (3.12)]. Data: Open circles ($\sqrt{s}=53$) Ref. 46(a), Chapt. III. Closed circles ($\sqrt{s}=31$, 45 and 63 GeV) Ref. 46 (b) (ϕ10)

Fig. 25. Predictions for $Ed\sigma(pp \to \gamma + X)/d^3p$ compared with the data. Dashed and solid lines as in Fig. 24. Data: ϕ Ref. 46(a). ϕ 46(b) (A^2 BC Collab.) (ϕ10). ϕ Ref. 48 (CCOR). ϕ Ref. 49. (All Refs. are from Chapt. III).

Fig. 26. Contributions of the Born terms to $Ed\sigma(\pi^- p \to \gamma + X)/d^3p$ and predictions for the ratio γ/π^0 with a π^- beam. (Solid lines represent calculations where Q^2-dependent distribution functions have been used.) (a) Input distributions of Eq. (3.16) (b) Input distributions of Eq. (3.18). The upper parts of the figure show the adopted $Ed\sigma(\pi^- p \to \pi^0 X)/d^3p \equiv \pi^0$(expt). In the lower parts

FIGURE CAPTIONS Cont'd.

Fig. 26. Cont'd.

the difference between solid and dashed lines shows the magnitude of scale violations. k_T-effects have been ignored.

Fig. 27. Same as in Fig. 26 but including k_T-effects. In the lower parts the difference between solid and dashed lines shows the magnitude of the k_T-effects in $\pi^- p \to \gamma + X$. (Scaling calculations are not represented).

Fig. 28. Contributions of the Born terms to $Ed\sigma(\bar{p}p \to \gamma + X)/d^3p$ and predictions for γ/π^0 with antiproton beams. (Solid lines represent calculations where Q^2-dependent distribution functions have been used). In the upper parts we also show the assumed $Ed\sigma(\bar{p}p \to \pi^0 + X)/d^3p = \pi^0(\text{expt})$. k_T-effects have been ignored.

Fig. 29. Same as in Fig. 28 but including k_T-effects. The dashed lines show the magnitude of the k_T-effects in $\bar{p}p \to \gamma + X$. (Scaling calculations are not presented).

Fig. 30. Kinematics of the large p_T event.

Fig. 31. Illustration of the determination[f11] of the gluon fragmentation function $D\pi^0/g = (D\pi^+/g + D\pi^-/g)/2$: Predictions for the difference $S_{\pi^-}^{\pi^0} - S_{\pi^+}^{\pi^0} = S_{\pi^-}^{\left(\frac{\pi^+ + \pi^-}{2}\right)} - S_{\pi^+}^{\left(\frac{\pi^+ + \pi^-}{2}\right)}$ as a function of the momentum sharing variable x_e for various photon trigger

FIGURE CAPTIONS. Cont'd.

Fig. 31. Cont'd.

momenta p_{T1}. Dashed lines: predictions with m=3 [Eq. (4.31)]. Solid lines: predictions with m=1.5 [Eq. (4.32)].

TABLE 1

c_0	c_1	c_2	c_3	c_0'	c_1'
-40.103	-20.813	2.507	-0.312	34.09	31.206
d_0	d_1	d_2	d_3	d_0'	d_1'
95.557	63.002	3.499	5.370	-62.349	-61.095

TABLE 2

j	$q_j(\pi^-)$	β_j	$\alpha_j(\bar{s})$	$q_j(\pi^+)$
1	$\bar{u}_v$	0.5	$0.5+4G\bar{s}$	u_v
2	d_v	0.5	$0.5+4G\bar{s}$	$\bar{d}_v$
3	ξ	0	$4+4G\bar{s}$	ξ
4	g_{π^-}	0	$2+9G\bar{s}$	g_{π^+}

TABLE 3

	Power of glue	$\alpha_g(\bar{s})$	β_g
Set 1	m=3	$3+9G\bar{s}$	0
Set 2	m=1.5	$1.5+9G\cdot\bar{s}$	0

TABLE 6

j \ k	0	1	2	3	4	5	6
1	0.85358	-1.43592	5.435853	-12.806	17.25334	-12.1401	3.45272
2							
3	0.19101	-1.93688	13.55434	-49.373499	95.11757	-91.44378	34.560229
4	5.194178	-64.749274	429.284274	-1455.01252	2592.4823	-2305.6614	806.091403

TABLE 7

j \ k	0	1	2	3	4	5	6
1	0.87893	-1.66438	6.37437	-15.140368	20.52295	-14.514812	4.146868
2							
3	0.214174	-2.33901	16.55565	-60.681266	117.283686	-112.961839	42.70748
4	5.56704	-73.1892	494.1894	-1696.9476	3056.3437	-2744.1249	967.6442

TABLE 4

j \ k	0	1	2	3	4	5	6
1	0.72371	-0.469321	1.67339	-3.769382	4.917588	-3.368919	0.935841
2							
3	0.081732	-0.430224	2.85859	-10.244338	19.945328	-19.594795	7.674978
4	2.993268	-23.188266	138.391734	-436.886643	735.087172	-622.157118	208.12003

TABLE 5

j \ k	0	1	2	3	4	5	6
1	0.812824	-1.096622	4.074562	-9.470639	12.634276	-8.816753	2.489275
2							
3	0.155498	-1.359682	9.34199	-33.719	64.7397	-62.1958	23.5622
4	4.551748	-51.259594	329.5952	-1093.478	1914.406	-1676.66	578.14738

TABLE 8

j \ k	0	1	2	3	4	5	6
1	0.8969	-1.835	7.0858	-16.92706	23.04371	-16.35683	4.6882
2							
3	0.23101	-2.64308	18.857896	-69.432981	134.55551	-129.822931	49.122313
4	5.818453	-79.16826	541.375917	-1876.025798	3404.689663	-3077.49264	1091.820477

TABLE 9

C_{gi} \ P_T	4	6	8
0	3.9264	4.6678	5.1195
1	-70.2774	-92.0677	-106.2639
2	760.2211	1095.149368	1203.5784
3	-4555.3334	-6256.6666	-7428.4322
4	15869.7321	22116.3671	26496.5277
5	-32881.7859	-46401.7226	-56029.3643
6	39842.9387	56855.17242	69136.9256
7	-26014.1585	-37498.7329	-45893.3309
8	7058.5568	10269.0621	12642.514

TABLE 10

C_{gi} \ P_T	4	6	8
0	3.2845	3.9732	4.3969
1	-53.5082	-71.2083	-82.9001
2	514.2917	707.9118	840.4489
3	-2773.9491	-3902.4251	-4693.8091
4	8764.3631	12546.4274	15250.9614
5	-16558.0482	-24065.1224	-29524.5597
6	18370.70029	27067.5187	33488.0221
7	011020.1921	-16443.3875	-20502.3020
8	2754.5911	4158.8554	5223.2054

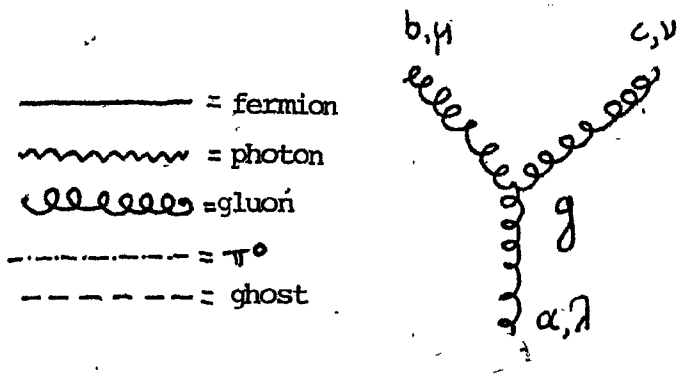

Fig. 1

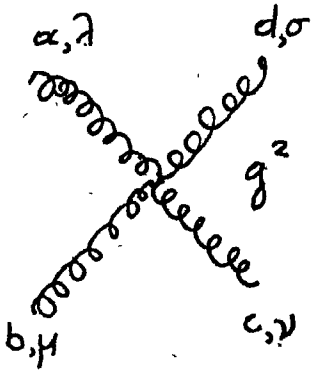

Fig. 2

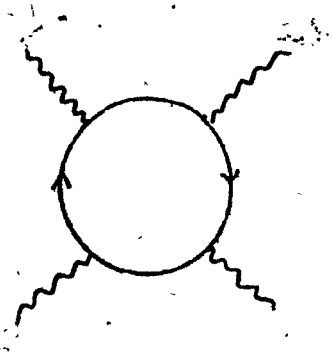

Fig. 3

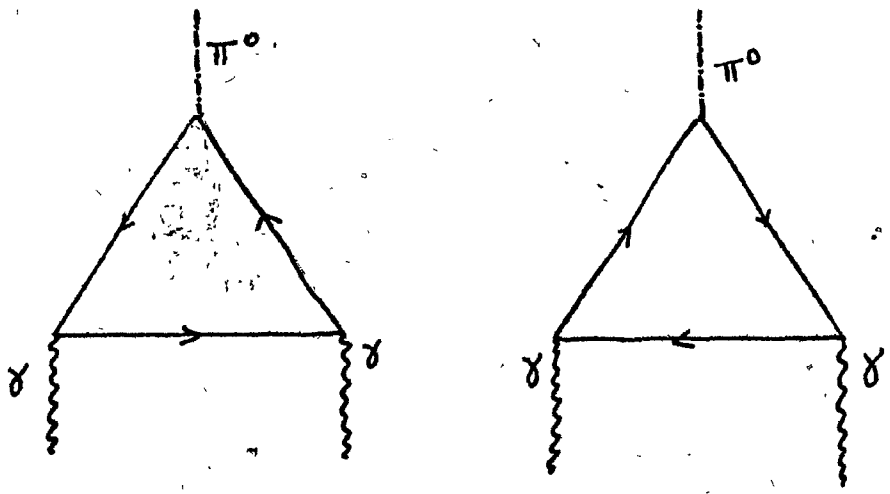

Fig. 4

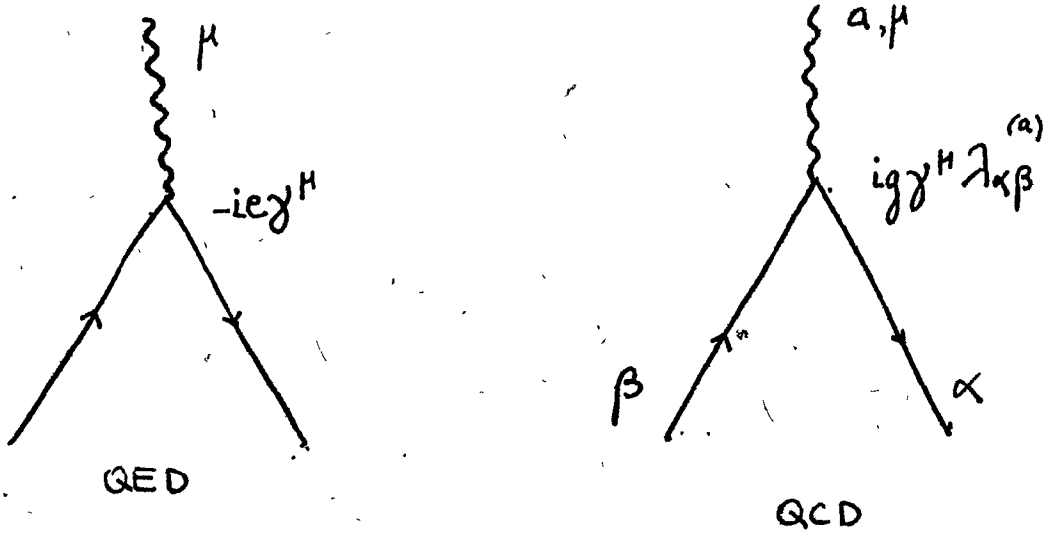

Fig.5

Fig.6

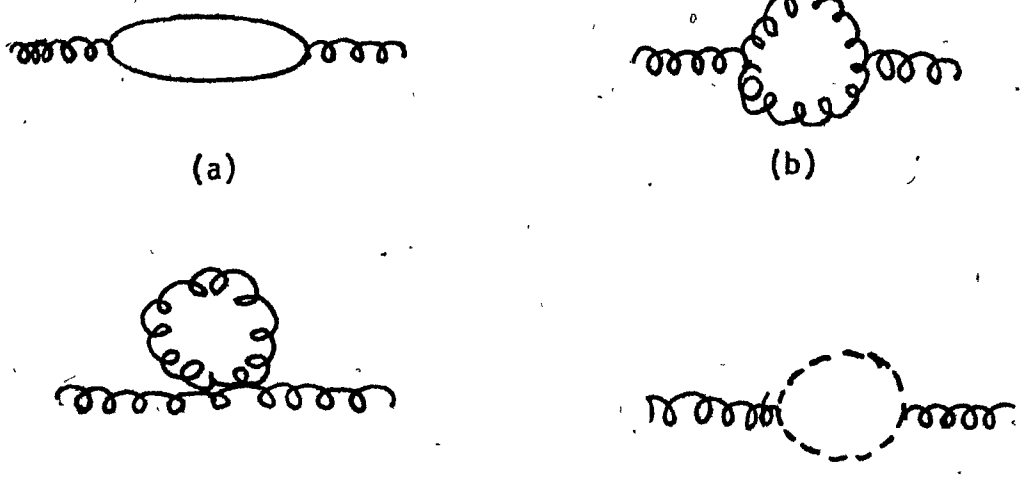

Fig.7

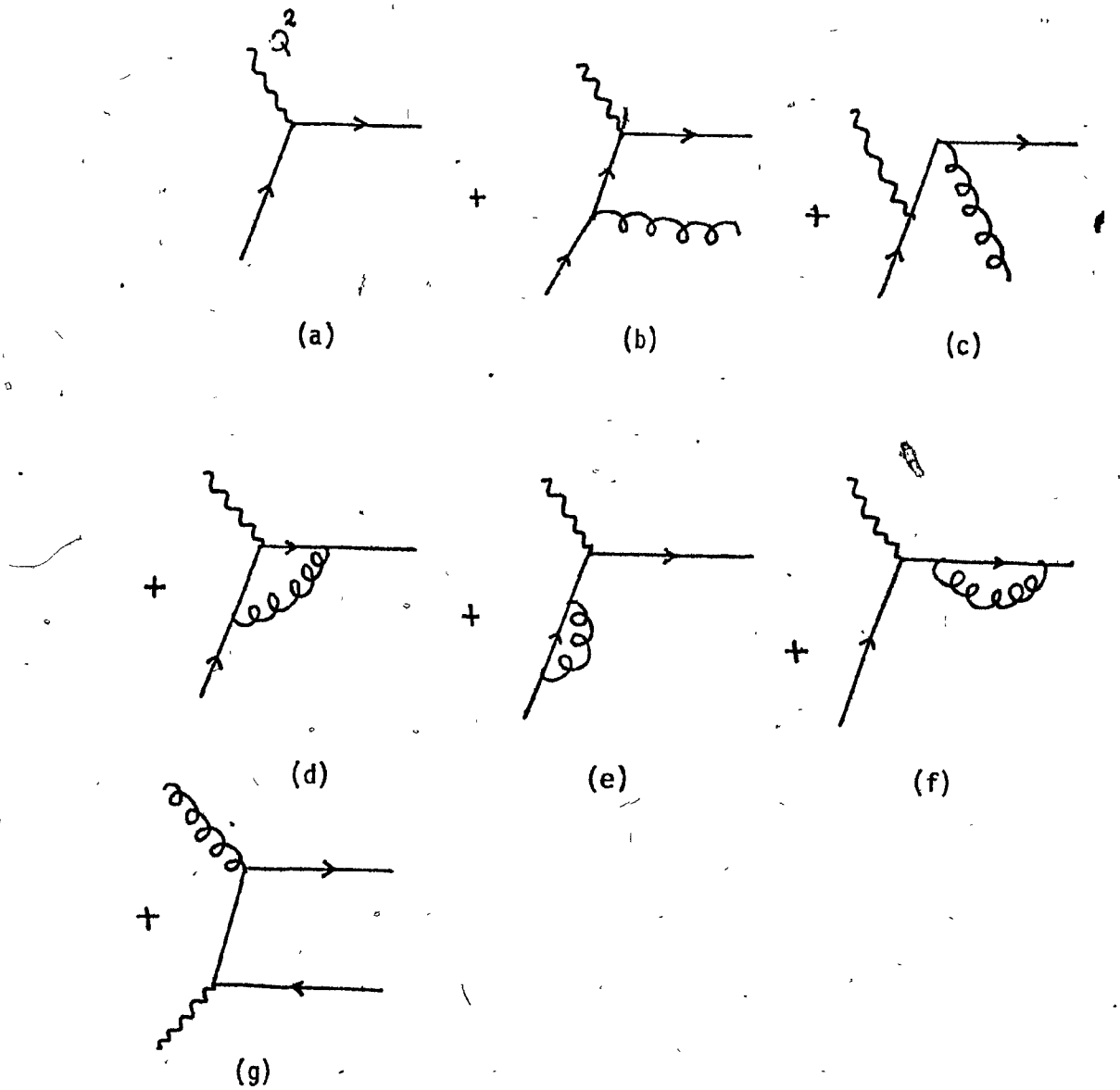

Fig.8

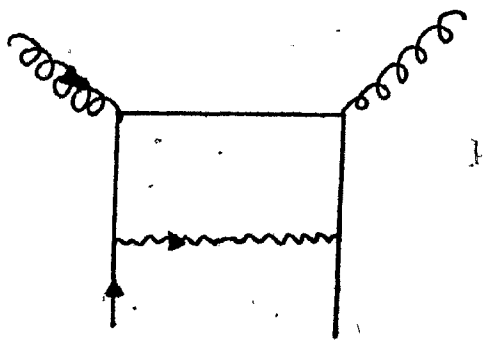

Fig.9

Mathematical Formulas

Intuitive Diagrams

a) $P_{qq}(z)$

$$P_{qq}(z)=\frac{4}{3}\left[\frac{1+z^2}{(1-z)_+}+\frac{3}{2}\delta(1-z)\right] \longleftrightarrow$$

b) $P_{qg}(z)$

$$P_{qg}(z)=\frac{1}{2}\left[z^2+(1-z)^2\right] \longleftrightarrow$$

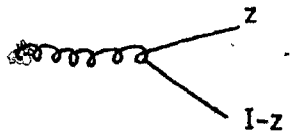

c) $P_{gq}(z)$

$$P_{gq}(z)=\frac{4}{3}\,\frac{1+(1-z)^2}{z} \longleftrightarrow$$

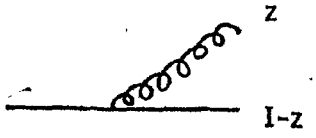

d) $P_{gg}(z)$

$$P_{gg}(z)=6\left[\frac{z}{(1-z)_+}+\frac{1-z}{z}+z(1-z)+\left(\frac{11}{12}-\frac{f}{18}\right)\delta(1-z)\right]$$

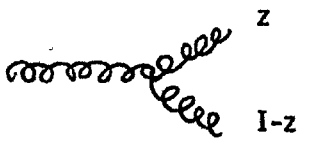

Fig. 10

$$E\frac{d\sigma}{d^3p}\ (h_1h_2 \to hX) = \sum_{\substack{\text{quarks}\\ \text{gluons}}}$$

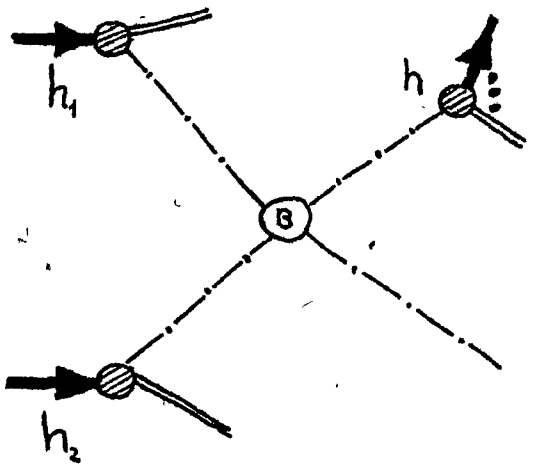

Fig.11

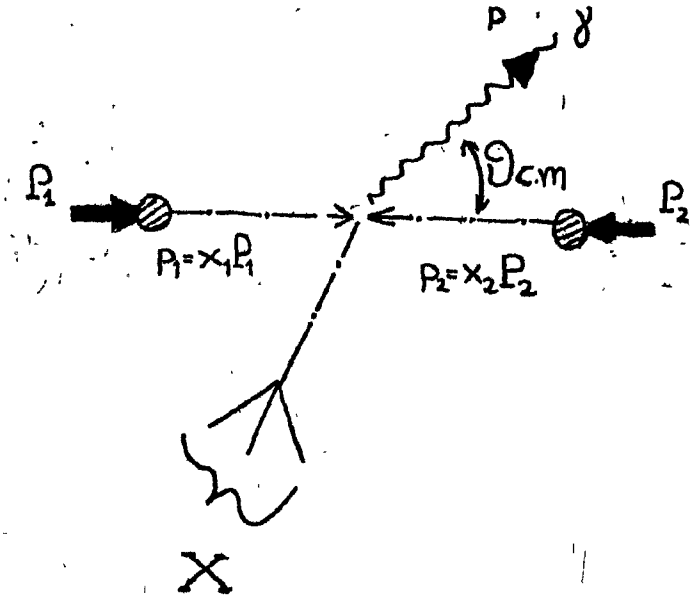

Fig.12

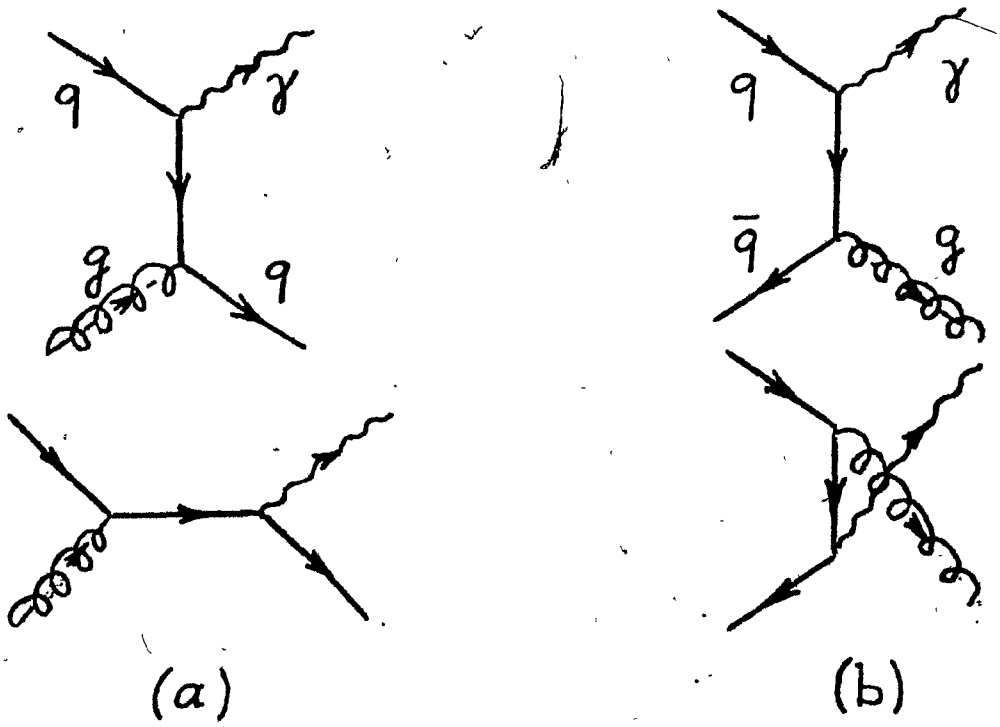

Fig. 13

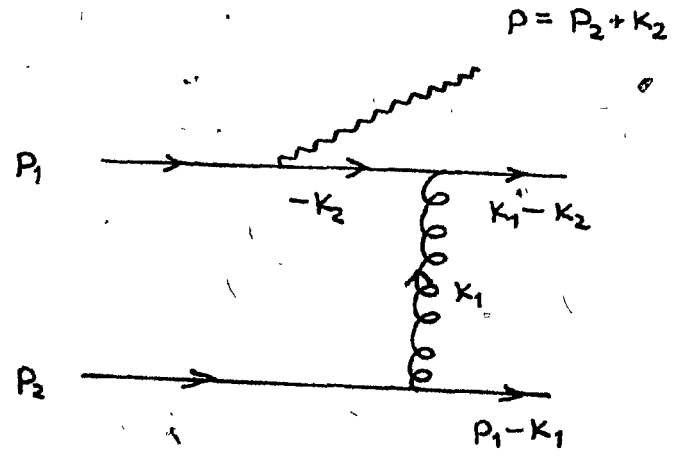

Fig.14

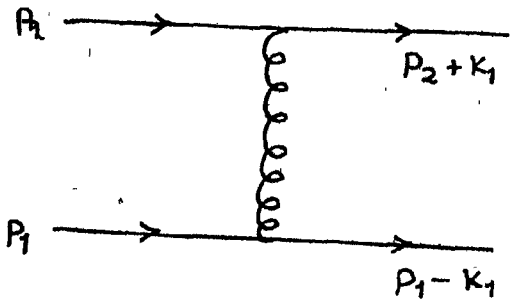

Fig.15

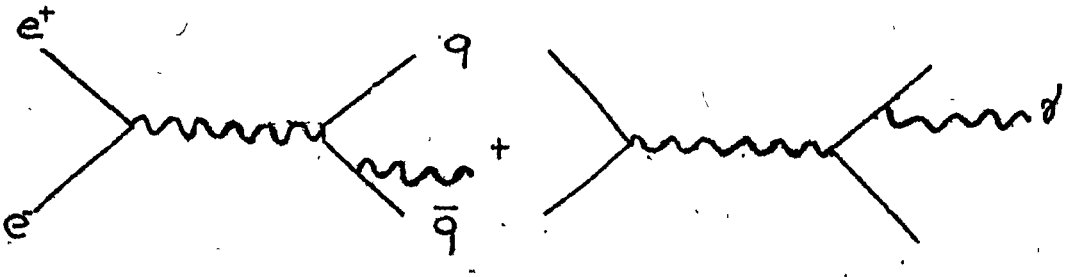

Fig.16

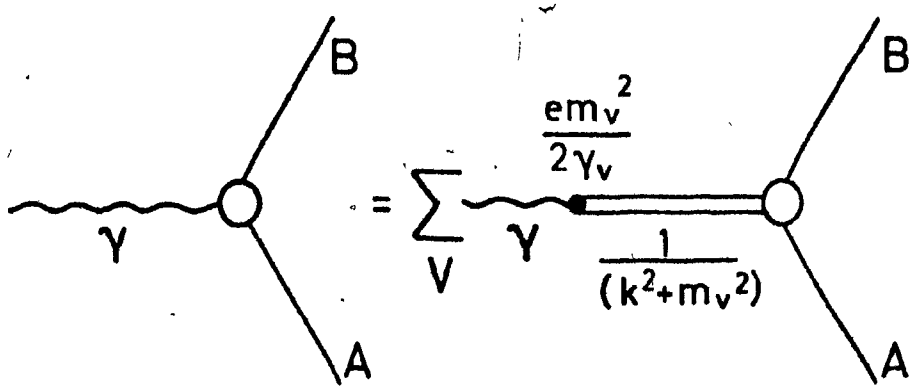

Fig.17

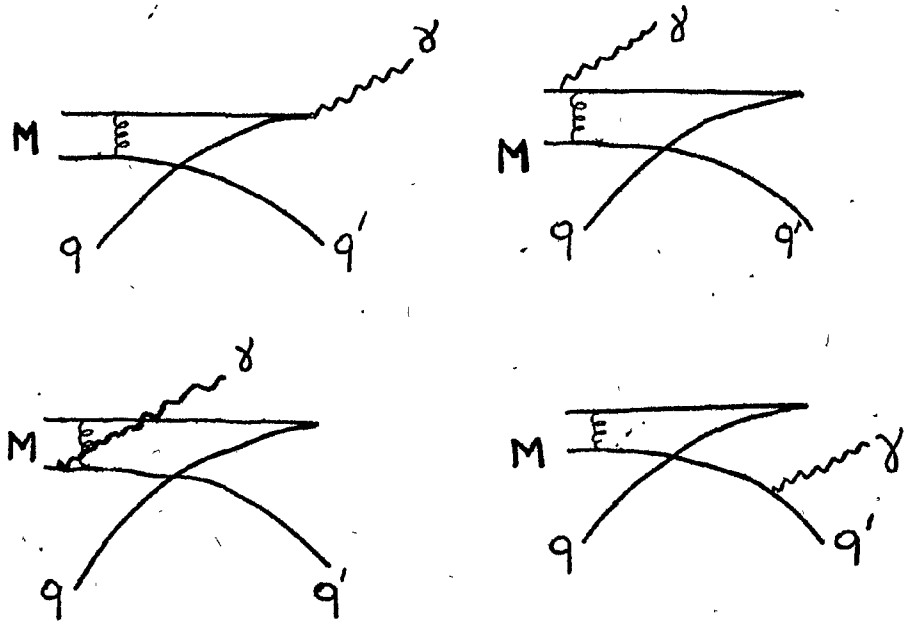

Fig.18

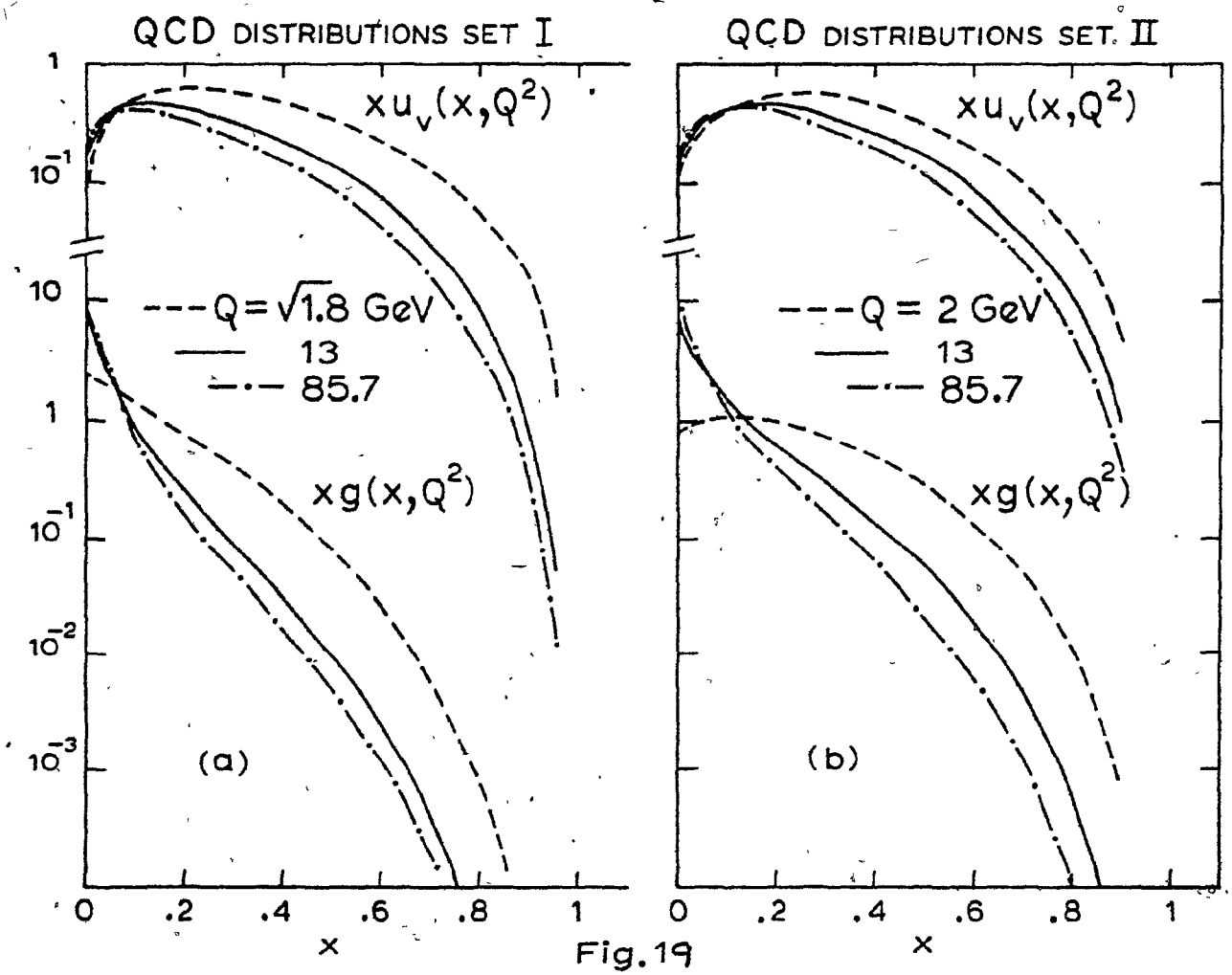
QCD DISTRIBUTIONS SET I
QCD DISTRIBUTIONS SET II
$xu_v(x,Q^2)$
$xg(x,Q^2)$
---Q=√1.8 GeV
13
85.7
---Q = 2 GeV
13
85.7
(a)
(b)
1
10^{-1}
10
1
10^{-1}
10^{-2}
10^{-3}
0
.2
.4
.6
.8
1
x

Fig. 19

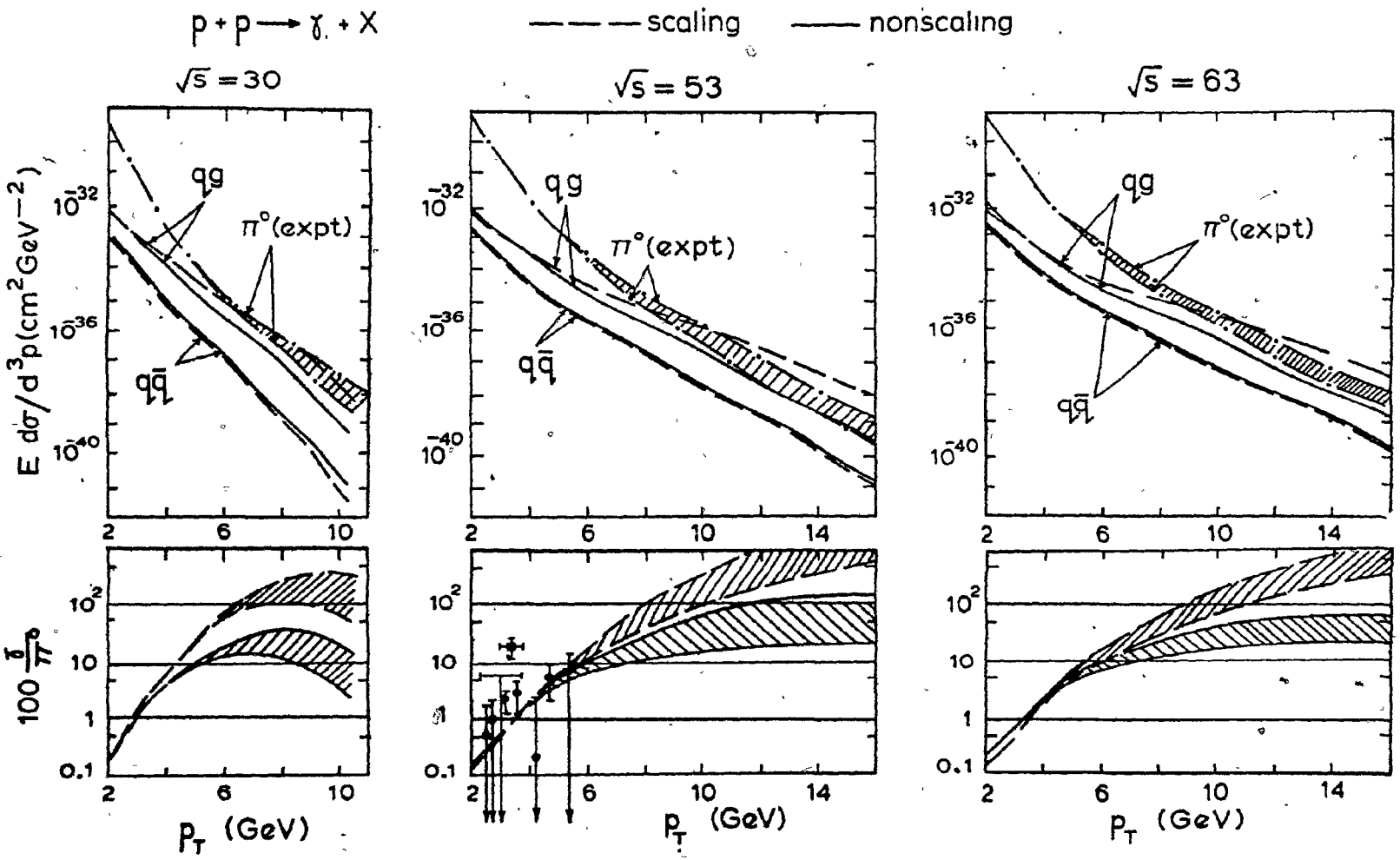
p + p → γ + X
scaling
nonscaling
√s = 30
√s = 53
√s = 63
E dσ/d³p(cm²GeV⁻²)
qg
π°(expt)
qq̄
100 γ/π°
P_T (GeV)
(a)
(b)
(c)

Fig.20

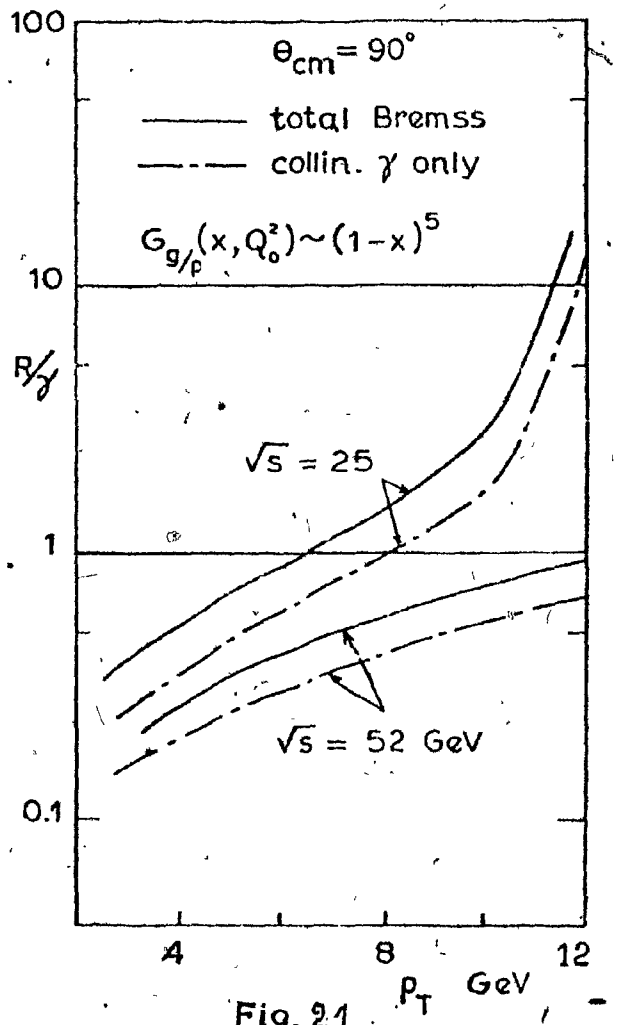
100
$\theta_{cm} = 90°$
total Bremss
collin. γ only
$G_{g/p}(x,Q_0^2) \sim (1-x)^5$
10
R/γ
$\sqrt{s}$ = 25
1
$\sqrt{s}$ = 52 GeV
0.1
4
8
12
p_T GeV

Fig. 21

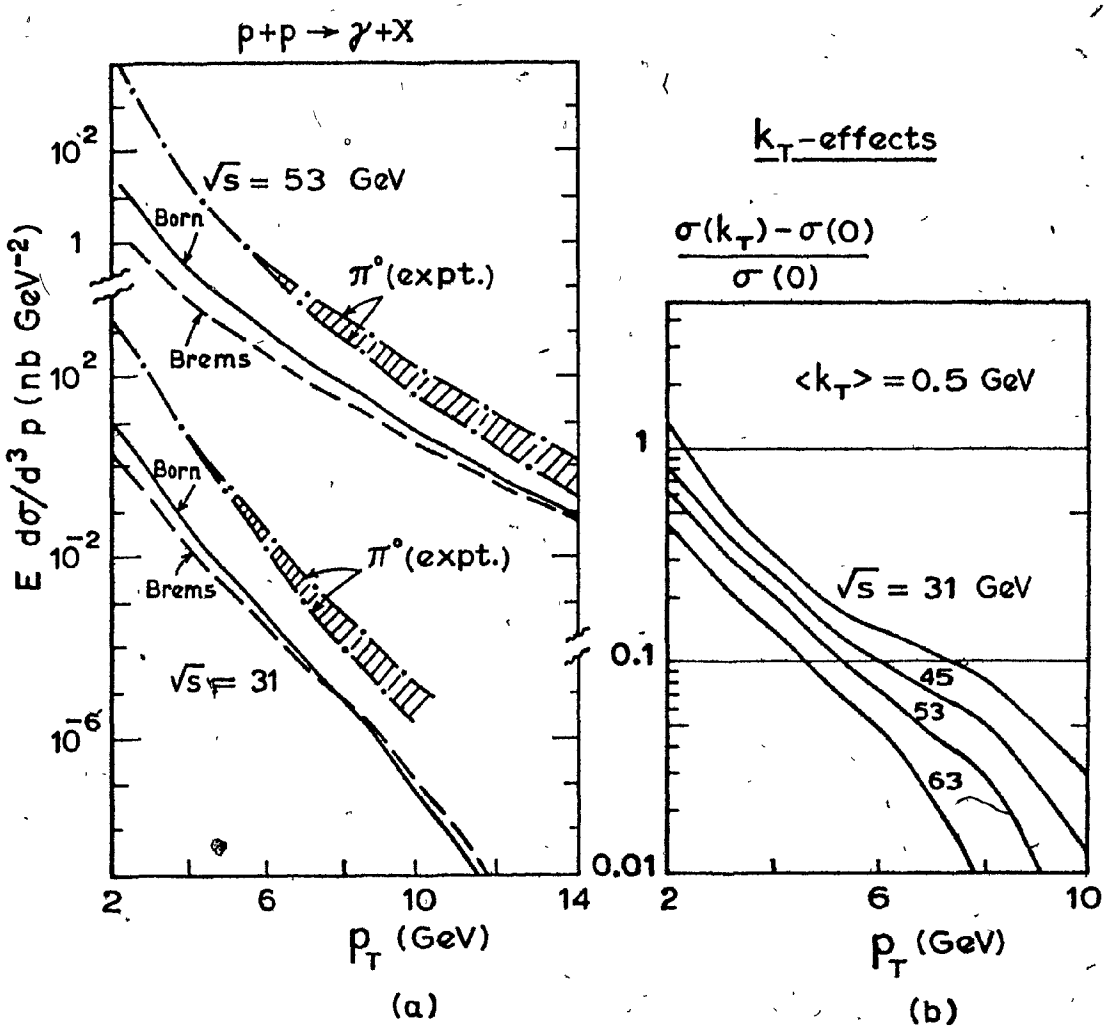
p+p → γ+X
E dσ/d³p (nb GeV⁻²)
√s = 53 GeV
Born
Brems
π°(expt.)
Born
Brems
π°(expt.)
√s = 31
p_T (GeV)
(a)
k_T-effects
σ(k_T) − σ(0) / σ(0)
<k_T> = 0.5 GeV
√s = 31 GeV
45
53
63
p_T (GeV)
(b)

Fig. 22

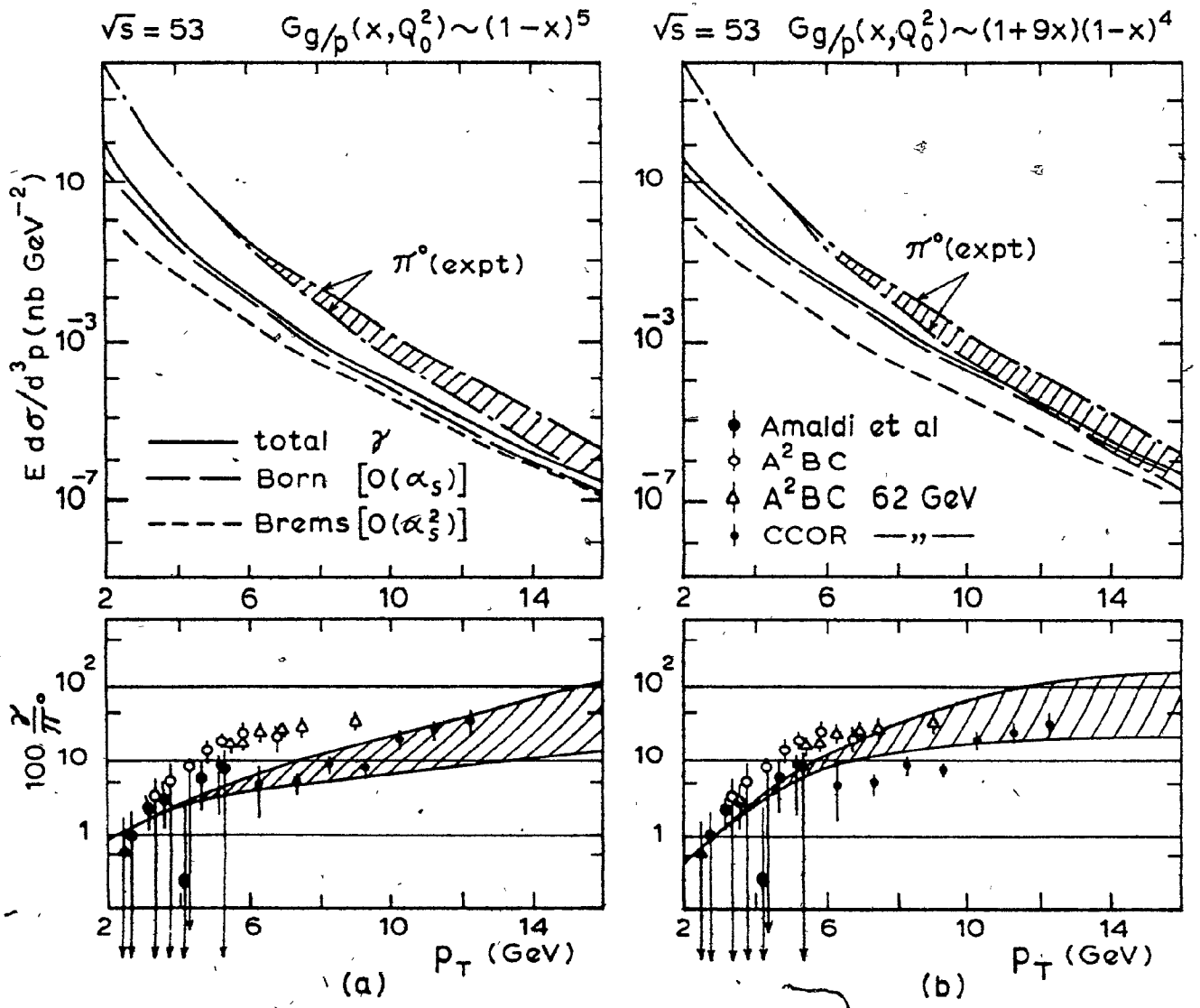
√s = 53 $G_{g/p}(x,Q_0^2) \sim (1-x)^5$
√s = 53 $G_{g/p}(x,Q_0^2) \sim (1+9x)(1-x)^4$
$E\,d\sigma/d^3p$ (nb GeV^{-2})
π^0(expt)
total γ
Born $[O(\alpha_s)]$
Brems $[O(\alpha_s^2)]$
Amaldi et al
A^2BC
A^2BC 62 GeV
CCOR —„—
$100\,\frac{\gamma}{\pi^0}$
p_T (GeV)
(a)
(b)

Fig.23

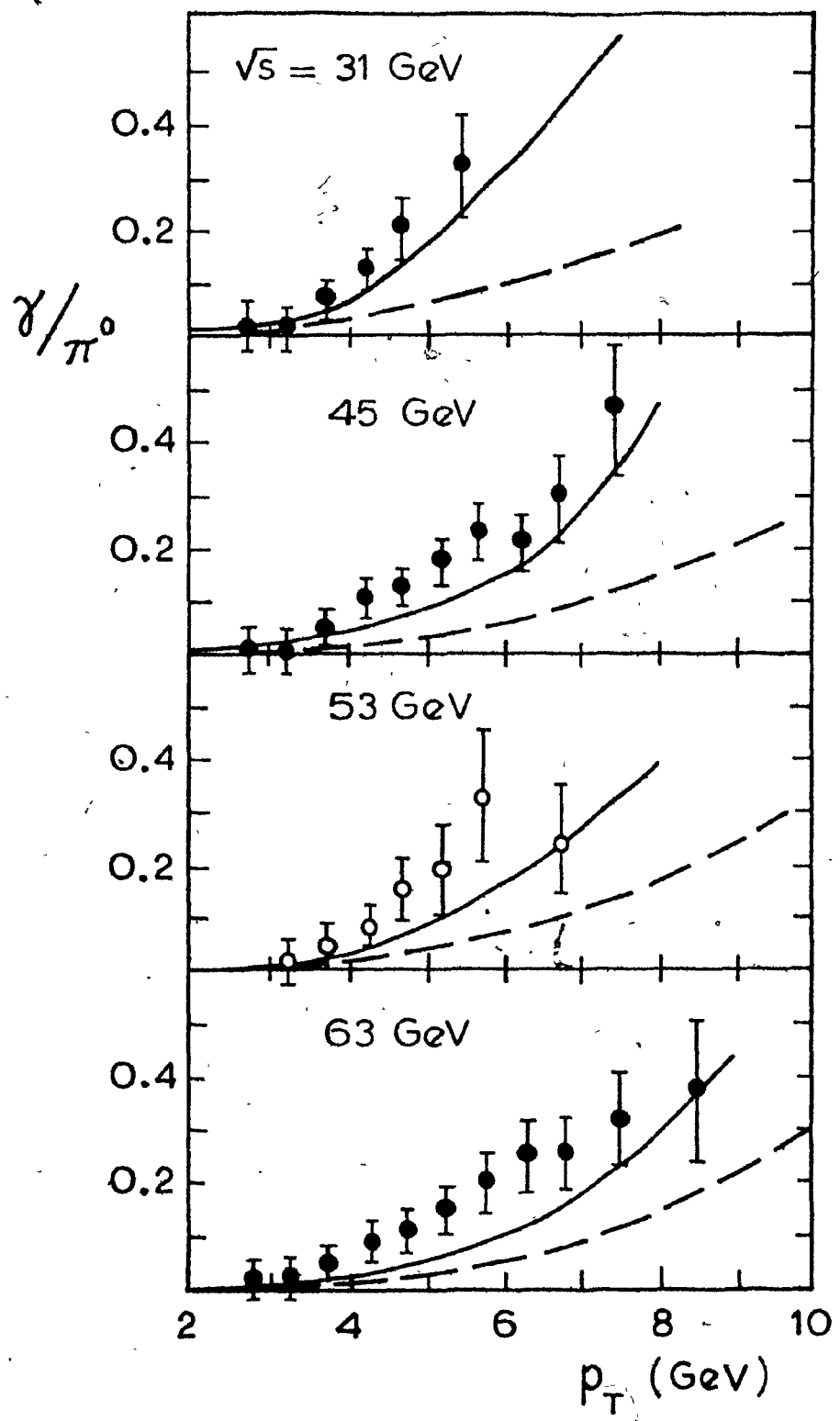

Fig. 24

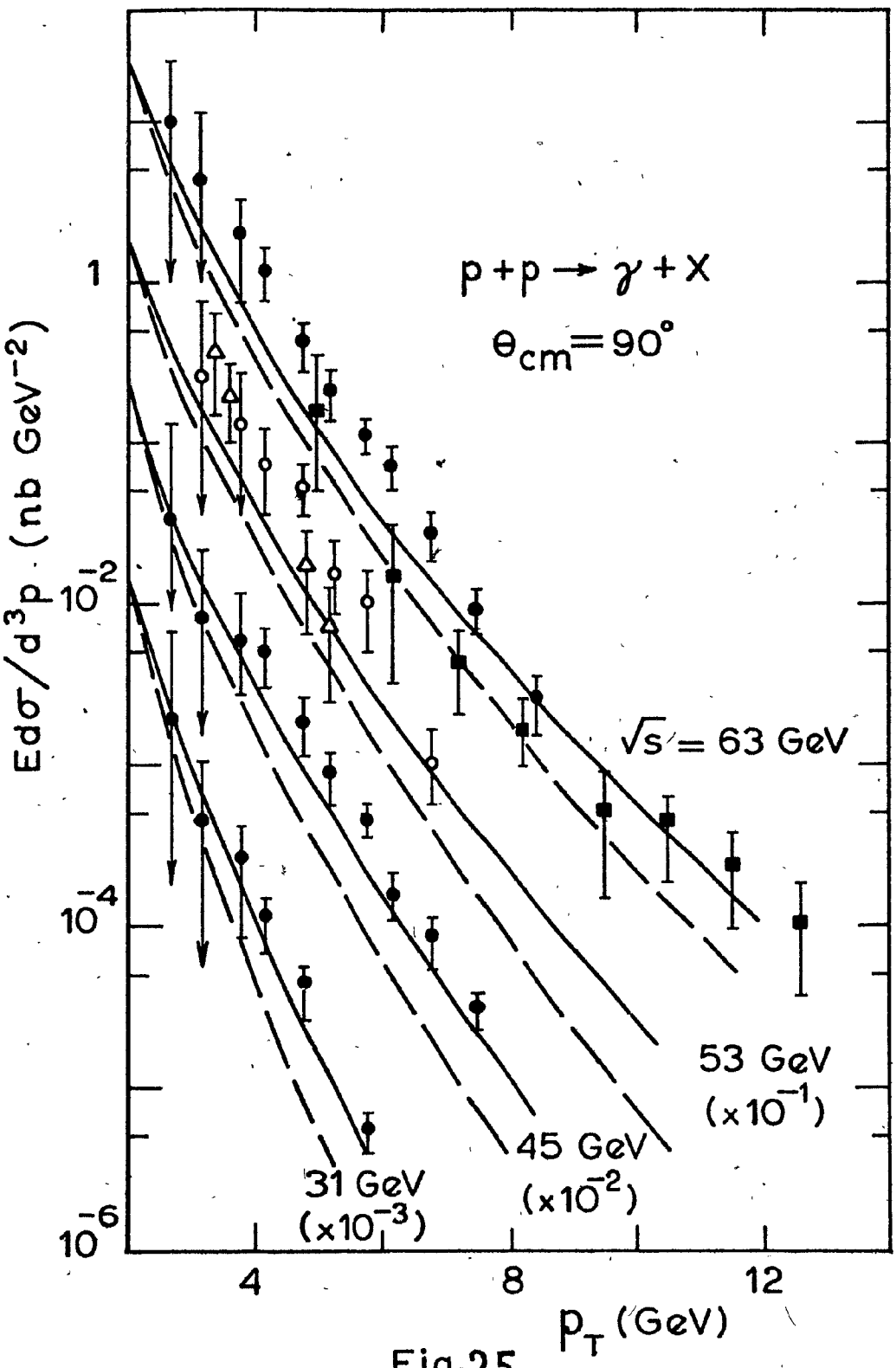
p + p → γ + X
θcm = 90°
√s = 63 GeV
53 GeV (×10⁻¹)
45 GeV (×10⁻²)
31 GeV (×10⁻³)
Ed³σ/d³p (nb GeV⁻²)
1
10⁻²
10⁻⁴
10⁻⁶
4
8
12
pT (GeV)

Fig.25

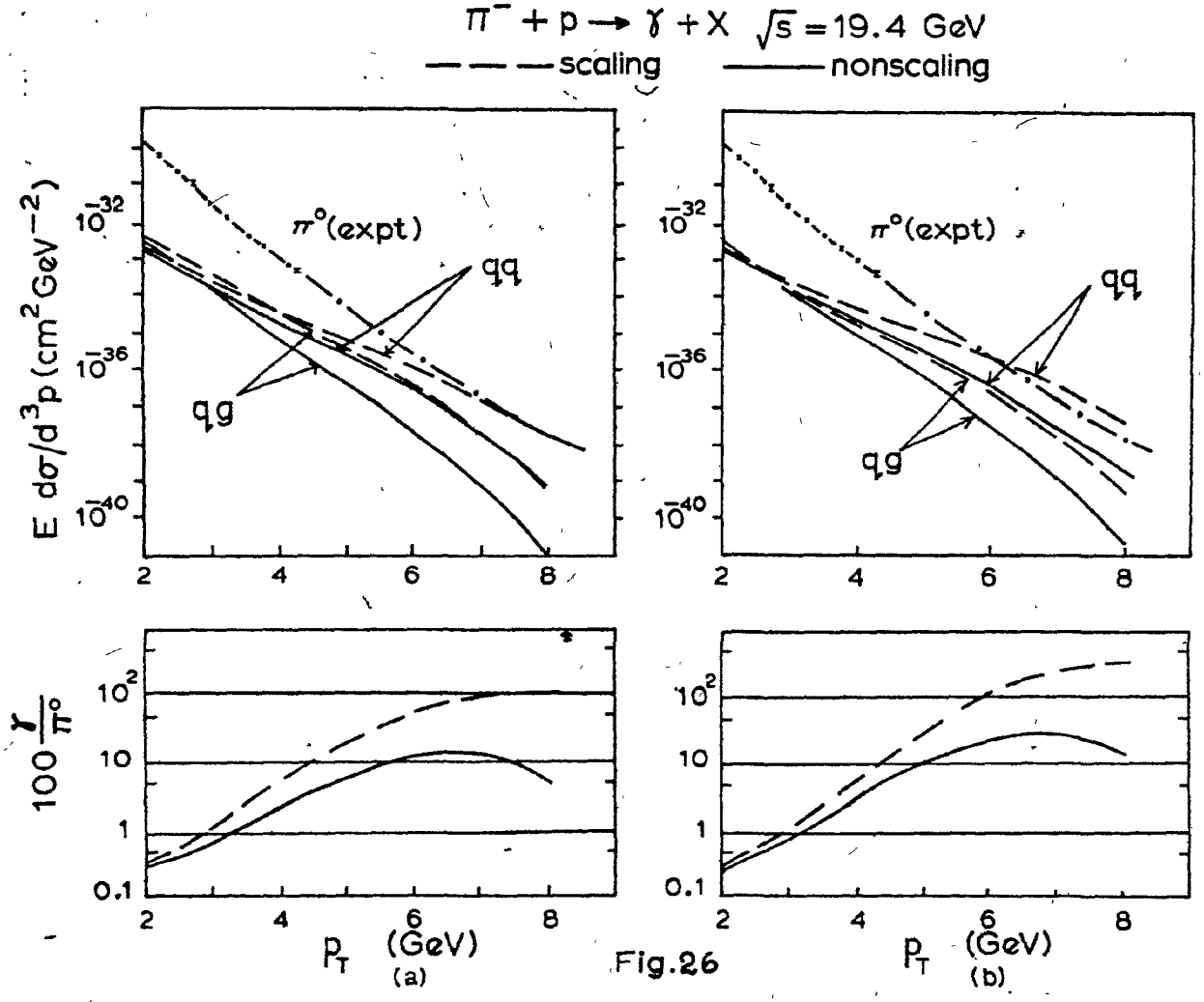
$\pi^- + p \rightarrow \gamma + X \quad \sqrt{s} = 19.4$ GeV
scaling
nonscaling
$E\, d\sigma/d^3p\ (cm^2 GeV^{-2})$
10^{-32}
10^{-36}
10^{-40}
π^0(expt)
qq
qg
2
4
6
8
$100\,\frac{\gamma}{\pi^0}$
10^2
10
1
0.1
p_T (GeV)
(a)
(b)

Fig.26

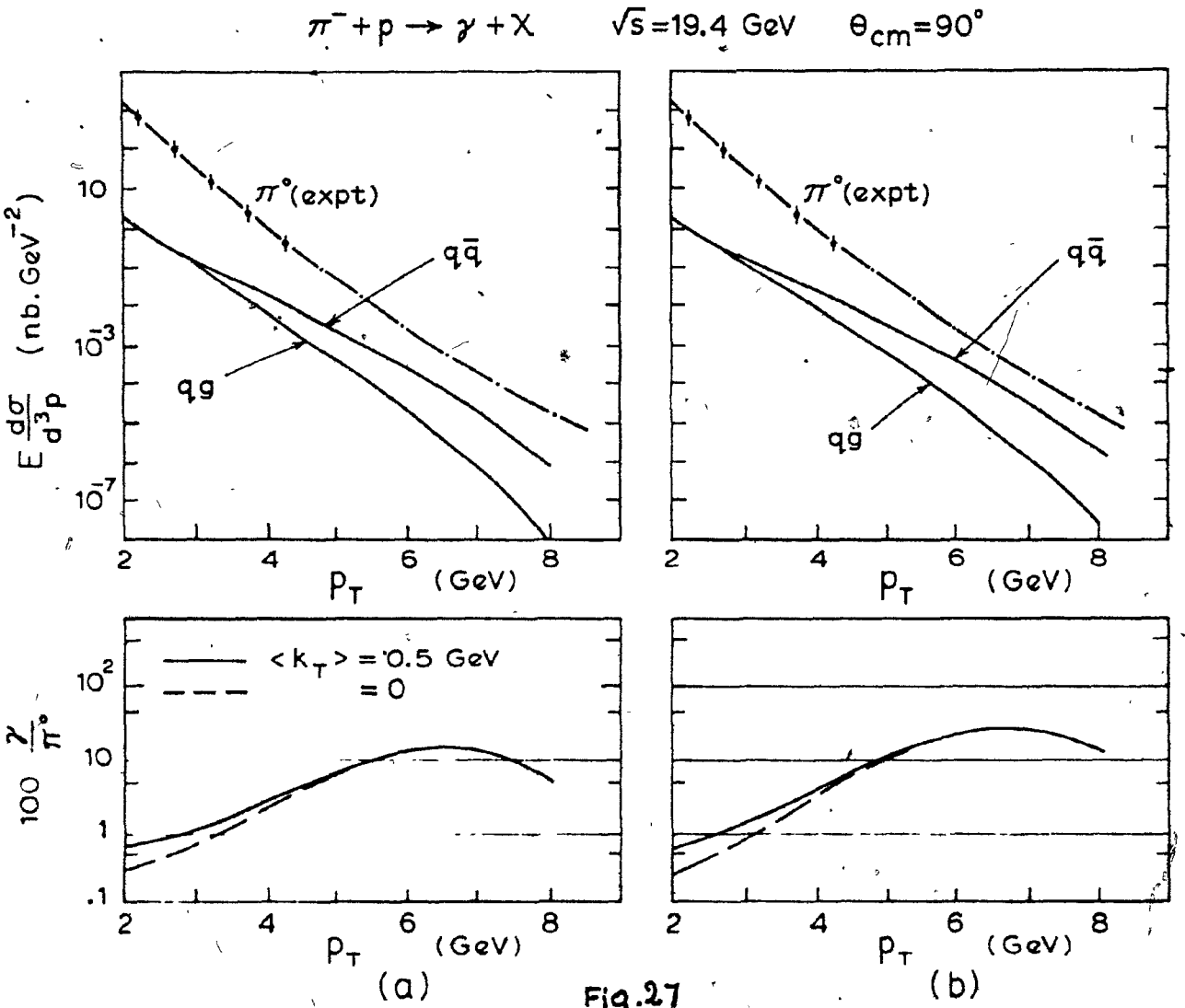
$\pi^- + p \rightarrow \gamma + X$ $\sqrt{s}$=19.4 GeV θ_{cm}=90°
$E\frac{d\sigma}{d^3p}$ (nb. GeV^{-2})
π^0(expt)
$q\bar{q}$
qg
$q\bar{q}$
qg
p_T (GeV)
$\frac{\gamma}{\pi^0}$
100
$\langle k_T \rangle$ = 0.5 GeV
= 0
p_T (GeV)
(a)
(b)

Fig.27

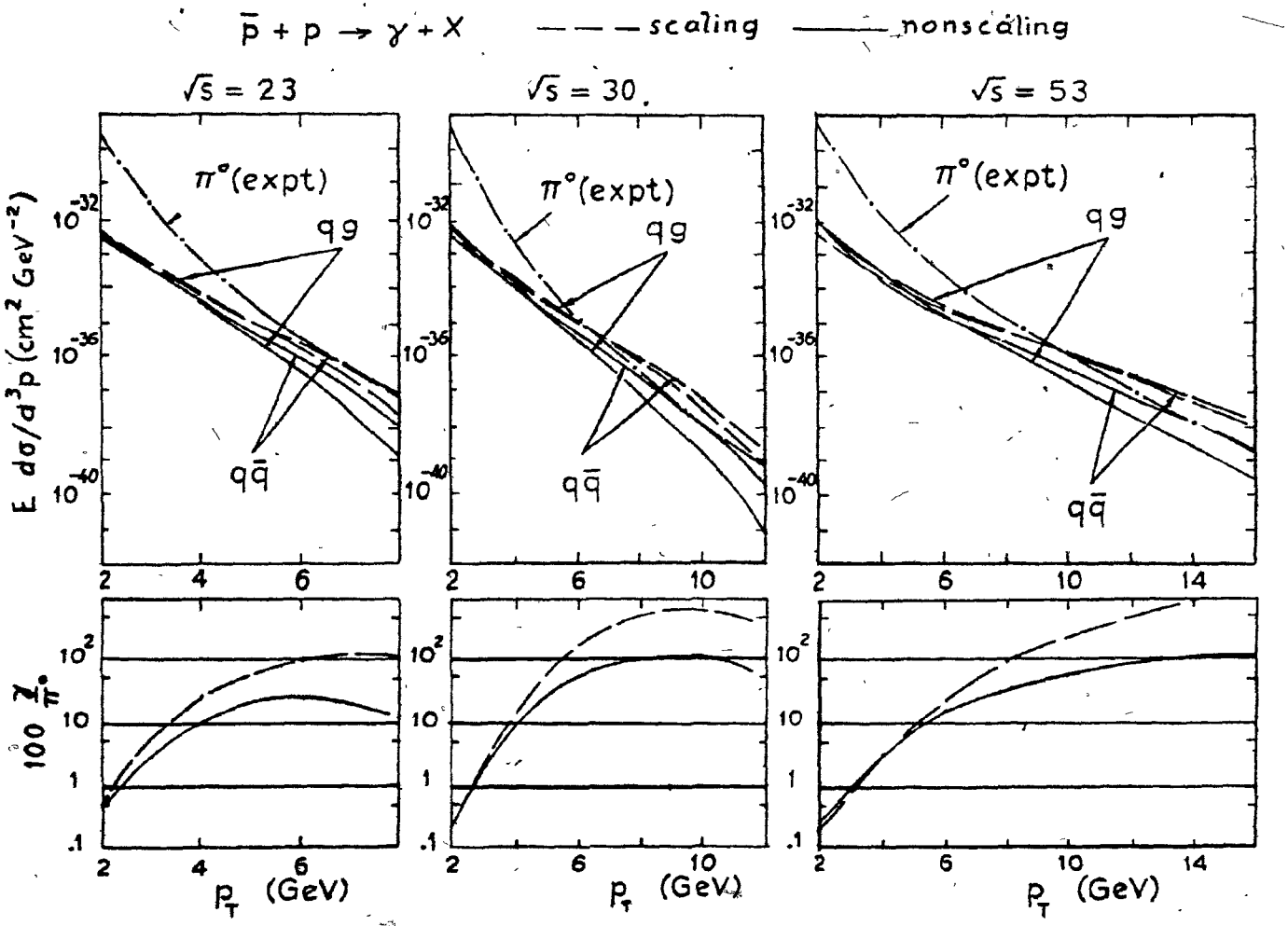
$\bar{p} + p \rightarrow \gamma + X$
scaling
nonscaling
$\sqrt{s} = 23$
$\sqrt{s} = 30$
$\sqrt{s} = 53$
π^0(expt)
qg
$q\bar{q}$
$E\, d\sigma/d^3p\ (cm^2\ GeV^{-2})$
$100\ \gamma/\pi^0$
p_T (GeV)

Fig. 28

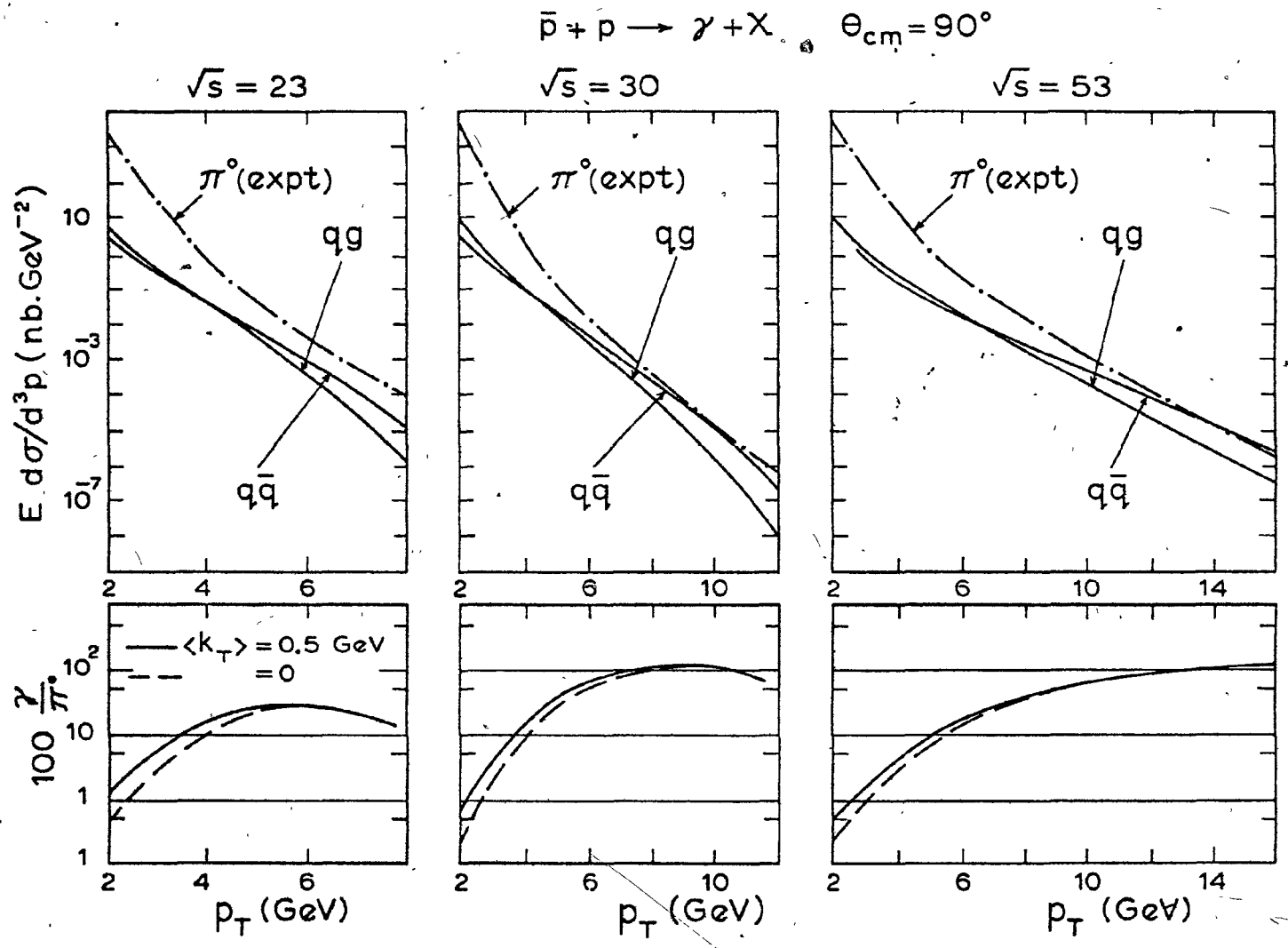
$\bar{p} + p \rightarrow \gamma + X$, $\theta_{cm} = 90°$
$\sqrt{s} = 23$
$\sqrt{s} = 30$
$\sqrt{s} = 53$
π^0(expt)
qg
$q\bar{q}$
$E\, d\sigma/d^3p$ (nb.GeV^{-2})
$\langle k_T \rangle = 0.5$ GeV
$= 0$
$100\ \frac{\gamma}{\pi^0}$
p_T (GeV)

Fig. 29

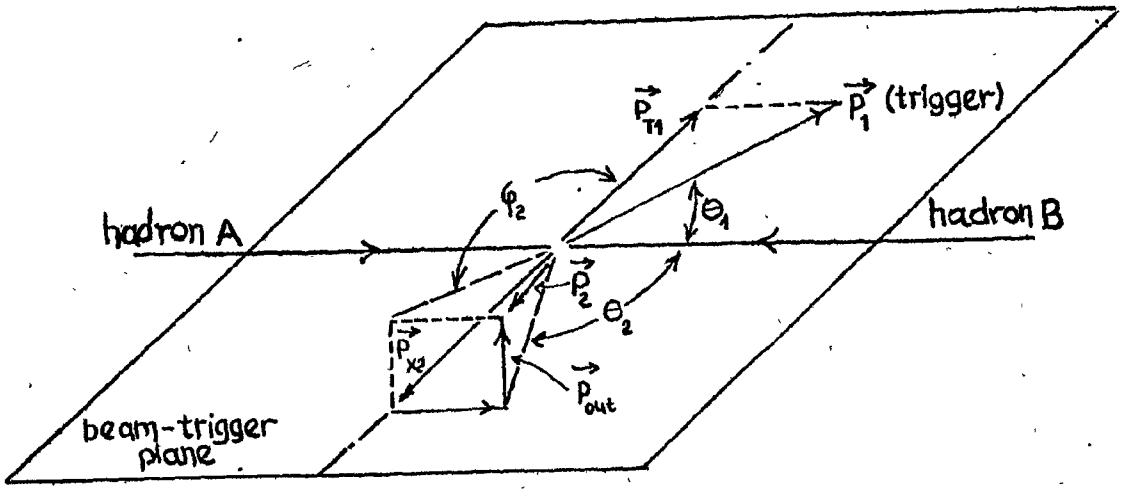
$\vec{P}_{T1}$
$\vec{P}_1$ (trigger)
φ_2
θ_1
hadron A
hadron B
$\vec{P}_2$
θ_2
$\vec{P}_{x2}$
$\vec{P}_{out}$
beam-trigger plane

Fig.30

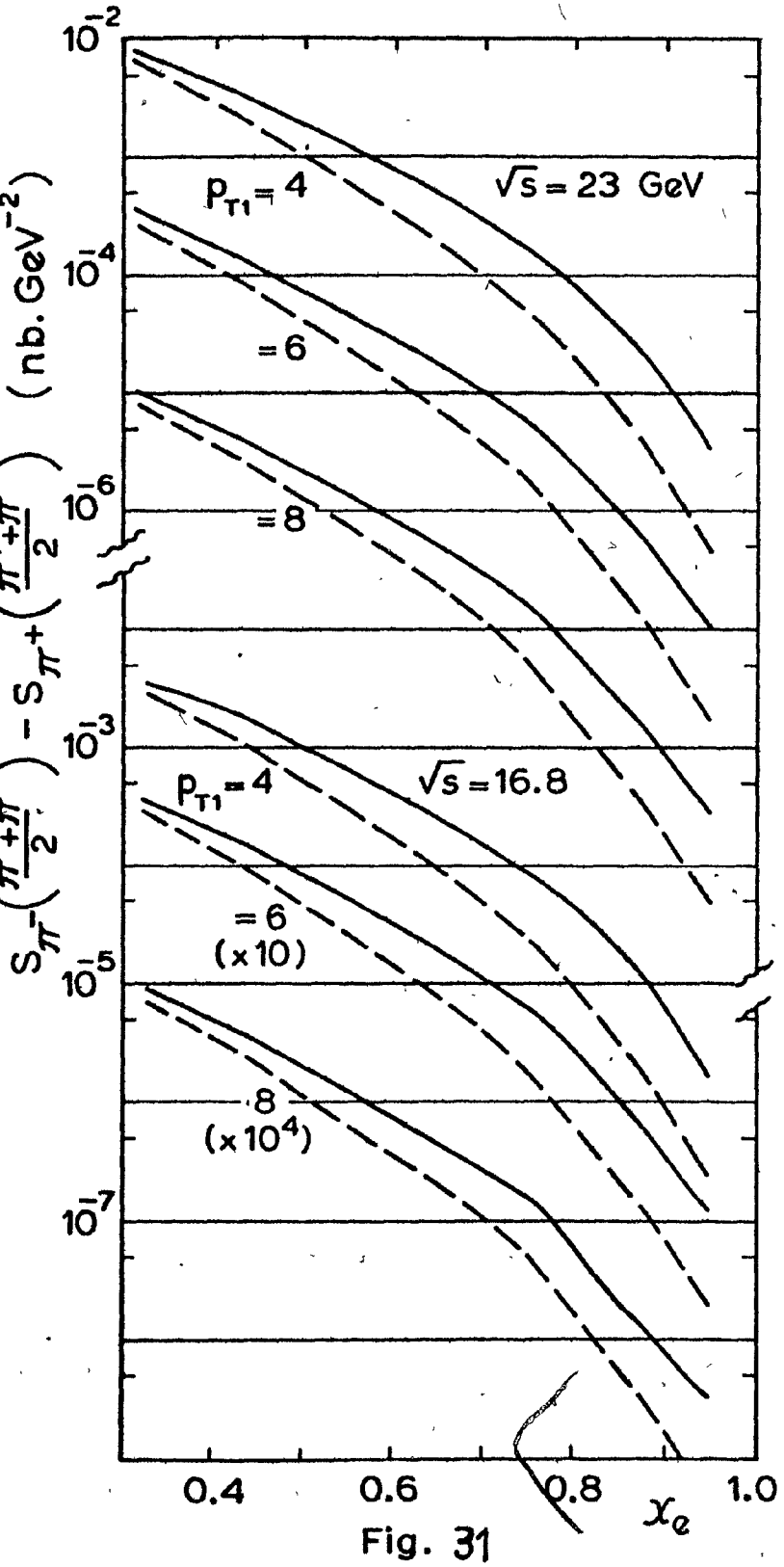
10^{-2}
10^{-4}
10^{-6}
10^{-3}
10^{-5}
10^{-7}
$S_{\pi^-}\left(\frac{\pi^+ + \pi^-}{2}\right) - S_{\pi^+}\left(\frac{\pi^+ + \pi^-}{2}\right)$ (nb. GeV^{-2})
$p_{T1} = 4$
$\sqrt{s} = 23$ GeV
$= 6$
$= 8$
$p_{T1} = 4$
$\sqrt{s} = 16.8$
$= 6$
$(\times 10)$
$= 8$
$(\times 10^4)$
0.4
0.6
0.8
1.0
x_e

Fig. 31